Contemporary Debates and Interdisciplinary Approaches In Natural Sciences and Mathematics

Editors::
Prof. Dr. Aybaba HANÇERLİOĞULLARI
Assoc. Prof. Dr. Cevat RAHABİ
Assist. Prof. Dr. Rezvan REZAIZADEH

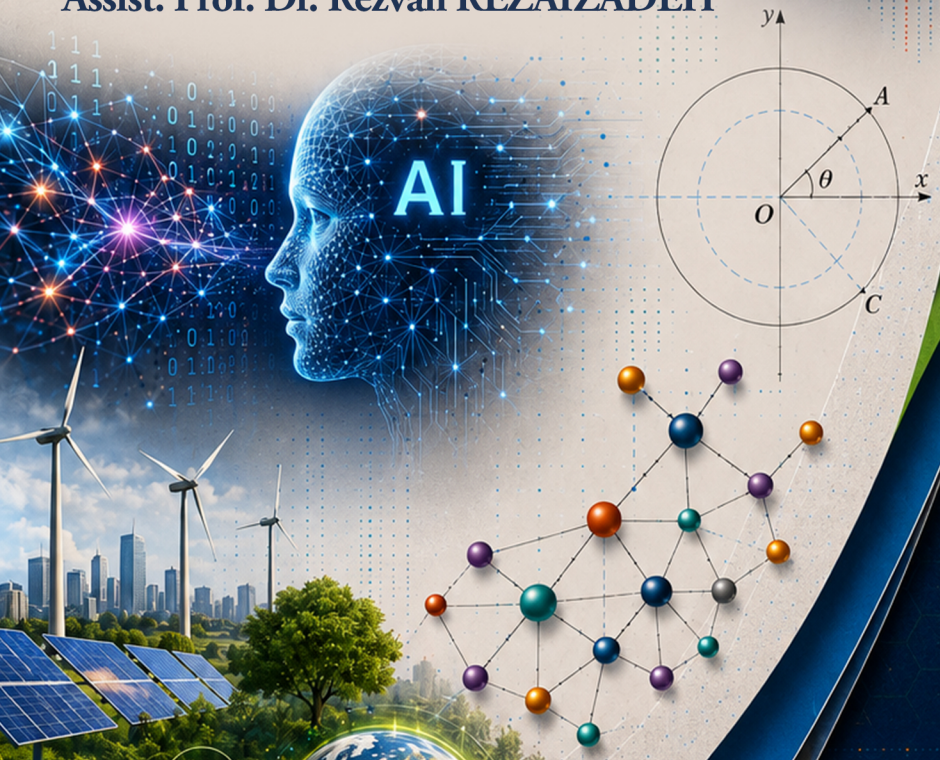

DUVAR

CONTEMPORARY DEBATES AND INTERDISCIPLINARY APPROACHES IN NATURAL SCIENCES AND MATHEMATICS

Editors:

Prof. Dr. Aybaba HANÇERLİOĞULLARI

Assoc. Prof. Dr. Cevat RAHABİ

Assist. Prof. Dr. Rezvan REZAIZADEH

Contemporary Debates and Interdisciplinary Approaches In Natural Sciences and Mathematics
Editors:: Prof. Dr. Aybaba HANÇERLİOĞULLARI
Assoc. Prof. Dr. Cevat RAHABİ
Assist. Prof. Dr. Rezvan REZAIZADEH

General Director: Berkan Balpetek
Cover and Page Design: Duvar Design
Printing : June-2026
Publisher Certificate No: 49837
E-ISBN: 978-625-8756-75-3

853 Sokak No:13 P.10 Kemeraltı-Konak/İzmir
Tel: 0 232 484 88 68
www.duvaryayinlari.com
duvarkitabevi@gmail.com

TABLE OF CONTENTS

CHAPTER-1

LINERIZED MODEL OF A PRES-STRESSED MAGNETO-ELECTRO-ELASTIC MATERIALS UNDER THE ACTION OF A DYNAMIC FORCE

Ahmet DAŞDEMİR[1]

1. INTRODUCTION

The rapid evolution of smart structures and multifunctional systems has propelled magneto-electro-elastic (MEE) materials to the forefront of interdisciplinary research, owing to their intrinsic ability to convert energy seamlessly and simultaneously among mechanical, electric, and magnetic fields. These composites, typically fabricated by uniting piezoelectric and piezomagnetic phases at the micro- or nano-scale, exhibit a remarkable magnetoelectric coupling effect that no single-phase constituent can achieve alone: an applied magnetic field can induce electric polarization, and conversely, an electric field can generate magnetization. This unique multi-physics characteristic renders MEE materials indispensable for a broad spectrum of advanced applications, ranging from ultra-sensitive magnetic field sensors and next-generation energy harvesters to contactless actuators and multi-state memory elements. In the vast majority of these engineering settings, however, the material rarely operates in a stress-free, static condition; particularly in embedded sensory or actuating layers, high-frequency resonators, and protective shielding under impact, the coexistence of a pre-stress state and dynamic loading fundamentally alters the constitutive behavior and the multi-field coupling landscape. Analytical approaches frequently become intractable when attempting to resolve these complex, fully coupled interactions accurately, thereby motivating the use of powerful numerical tools such as the finite element method.

These developments have led researchers to conduct further theoretical investigations on magneto-electro-elastic (MEE) materials. Ke and Wang comprehensively studied the effects of external electric and magnetic potentials and a uniform temperature rise on MEE nanobeams [1]. Lim et al. proposed a novel nonlocal strain gradient theory (NSGT) that unifies the nonlocal elasticity and strain gradient theories and applied it to wave propagation problems [2]. Jandaghian and

[1] Assoc.Prof., Department of Mathematics, Faculty of Science, Kastamonu University, Türkiye, ahmetdasdemir37@gmail.com, (ORCID: 0000-0001-8352-2020)

Rahmani developed a magneto-electro-thermo-elastic (METE) nanobeam model to regulate the variation and distribution of electric and magnetic potentials through the beam thickness and presented numerical solutions using the differential quadrature method [3]. Trinh et al. examined the mechanical behavior of functionally graded microbeams by combining the modified couple stress theory with various shear deformation theories [4]. Ebrahimi et al. analyzed the free vibration of porous functionally graded MEE plates resting on an elastic foundation under various boundary conditions using the Euler–Bernoulli beam theory [5]. Kiran and Kattimani investigated the free and static vibration of functionally graded skew MEE plates through a power-law distribution using a finite element model [6]. Sahmani and Aghdam applied the nonlocal strain gradient shell model to the axial buckling and postbuckling analysis of MEE cylindrical nanoshells, highlighting scale-dependent stiffening-softening effects [7]. Ebrahimi, Barati, and Mahesh modeled the influence of nonlocal stresses on the free vibration of curved functionally graded MEE nanobeams based on the Euler–Bernoulli beam theory [8]. Habibi et al. investigated the size-dependent free vibration of MEE nanobeams in a thermal environment using the modified couple stress theory [9]. Sahmani and Khandan employed the NSGT to analyze the nonlinear buckling behavior of MEE cylindrical nano-composite panels under electrostatic and magnetostatic effects [10]. Milan and Ayatollahi observed the transient response of a system consisting of two dissimilar functionally graded MEE layers weakened by a screw dislocation and subjected to magneto-electro-mechanical impacts by means of the distributed dislocation technique [11]. Hong et al. developed a functionally graded MEE Timoshenko microbeam model using variational approaches [12]. Danesh and Javanbakht comparatively examined the free vibration properties of nonlocal nanobeams with different crystalline core configurations [13]. Sui et al. solved the frictional contact problem of a MEE half-space over which a perfectly conducting rigid spherical punch slides using a semi-analytical method [14]. Zhou and Qu proposed an isogeometric analysis method for the static and dynamic analysis of MEE structures under both thermal and mechanical interactions [15]. Van Ke et al. investigated the flexoelectric effect on the bending and free vibration characteristics of piezoelectric sandwich functionally graded porous nanoplates via the nonlocal strain gradient theory [16]. Van Thom et al. analyzed the mechanical responses of nanoplates resting on viscoelastic foundations in multi-physical environments using classical plate theory [17]. Wang, Zhou and Chai employed an enriched finite element method within a layerwise model to analyze the static response of functionally graded MEE structures in a hygrothermal environment [18].

This chapter develops, in a rigorous and self-contained manner, a fully coupled finite element model for a pre-stressed MEE material subjected to a dynamic force,

explicitly embedding the nonlinear influence of the initial stress field onto the stiffness, piezoelectric, piezomagnetic, and magnetoelectric tensors within the formulation. Consequently, the work unlocks the possibility of predicting with high fidelity critical phenomena, most notably stress-mediated magneto-electric coupling enhancement and resonance frequency shifts, that are experimentally observed yet notoriously difficult to capture numerically.

2. STATEMENT OF PROBLEM

In this study, a two-dimensional magneto-electro-elastic (MEE) medium is considered. The material is assumed to be linearly elastic, homogeneous, isotropic, and orthogonally polarized. The geometry of the plate and its physical configuration are illustrated in Figure 1. Let V denote the volume occupied by the plate, while Γ represents the entire boundary of the domain. It should be emphasized that Γ consists of four boundary segments. Throughout the formulation, Cartesian coordinates x_1 and x_2 are employed. The coordinate system is selected such that the plane Ox_1x_2 passes through the middle surface of the plate.

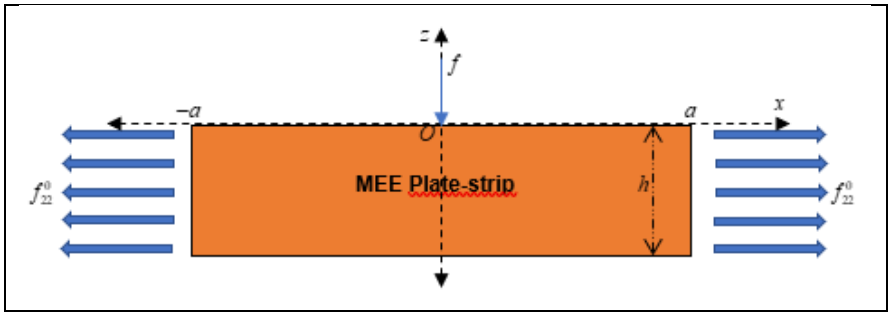

Figure 1 Geometry of problem

For the MEE medium, the constitutive behavior is described through generalized Hooke-type relations as follows [19]:

$$\mathbf{\Sigma} = [C]\mathbf{S} - [e]\mathbf{E} - [f]\mathbf{H}, \tag{1.a}$$

$$\mathbf{D} = [e]^T\mathbf{S} + [h]\mathbf{E} + [g]\mathbf{H}, \tag{1.b}$$

$$\mathbf{B} = [f]^T\mathbf{S} + [g]\mathbf{E} + [\mu]\mathbf{H}. \tag{1.c}$$

In the above expressions, Σ and S denote the stress and strain tensors, respectively. The vectors E and H correspond to the electric and magnetic field

intensities, whereas D and B represent the electric displacement and magnetic induction vectors. Furthermore, $[C]$, $[e]$, $[f]$, $[h]$, $[g]$, and $[\mu]$ stand for the elastic, piezoelectric, piezomagnetic, dielectric, magnetoelectric, and magnetic property matrices, respectively. The explicit forms of these quantities are given by

$$\mathbf{\Sigma} = \{\sigma_{11} \quad \sigma_{22} \quad \sigma_{12}\}^T, \ \mathbf{S} = \{S_{11} \quad S_{22} \quad S_{12}\}^T \tag{2.a}$$

$$\mathbf{D} = \{D_1 \quad D_2\}^T, \ \mathbf{E} = \{E_1 \quad E_2\}^T \tag{2.b}$$

$$\mathbf{B} = \{B_1 \quad B_2\}^T, \ \mathbf{H} = \{H_1 \quad H_2\}^T \tag{2.c}$$

$$[C] = [c_{ij}]_{3\times3}, \ [e] = [e_{ij}]_{3\times2}, \ [f] = [f_{ij}]_{3\times2} \tag{2.d}$$

$$[h] = [h_{ij}]_{2\times2}, \ [g] = [g_{ij}]_{2\times2}, \ [\mu] = [\mu_{ij}]_{2\times2} \tag{2.e}$$

It is worth mentioning that the numerical values of the entries appearing in these matrices depend on the chosen polarization direction of the material.

The kinematic relations of the MEE plate are expressed through the strain-displacement, electric potential-electric field, and magnetic potential-magnetic field relationships:

$$\mathbf{S} = \mathbf{L}_u \mathbf{U}, \ \mathbf{E} = \mathbf{L}\varphi, \text{ and } \mathbf{H} = \mathbf{L}\psi, \tag{3}$$

where ϕ and ψ denote the electric and magnetic potentials, respectively. Moreover,

$$\mathbf{U} = \begin{Bmatrix} u_1 \\ u_2 \end{Bmatrix}, \ \mathbf{L}_u = \begin{bmatrix} \dfrac{\partial}{\partial x_1} & 0 & \dfrac{\partial}{\partial x_2} \\ 0 & \dfrac{\partial}{\partial x_2} & \dfrac{\partial}{\partial x_1} \end{bmatrix}^T, \text{ and } \mathbf{L} = \begin{Bmatrix} \dfrac{\partial}{\partial x_1} \\ \dfrac{\partial}{\partial x_2} \end{Bmatrix}. \tag{4}$$

During the manufacturing stage, the plate-strip is first subjected to a uniform static normal preload and subsequently brought into contact with a rigid half-space. Afterward, a time-dependent harmonic excitation of frequency ω, represented by $e^{i\omega t}$, acts on the system. Consequently, the analysis concerns wave propagation in a medium that already possesses an initial stress field.

The prestressed configuration is established under the assumptions that the initial load remains static and spatially uniform, and that the incremental deformations generated during dynamic motion are significantly smaller than the pre-existing

deformation state. Under these conditions, the framework of the three-dimensional linearized theory of elasticity with initial stresses (TLTESIS) is applicable, allowing nonlinear contributions associated with prestressing to be neglected.

Accordingly, the initial stress distribution is taken as

$$\sigma_{11}^{\ 0} = q, \text{ and } \sigma_{ij}^{\ 0} = 0 \text{ for } ij \neq 11, \tag{5}$$

where $i, j = 1, 2$. Here, q is a constant preload parameter associated with each layer, while the superscript "0" designates quantities evaluated in the initial equilibrium state.

Making use of the constitutive relations in Eq. (1), the initial electric displacement and magnetic induction induced by the prestress can be obtained as

$$d = \frac{e_{33}\left(c_{11}+c_{12}\right)-2c_{13}e_{31}}{c_{33}\left(c_{11}+c_{12}\right)-2c_{13}^{\ 2}}q \text{ and } b = \frac{f_{33}\left(c_{11}+c_{12}\right)-2c_{13}f_{31}}{c_{33}\left(c_{11}+c_{12}\right)-2c_{13}^{\ 2}}q, \tag{6}$$

The parameters d and b correspond to the initial electric displacement and initial magnetic induction generated by the applied prestress. These quantities quantify the electromechanical and magnetomechanical response of the MEE material arising from its intrinsic constitutive characteristics.

Assuming harmonic time dependence for all field variables, i.e., $g = \bar{g}\mathrm{e}^{\mathrm{i}\omega t}$, the common factor $e^{i\omega t}$ may be separated from the governing equations. In this notation, $\mathrm{i} = \sqrt{-1}$ is the imaginary unit, e denotes the exponential constant, and g represents any field quantity. The overbar indicates the corresponding amplitude. For computational convenience, dimensionless coordinates are introduced through $\hat{x}_i = x_i / h$. Thereafter, the hats and overbars are omitted for notational simplicity.

Under these assumptions, the governing equations describing the mechanical, electrical, and magnetic behavior of the MEE plate-strip are as follows (Maugin [20], Guz [21], and Fulin et al. [22]):

$$\sigma_{11,1} + \sigma_{12,2} + qu_{1,11} + \rho\omega^2 h^2 u_1 = 0, \tag{7.a}$$

$$\sigma_{21,1} + \sigma_{22,2} + qu_{2,11} + \rho\omega^2 h^2 u_2 = 0, \tag{7.b}$$

$$D_{1,1} + D_{2,2} + D_1^{\ 0} E_{1,1} + D_1^{\ 0} E_{2,2} = 0, \tag{7.c}$$

$$B_{1,1} + B_{2,2} + B_1^{\ 0} H_{1,1} + B_1^{\ 0} H_{2,2} = 0. \tag{7.d}$$

In these equations, σ_{ij} , D_i , B_i , u_i , E_i , and H_i denote the stress, electric displacement, magnetic induction, displacement, electric field, and magnetic field components, respectively, while ρ represents the mass density. Repeated indices imply summation according to Einstein notation, and a comma followed by an index denotes partial differentiation with respect to the corresponding spatial coordinate. The boundary and contact conditions adopted in the analysis are summarized below.

i-) Robin initial stress conditions

$$\left(\sigma_{11}+qu_{1,1}\right)\Big|_{x_1=\mp a^*}=0\,,\ \left(\sigma_{21}+qu_{2,1}\right)\Big|_{x_1=\mp a^*}=0\,, \tag{8.a}$$

$$\left(D_1+dE_1\right)\Big|_{x_1=\mp a^*}=0\,,\left(D_2+dE_2\right)\Big|_{x_1=\mp a^*}=0\,, \tag{8.b}$$

$$\left(B_1+bH_1\right)\Big|_{x_1=\mp a^*}=0\,,\ \left(B_2+bH_2\right)\Big|_{x_1=\mp a^*}=0\,, \tag{8.c}$$

ii-) Dynamic loading conditions

$$\sigma_{12}\big|_{x_2=0}=0\,,\ \sigma_{22}\big|_{x_2=0}=-p\delta\left(x_1\right),\ D_i\big|_{x_2=0}=0\,,\ B_i\big|_{x_2=0}=0\,, \tag{8.d}$$

iii-) Short circuit conditions

$$u_i\big|_{x_2=-1}=0\,,\ \varphi\big|_{x_2=0,-1}=0\,,\ \psi\big|_{x_2=0,-1}=0\,. \tag{8.e}$$

Here, p_0 denotes the amplitude of the applied external load, whereas $\delta(\cdot)$ is the Dirac delta distribution.

The boundary and contact conditions expressed in Eq. (8) dictate the mechanical, electrical, and magnetic interactions at the domain limits, carrying specific physical implications for the magneto-electro-elastic (MEE) plate-strip:

- Eq. (8.a)-Robin Mechanical Conditions: These expressions define the traction-free state at the lateral surfaces of the plate. The integration of the gradient terms $qu_{1,1}$ and $qu_{2,1}$ physically accounts for the geometric stiffness or softening effects. It shows how the initial static normal stress modulates the dynamic stress distribution during deformation.
- Eq. (8.b)& (8.c)-Robin-Type Electromagnetic Conditions: Correspondingly, these equations establish the effective electric displacement and magnetic

induction boundary constraints along the lateral edges. They mathematically represent how the baseline biasing electrical d and magnetic b fields, induced solely by the primary pre-stress, alter the dynamic electrical and magnetic flux balances across these boundaries.

- Eq. (8.d)-Dynamic Loading and Surface Insulation: This set governs the multi-physical load profile applied to the upper boundary. The condition $\sigma_{12}=0$ indicates a shear-free top surface. Meanwhile, $\sigma_{22}=-p_0\delta(x_1)$ models a time-harmonic, concentrated normal line load of magnitude p_0 acting strictly at the origin point. Furthermore, the constraints $D_i=0$ and $B_i=0$ mean that this surface is perfectly insulated against external free electric charges and magnetic fluxes, representing an open-circuit state.
- Eq. (8.e)-Short-Circuit and Potential Constraints: These conditions specify that both the upper and lower surfaces are electrically grounded (short-circuited, $\varphi=0$) and that the dynamic magnetic potential is forced to vanish ($\psi=0$). Physically, these boundaries serve as reference planes that confine the internal electric and magnetic fields within the MEE medium.

3. FINITE ELEMENT MODEL

In this section, a finite element framework is established to obtain an approximate numerical solution of the magneto-electro-elastic plate problem. The development of the formulation begins with the derivation of the weak form of the governing equations. To this end, let V denote the displacement test function, while Φ and Ψ represent the test functions associated with the electric and magnetic potentials, respectively. These functions are selected such that they satisfy the admissibility requirements imposed by the boundary and contact conditions of the problem.

Multiplying the governing equations, expressed in vector–matrix notation, by the corresponding test functions and integrating over the entire domain V, one obtains

$$0=\int_V\left[\mathbf{V}^T\left(\boldsymbol{\Sigma}+\boldsymbol{\Sigma}^0\mathbf{S}\right)_{,j}+\rho\omega^2h^2\mathbf{V}^T\mathbf{U}\right]dV+\int_V\boldsymbol{\Phi}^T\left(\mathbf{D}+\mathbf{D}^0\mathbf{E}^T\right)_{,i}dV+\int_V\boldsymbol{\Psi}^T\left(\mathbf{B}+\mathbf{B}^0\mathbf{H}^T\right)_{,i}dV, \tag{9}$$

where the notation "v" indicates quantities associated with the test functions.

By applying the Gauss–Ostrogradsky divergence theorem, the volume integrals involving spatial derivatives can be transformed into equivalent boundary and domain contributions. Consequently, Eq. (9) can be rewritten in the form

$$\begin{aligned}&\rho\omega^2 h^2 \int_V \mathbf{V}^T \mathbf{U} dV - \int_V \begin{bmatrix} \mathbf{S}_v{}^T \left(\boldsymbol{\Sigma} + \boldsymbol{\Sigma}^0 \mathbf{S}\right) + \mathbf{E}_v{}^T \left(\mathbf{D} + \mathbf{D}^0 \mathbf{E}^T\right) \\ + \mathbf{H}_v{}^T \left(\mathbf{B} + \mathbf{B}^0 \mathbf{H}^T\right) \end{bmatrix} dV \\ &= \int_\Gamma \begin{bmatrix} \mathbf{V}^T \left(\boldsymbol{\Sigma} + \boldsymbol{\Sigma}^0 \mathbf{S}\right) \cos\left(\mathbf{n}, x_j\right) + \boldsymbol{\Phi}^T \left(\mathbf{D} + \mathbf{D}^0 \mathbf{E}^T\right) \cos\left(\mathbf{n}, x_i\right) \\ + \boldsymbol{\Psi}^T \left(\mathbf{B} + \mathbf{B}^0 \mathbf{H}^T\right) \cos\left(\mathbf{n}, x_i\right) \end{bmatrix} d\Gamma \end{aligned}, \tag{10}$$

where $\mathbf{n}$ denotes the outward unit normal vector to the boundary and $\cos(n, x_i)$ represents the associated direction cosine.

Considering the decomposition of the boundary Γ together with the prescribed boundary-contact conditions introduced in Eq. (8), the weak form can be further simplified as

$$\int_V \begin{bmatrix} \mathbf{S}_v{}^T \left(\boldsymbol{\Sigma} + \boldsymbol{\Sigma}^0 \mathbf{S}\right) + \mathbf{E}_v{}^T \left(\mathbf{D} + \mathbf{D}^0 \mathbf{E}^T\right) + \mathbf{H}_v{}^T \left(\mathbf{B} + \mathbf{B}^0 \mathbf{H}^T\right) \\ -\rho\omega^2 h^2 \mathbf{V}^T \mathbf{U} \end{bmatrix} dV = \int_{\Gamma_2} \mathbf{V}^T \mathbf{f} d\Gamma_2 , \tag{11}$$

where the vector $\mathbf{f}$ arises from the externally applied dynamic loading conditions. Thus, the weak formulation governing the present problem is obtained.

Having established the weak statement, the variational form of the problem is constructed through Hamilton's principle together with the principle of virtual work [23]. Replacing the test functions by their corresponding virtual quantities yields

$$\int_V \begin{bmatrix} \delta\mathbf{S}^T \left(\boldsymbol{\Sigma} + \boldsymbol{\Sigma}^0 \mathbf{S}\right) + \delta\mathbf{E}^T \left(\mathbf{D} + \mathbf{D}^0 \mathbf{E}^T\right) \\ + \delta\mathbf{H}^T \left(\mathbf{B} + \mathbf{B}^0 \mathbf{H}^T\right) - \rho\omega^2 h^2 \delta\mathbf{U}^T \mathbf{U} \end{bmatrix} dV = \int_{\Gamma_2} \delta\mathbf{U}^T \mathbf{f} d\Gamma_2 \tag{12}$$

Substituting the constitutive relations given previously in Eq. (2) into Eq. (12) allows the problem to be expressed through a total potential functional. Accordingly,

$$\delta\left(\omega^2 \boldsymbol{K} - \boldsymbol{P} - \boldsymbol{M}\right) = 0 , \tag{13}$$

where K , P , and M denote the kinetic energy, total potential energy, and external work functional, respectively.

To discretize the problem, a nine-node quadrilateral finite element is adopted. For each node, four independent degrees of freedom are considered, namely two mechanical displacement components, one electric potential, and one magnetic potential. Let V_h denote the finite element partition of the computational domain such that

$$V_h \subset V \text{ , } V_{h_1} \cap V_{h_2} = \varnothing \text{, and } V = \bigcup V_h \text{.} \tag{14}$$

Within this discretized framework, the displacement field, electric field, magnetic field, and their virtual counterparts are approximated by nodal interpolation functions. Accordingly,

$$\mathbf{U}^h = \mathbf{N}_u \mathbf{U}^{eh} \text{, } \mathbf{E}^h = \mathbf{N}\mathbf{E}^{eh} \text{, } \mathbf{H}^h = \mathbf{N}H^{eh} \text{,} \tag{15.a}$$

$$\delta\mathbf{U}^h = \mathbf{N}_u \delta\mathbf{U}^{eh} \text{, } \delta\mathbf{E}^h = \mathbf{N}_\varphi \delta\mathbf{E}^{eh} \text{, and } \delta\mathbf{H}^h = \mathbf{N}\delta\mathbf{H}^{eh} \text{.} \tag{15.b}$$

The corresponding nodal vectors and matrices are defined as

$$\mathbf{U}^e = \begin{bmatrix} u_{ui} \end{bmatrix}^T = \begin{bmatrix} u_{1i} & u_{2i} \end{bmatrix}^T \text{, } \mathbf{E}^e = \begin{bmatrix} E_{\varphi i} \end{bmatrix}^T = \begin{bmatrix} E_{1i} & E_{2i} \end{bmatrix}^T \text{,} \tag{16.a}$$

$$\mathbf{H}^e = \begin{bmatrix} H_{\psi i} \end{bmatrix}^T = \begin{bmatrix} H_{1i} & H_{2i} \end{bmatrix}^T \text{, } \mathbf{N}_u = \begin{bmatrix} N_{u1} & N_{u2} & \dots & N_{u9} \end{bmatrix} \text{,} \tag{16.b}$$

$$N_{ui} = n_i I_u \text{, and } \mathbf{N} = \begin{bmatrix} n_1 & n_2 & \dots & n_9 \end{bmatrix} \text{.} \tag{16.c}$$

Here, u_i represents the nodal displacement vector, E_i the nodal electric potential variable, H_i the nodal magnetic potential variable, and n_i the interpolation (shape) function associated with the i th node. The matrix I_u denotes the identity matrix. The dimensions of the shape-function matrices are 3×27 for $\mathbf{N}_u$ and 1×9 for $\mathbf{N}$.

The interpolation functions employed in the present study correspond to the standard quadratic Lagrange family commonly used for nine-node isoparametric finite elements, as described by Hutton [24].

Using these interpolations, the strain vector $\mathbf{S}^h$, the electric field vector $\mathbf{E}^h$ and the magnetic field vector $\mathbf{H}^h$ may be expressed directly in terms of the nodal

displacement vector $\mathbf{U}^h$, the nodal electric potential φ^e, and the nodal magnetic potential ψ^e respectively. Therefore,

$$\mathbf{S}^h = \mathbf{L}_u \mathbf{N}_u \mathbf{U}^{eh} = \mathbf{B}_u \mathbf{U}^{eh},\ \mathbf{E}^h = \mathbf{L}\mathbf{N}\varphi^{eh} = \mathbf{B}\varphi^{eh}, \text{ and } \mathbf{H}^h = \mathbf{L}\mathbf{N}\psi^{eh} = \mathbf{B}\psi^{eh}, \quad (17)$$

In these expressions, $\mathbf{B}_u$ and $\mathbf{B}$ are the strain–displacement type matrices that govern the internal force calculations. Their matrix forms are

$$\mathbf{B}_u = \begin{bmatrix} B_{u1} & B_{u2} & \dots & B_9 \end{bmatrix},\ \mathbf{B} = \begin{bmatrix} B_1 & B_2 & \dots & B_9 \end{bmatrix}, \quad (18.a)$$

$$\begin{bmatrix} B_{ui} \end{bmatrix} = \begin{bmatrix} \dfrac{\partial n_i}{\partial x_1} & 0 & \dfrac{\partial n_i}{\partial x_2} \\ 0 & \dfrac{\partial n_i}{\partial x_2} & \dfrac{\partial n_i}{\partial x_1} \end{bmatrix}^T, \text{ and } \begin{bmatrix} B_i \end{bmatrix} = \begin{bmatrix} \dfrac{\partial n_i}{\partial x_1} & \dfrac{\partial n_i}{\partial x_2} \end{bmatrix}^T. \quad (19.b)$$

To facilitate the assembly procedure and ensure compatibility between local and global coordinate systems, the element formulation is expressed in normalized coordinates. The shape functions are initially defined in terms of the local Cartesian coordinates x_1^e and x_2^e. Employing the isoparametric concept, these coordinates are represented through the natural coordinates (r,s) according to

$$\mathbf{x}^e = \sum_{i=1}^{9} N_i(p,r,s)\,\mathbf{x}_i^e,\ \mathbf{x}^e = \begin{bmatrix} \mathbf{x}_1^e & \mathbf{x}_2^e \end{bmatrix}^T, \text{ and } \mathbf{x}_i^e = \begin{bmatrix} \mathbf{x}_{i1}^e & \mathbf{x}_{i2}^e \end{bmatrix}^T, \quad (20)$$

where the nodal coordinates of the parent element are denoted by x_i^e.

Because the finite elements considered here possess smooth geometries, the determinant of the Jacobian matrix $\mathbf{J}$ remains positive throughout the element domain. Consequently, the Jacobian is nonsingular and therefore invertible. This property allows the parent element geometry to be mapped onto the standard square domain $\tilde{V} = [-1,1] \times [-1,1]$.

Substituting the isoparametric relations into the variational formulation yields the element-level matrix equation

$$\delta\left(\frac{1}{2}\int_{\tilde{V}}\begin{bmatrix}\omega^2\left(\mathbf{U}^{eh}\right)^T\tilde{\mathbf{M}}_{uu}{}^e\mathbf{U}^{eh}-\left(\mathbf{U}^{eh}\right)^T\tilde{\mathbf{K}}_{uu}{}^e\mathbf{U}^{eh}\\ -\left(\mathbf{U}^{eh}\right)^T\tilde{\mathbf{K}}_{u\varphi}{}^e\varphi^{eh}-\varphi^{eh}\tilde{\mathbf{K}}_{\varphi u}{}^e\mathbf{U}^{eh}\\ -\left(\mathbf{U}^{eh}\right)^T\tilde{\mathbf{K}}_{u\psi}{}^e\psi^{eh}-\psi^{eh}\tilde{\mathbf{K}}_{\psi u}{}^e\mathbf{U}^{eh}\\ -\varphi^{eh}\tilde{\mathbf{K}}_{\varphi\psi}{}^e\psi^{eh}-\varphi^{eh}\tilde{\mathbf{K}}_{\varphi\psi}{}^e\psi^{eh}\\ -\varphi^{eh}\tilde{\mathbf{K}}_{\varphi\varphi}{}^e\varphi^{eh}-\psi^{eh}\tilde{\mathbf{K}}_{\psi\psi}{}^e\psi^{eh}\end{bmatrix}|\mathbf{J}|\,dV-\int_{\tilde{\Gamma}_2}\left(\mathbf{U}^{eh}\right)^T\tilde{\mathbf{F}}^e|\mathbf{J}|\,d\tilde{\Gamma}_2\right)=0, \tag{21}$$

where

$$\tilde{\mathbf{M}}_{uu}{}^e=\rho h^2\mathbf{N}_u{}^T\mathbf{N}_u, \tag{22.a}$$

$$\tilde{\mathbf{K}}_{uu}{}^e=\mathbf{B}_u{}^T\left([C]+\boldsymbol{\Sigma}^0\right)\left([C]+\boldsymbol{\Sigma}^0\right)^T\mathbf{B}_u, \tag{22.b}$$

$$\tilde{\mathbf{K}}_{u\varphi}{}^e=\mathbf{B}_u{}^T\left([C]+\boldsymbol{\Sigma}^0\right)\left([e]+\frac{1}{2}\left(\mathbf{D}^0\right)^T\right)\tilde{\mathbf{B}}, \tag{22.c}$$

$$\tilde{\mathbf{K}}_{\varphi u}{}^e=\tilde{\mathbf{B}}^T\left([e]^T+\frac{1}{2}\mathbf{D}^0\right)^T\left([C]+\boldsymbol{\Sigma}^0\right)^T\mathbf{B}_u, \tag{22.d}$$

$$\tilde{\mathbf{K}}_{u\psi}{}^e=\mathbf{B}_u{}^T\left([C]+\boldsymbol{\Sigma}^0\right)\left([f]+\frac{1}{2}\left(B^0\right)^T\right)\tilde{\mathbf{B}}, \tag{22.e}$$

$$\tilde{\mathbf{K}}_{u\psi}{}^e=\tilde{\mathbf{B}}^T\left([f]^T+\frac{1}{2}B^0\right)\left([C]+\boldsymbol{\Sigma}^0\right)^T\mathbf{B}_u{}^T, \tag{22.f}$$

$$\tilde{\mathbf{K}}_{\varphi\psi}{}^e=\tilde{\mathbf{B}}^T\left([e]^T+\frac{1}{2}\mathbf{D}^0\right)^T\left([f]^T+\frac{1}{2}B^0\right)\tilde{\mathbf{B}}, \tag{22.g}$$

$$\tilde{\mathbf{K}}_{\psi\varphi}{}^e=\tilde{\mathbf{B}}^T\left([f]^T+\frac{1}{2}B^0\right)^T\left([e]^T+\frac{1}{2}\mathbf{D}^0\right)\tilde{\mathbf{B}}, \tag{22.h}$$

$$\tilde{\mathbf{K}}_{\varphi\varphi}{}^e=\tilde{\mathbf{B}}^T[\gamma][\gamma]\tilde{\mathbf{B}},\ \tilde{\mathbf{K}}_{\psi\psi}{}^e=\tilde{\mathbf{B}}^T[\psi][\psi]\tilde{\mathbf{B}}, \text{ and } \tilde{\mathbf{F}}^e=\mathbf{N}_u{}^T\mathbf{f}. \tag{22.i}$$

The matrix $\tilde{\mathbf{K}}_{uu}{}^e$ corresponds to the elemental mechanical stiffness matrix, while $\tilde{\mathbf{K}}_{u\varphi}{}^e$ and $\tilde{\mathbf{K}}_{\varphi u}{}^e$ describe the electroelastic coupling effects. Similarly, $\tilde{\mathbf{K}}_{u\psi}{}^e$ and $\tilde{\mathbf{K}}_{\psi u}{}^e$ characterize the magnetoelastic interactions. The matrices $\tilde{\mathbf{K}}_{\varphi\psi}{}^e$ and $\tilde{\mathbf{K}}_{\varphi\psi}{}^e$

account for magnetoelectric coupling. Furthermore, $\tilde{\mathbf{K}}_{\varphi\varphi}{}^{e}$ and $\tilde{\mathbf{K}}_{\psi\psi}{}^{e}$ denote the electric and magnetic coefficient matrices, respectively. The matrix $\tilde{\mathbf{M}}_{uu}{}^{e}$ represents the elemental mass matrix, whereas $\tilde{\mathbf{F}}^{e}$ is the elemental load vector.

Rearranging the terms of Eq. (22) with respect to the unknown nodal quantities leads to the following system of algebraic equations at the element level:

$$\left(\mathbf{K}_{uu}{}^{e}-\omega^{2}\mathbf{M}_{uu}{}^{e}\right)\mathbf{U}^{eh}+\mathbf{K}_{u\varphi}{}^{e}\boldsymbol{\varphi}^{eh}+\mathbf{K}_{u\psi}{}^{e}\boldsymbol{\psi}^{eh}=\mathbf{F}^{e}, \tag{23.a}$$

$$\mathbf{K}_{\varphi u}{}^{e}\mathbf{U}^{eh}+\mathbf{K}_{\varphi\varphi}{}^{e}\boldsymbol{\varphi}^{eh}+\mathbf{K}_{\varphi\psi}{}^{e}\boldsymbol{\psi}^{eh}=0, \tag{23.b}$$

$$\mathbf{K}_{\psi u}{}^{e}\mathbf{U}^{eh}+\mathbf{K}_{\varphi\psi}{}^{e}\boldsymbol{\psi}^{eh}+\mathbf{K}_{\psi\psi}{}^{e}\boldsymbol{\psi}^{eh}=0. \tag{23.c}$$

Here, the matrix $\mathbf{K}_{uu}{}^{e}$ denotes the local stiffness contribution, while $\mathbf{K}_{u\varphi}{}^{e}$ and $\mathbf{K}_{\varphi u}{}^{e}$ represent the local electro-elastic coupling matrices. Similarly, $\mathbf{K}_{u\psi}{}^{e}$ and $\mathbf{K}_{\psi u}{}^{e}$ stand for the local magneto-elastic coupling matrices, and $\mathbf{K}_{\varphi\psi}{}^{e}$ along with $\mathbf{K}_{\psi\varphi}{}^{e}$ correspond to the local magneto-electric coupling matrices. The term $\mathbf{K}_{\varphi\varphi}{}^{e}$ is the local electric stiffness matrix, and $\mathbf{K}_{\psi\psi}{}^{e}$ is the local magnetic stiffness matrix. Additionally, $\mathbf{M}_{uu}{}^{e}$ is the local mass matrix, and $\mathbf{F}^{e}$ is the local nodal force vector. It is important to observe that the following symmetry relations hold: $\mathbf{K}_{u\varphi}{}^{e}$ and $\mathbf{K}_{\varphi u}{}^{e}$ are symmetric with respect to each other; likewise, $\mathbf{K}_{u\psi}{}^{e}$ and $\mathbf{K}_{\psi u}{}^{e}$ are symmetric; and $\mathbf{K}_{\varphi\psi}{}^{e}$ together with $\mathbf{K}_{\psi\varphi}{}^{e}$ also satisfy the same property. In mathematical terms, this means:

$$\mathbf{K}_{u\varphi}{}^{e}=\left[\mathbf{K}_{\varphi u}{}^{e}\right]^{T},\ \mathbf{K}_{u\psi}{}^{e}=\left[\mathbf{K}_{\psi u}{}^{e}\right]^{T},\ \text{and}\ \mathbf{K}_{\varphi\psi}{}^{e}=\left[\mathbf{K}_{\varphi\psi}{}^{e}\right]^{T}. \tag{24}$$

At this stage, we have derived the local algebraic system of equations defined over the master element, which is presented in Eq. (23). Moreover, Eq. (24) demonstrates that the resulting solution matrix is real, symmetric, and positive definite. This property guarantees that Eq. (23) admits a unique solution. As noted earlier, the numerical quantities to be computed are expected to follow a standard pattern. Hence, these local numerical values obtained on the master element can be mapped to their corresponding positions in the global system through an appropriate node-based transformation. Following this comprehensive procedure, we finally obtain the global system of equations given below:

$$\left\{\tilde{\mathbf{K}}_{uu}-\omega^2\tilde{\mathbf{M}}_{uu}\right\}\tilde{\mathbf{U}}+\tilde{\mathbf{K}}_{u\varphi}\tilde{\mathbf{\Phi}}+\tilde{\mathbf{K}}_{u\psi}\mathbf{\Psi}=\tilde{\mathbf{F}}_{u}\,, \tag{25.a}$$

$$\tilde{\mathbf{K}}_{\varphi u}\tilde{\mathbf{U}}+\tilde{\mathbf{K}}_{\varphi\varphi}\tilde{\mathbf{\Phi}}+\tilde{\mathbf{K}}_{u\psi}\mathbf{\Psi}=0\,, \tag{25.b}$$

$$\tilde{\mathbf{K}}_{\psi u}\tilde{\mathbf{U}}+\tilde{\mathbf{K}}_{\varphi\psi}\tilde{\mathbf{\Phi}}+\tilde{\mathbf{K}}_{\psi\psi}\mathbf{\Psi}=0\,, \tag{25.c}$$

The boldface symbols denote the assembled global counterparts of the corresponding elemental matrices.

It should be emphasized that the assembled system remains real and symmetric; however, it is not initially positive definite due to the imposed boundary-contact constraints introduced in Eq. (8). Moreover, examination of the loading conditions reveals that only a limited number of entries of the global force vector are nonzero.

To overcome these numerical difficulties, a mesh-refinement procedure is applied. After refinement, the resulting algebraic system becomes symmetric, real, and positive definite. Consequently, the unknown displacement, electric potential, and magnetic potential fields can be determined uniquely.

Finally, once the primary nodal variables have been obtained, the constitutive equations are employed to recover the secondary field quantities, including stresses, electric displacements, and magnetic induction components. In this way, the complete numerical solution of the magneto-electro-elastic problem is achieved.

Acknowledgements. The Scientific and Technical Research Council of Turkey (TUBITAK) funded this work under project no 125M293.

REFERENCES

1- Ke, L.-L., & Wang, Y.-S. (2014). Free vibration of size-dependent magneto-electro-elastic nanobeams based on the nonlocal theory. Physica E: Low-Dimensional Systems and Nanostructures, 63, 52–61.

2-Lim, C. W., Zhang, G., & Reddy, J. N. (2015). A higher-order nonlocal elasticity and strain gradient theory and its applications in wave propagation. Journal of the Mechanics and Physics of Solids, 78, 298–313.

3-Jandaghian, A. A., & Rahmani, O. (2016). Free vibration analysis of magneto-electro-thermo-elastic nanobeams resting on a Pasternak foundation. Smart Materials and Structures, 25(3), 035023.

4-Trinh, L. C., Nguyen, H. X., Vo, T. P., & Nguyen, T.-K. (2016). Size-dependent behaviour of functionally graded microbeams using various shear deformation theories based on the modified couple stress theory. Composite Structures, 154, 556–572.

5-Ebrahimi, F., Jafari, A., & Barati, M. R. (2017). Vibration analysis of magneto-electro-elastic heterogeneous porous material plates resting on elastic foundations. Thin-Walled Structures, 119, 33–46.

6-Kiran, M. C., & Kattimani, S. C. (2018). Free vibration and static analysis of functionally graded skew magneto-electro-elastic plate. Smart Structures and Systems, 21(4), 493–519.

7-Sahmani, S., & Aghdam, M. M. (2018). Nonlocal strain gradient shell model for axial buckling and postbuckling analysis of magneto-electro-elastic composite nanoshells. Composites Part B: Engineering, 132, 258–274.

8-Ebrahimi, F., Barati, M. R., & Mahesh, V. (2019). Dynamic modeling of smart magneto-electro-elastic curved nanobeams. Advances in Nano Research, 7(3), 145–156.

9-Habibi, B., Beni, Y. T., & Mehralian, F. (2019). Free vibration of magneto-electro-elastic nanobeams based on modified couple stress theory in thermal environment. Mechanics of Advanced Materials and Structures, 26, 601–613.

10-Sahmani, S., & Khandan, A. (2019). Size dependency in nonlinear instability of smart magneto-electro-elastic cylindrical composite nanopanels based upon nonlocal strain gradient elasticity. Microsystem Technologies, 25, 2171–2186.

11-Milan, A. G., & Ayatollahi, M. (2020). Transient analysis of multiple interface cracks between two dissimilar functionally graded magneto-electro-elastic layers. Archive of Applied Mechanics, 90(8), 1829–1844.

12-Hong, J., Wang, S., Zhang, G., & Mi, C. (2021). On the bending and vibration analysis of functionally graded magneto-electro-elastic Timoshenko microbeams. Crystals, 11(10), 1206.

13-Danesh, H., & Javanbakht, M. (2022). Free vibration analysis of nonlocal nanobeams: A comparison of the one-dimensional nonlocal integral Timoshenko beam theory with the two-dimensional nonlocal integral elasticity theory. Mathematics and Mechanics of Solids, 27, 557–576.

14- Sui, Y., Wang, W., & Zhang, H. (2022). Effects of electromagnetic fields on the contact of magneto-electro-elastic materials. International Journal of Mechanical Sciences, 223, 107283.

15-Zhou, L., & Qu, F. (2023). The magneto-electro-elastic coupling isogeometric analysis method for the static and dynamic analysis of magneto-electro-elastic structures under thermal loading. Composite Structures, 315, 116984.

16-Van Ke, T., Van Minh, P., Dung, N. T., et al. (2024). Flexoelectric effect on bending and free vibration behaviors of piezoelectric sandwich FGP nanoplates via nonlocal strain gradient theory. Journal of Vibration Engineering & Technologies, 12, 6567–6596.

17-Van Thom, D., Van Minh, C., Van Minh, P., et al. (2024). Mechanical responses of nanoplates resting on viscoelastic foundations in multi-physical environments. European Journal of Mechanics-A/Solids, 106, 105309.

18-Wang, J., Zhou, L., & Chai, Y. (2024). The adaptive hygrothermo–magneto–electro–elastic coupling improved enriched finite element method for functionally graded magneto–electro–elastic structures. Thin-Walled Structures, 200, 111970.

19-Yang, J. (2024). Theory of electromagnetoelasticity. World Scientific.

20-Maugin, G. A. (1988). Continuum mechanics of electromagnetic solids. North-Holland.

21-Guz, A. N. (1973). Stability of elastic bodies under finite deformations. Naukova Dumka.

22-Fulin, S., Zikun, W., & Zhonghua, L. (1997). An exact analysis of thermal buckling of piezoelectric laminated plates. Acta Mech. Solida Sin, 10(2), 95-107.

23-Zienkiewicz, O. C. and Taylor, R. L. (1989) The finite element method, basic formulation and linear problems. McGraw-Hill, London

24-Hutton, D. (2004) Fundamentals of finite element analysis. McGraw-Hills, New York, pp 191–192

CHAPTER -2

SUSTAINABILITY OPTIMIZATION OF SODIUM-ION, LITHIUM-ION AND SOLID-STATE BATTERY SYSTEMS FOR FUTURE ELECTRIC PLATFORMS

Majid MONAJJEMI[1], Aybaba HANÇERLİOĞULLARI[2]
Rezvan REZAIZADEH[3], İlknur ŞAHİN[4], Fatemeh MOLLAAMIN[5]

1. INTRODUCTION

Sodium-ion, Lithium-ion and Solid-state batteries are three main technologies addressing different needs in energy storage. Lithium-ion batteries, with their high energy density, are standard in electric vehicles, while sodium-ion batteries stand out as an economical alternative due to their low cost and abundant raw materials . Solid-state batteries, with their non-flammable structure and very high energy density, are seen as the safe, long-range battery technology of the future. Lithium-ion batteries operate through the reversible movement of Li^+ ions between the anode and cathode during charging and discharging. During discharge, lithium ions leave the anode and migrate through the electrolyte toward the cathode, while electrons flow through the external circuit and deliver useful electrical energy. During charging, this process is reversed [1,2].Lithium-ion batteries are the cornerstone of current technology, offering high energy density and long lifespan. Specifically, lithium-ion batteries are lightweight, offer high energy density in a small space, and have a long charging cycle life of 2000-5000+ cycles. However, raw materials are quite expensive, rare, and carry a fire risk due to the liquid electrolyte. In terms of applications, they offer significant advantages in electric vehicles, smartphones, and laptops. Sodium-ion batteries offer a cheaper and more sustainable alternative to lithium-ion batteries. Na-ion batteries, whose raw material is salt, are environmentally friendly, low-cost, offer fast charging, and provide better

[1] *Prof. Dr., Department of Biologica/Faculty of Science, Kastamonu University, Turkey, mmonajjemi@kastamonu.edu.tr, (ORCID: 0000-0002-6665-837X)
[2] Prof. Dr., Department of Physisc/Faculty of Science, Kastamonu University, Turkey, aybaba@kastamonu.edu.tr, (ORCID: 0000-0000-1700-8480)
[3] Assist.Prof. Dr., Department of Enginering/Faculty of Basic Science, University of Applied Science, Iran, r.rezaeizade@gmail.com , (ORCID: 0000-0001-6219-6174)
[4] PhD, Department of Mathematics and Science Education, Faculty of Graduate School of Natural and Applied Sciences, Middle East Technical University, Türkiye. ilknurs@metu.edu.tr, (0000-0002-4383-3817)
[5] Accos.Prof. Dr., Department of Biomedical Enginnering/Faculty of Enginnering andArchitecture,KastamonuUniversity,Turkey,fmollaamin@kastamonu.edu.tr,(ORCID: 0000-0002-6896-336X)

performance in cold weather. However, their disadvantages include lower energy density compared to lithium, and therefore they can be heavier/larger. In terms of applications, they are widely used in energy storage systems (ESS), low-range electric vehicles, and electric bicycles. 3. Solid-state batteries are a new generation technology that uses a solid electrolyte instead of a liquid electrolyte. Their advantages include high safety, non-flammability, much higher energy density compared to liquid electrolyte batteries, and faster charging. However, some disadvantages include high production costs and difficulties in mass production with current technology. They are widely used in high-performance electric vehicles, aviation, and high-end electronic devices.For graphite anode, the simplified discharge reaction can be written as,

$$Li_xC_6 \rightarrow C_6 + xLi^{+} + xe^{-}$$

During charging, the reverse reaction occurs,

$$C_6 + xLi^{+} + xe^{-} \rightarrow Li_xC_6$$

These reactions describe the insertion and extraction of lithium ions within the layered structure of graphite. On the cathode side, layered oxides such as NMC and NCA, or olivine-type materials such as LFP, reversibly host lithium ions within their crystal structures [2, 3]. The performance of a lithium-ion cell depends not only on the theoretical capacity of the active materials but also on electrolyte conductivity, electrode porosity, electrode thickness, ion diffusion, electronic conductivity, interfacial stability, operating temperature, and current density [5,17].The success of lithium-ion batteries in electric vehicles is mainly associated with their relatively high energy density. Gravimetric energy density can be expressed as;

$$Ed = m/E$$

Where, Ed is the specific energy, E the stored energy, and m is the battery mass. Higher energy density allows a vehicle to store more usable energy for a given battery mass, which can increase driving range. However, vehicle range is not determined by battery capacity alone. Aerodynamics, vehicle mass, tire rolling resistance, motor-inverter efficiency, thermal management, driving profile, and battery management algorithms also play decisive roles [16,18].The driving range of an electric vehicle may be expressed in simplified form as;

$$R = E_{use} / e_c$$

Where, R is the driving range, E_{use} the usable battery energy, and ec is the energy consumption per unit distance. For instance, if a vehicle has 60 kWh of usable battery energy and consumes 15 kWh/100 km, its approximate range is 400 km. If the same vehicle reduces its consumption to 12kWh/100 km through aerodynamic improvement, mass reduction, efficient thermal management, and optimized power electronics, the range may increase to approximately 500 km. This example shows that range extension is a complete vehicle optimization problem, not merely a battery-capacity problem [16,18].

2. PHYSICAL BACIS OF SODIUM-ION BATTERIES

Sodium ion (Na-ion) batteries offer an economical alternative to lithium, using sodium salt, which is more abundant and cheaper in nature. Compared to lithium technology, they are cheaper, perform better in extreme cold, and are safer. However, their energy density is lower; meaning a larger and heavier battery is needed to obtain the same power. They are widely used in inexpensive city vehicles where range is not critical, and in home energy storage systems.One of the most important advantages of solid-state batteries is their potential compatibility with lithium metal anodes. Lithium metal has a much higher theoretical capacity than graphite, and its use could significantly increase battery energy density [11, 12]. However, this advantage depends strongly on the stability of the interface between the lithium metal anode and the solid electrolyte [13-15]Solid electrolytes can be broadly classified into sulfide-based, oxide-based, polymer-based, and composite systems. Sulfide electrolytes may provide high ionic conductivity and favorable mechanical contact, but they are often sensitive to moisture and may require careful processing [14]. Oxide electrolytes generally exhibit high chemical and thermal stability, but their rigidity and brittleness can make interfacial contact more difficult [13-15]. Polymer electrolytes are flexible and processable, but their ionic conductivity at room temperature may be insufficient for high-power applications [12,13]

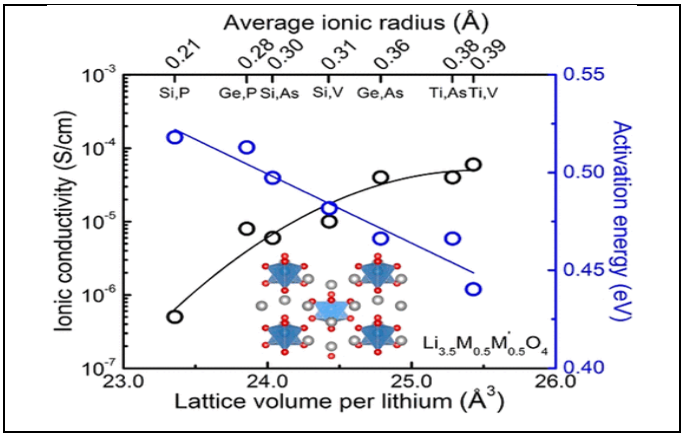

Figure1. Lithium ions motion in the crystal stucture [11-15]

Despite these challenges, solid-state batteries are considered among the most important future technologies for electric aircraft, long-range electric vehicles, high-safety defense platforms, and submarine auxiliary power systems [11-21].

In figure -1 shows the relationship between the movement of lithium ions and the crystal structure properties. The X-axis represents the lattice volume per lithium ion, indicating how much free space is available for Li in the crystal, the Y-axis describes ionic conductivity on the right side, and activation energy on the left side. In Figure 1, as the lattice volume increases, ionic conductivity increases, while activation energy decreases. As the area in which lithium ions move in the crystal increases, the ions move more easily, and the material becomes a better ion conductor.

3. PHYSCIAL PARAMETER OF ELECTRIC VEHICLE RANGE

The range of an electric vehicle is not determined by battery capacity alone. During operation, the energy stored in the battery is consumed by rolling resistance, aerodynamic drag, acceleration, climbing resistance, thermal loads, auxiliary systems, and internal battery losses [16,18].A simplified expression for total energy(Etotal) demand may be written as;

$$E_{total}=E_{rolling}+E_{drag}+E_{acceleration+}E_{grade}+E_{thermal+}E_{auxiliary}$$

Rolling resistance is given by, where Cr is the rolling resistance coefficient, mis vehicle G gravitational forces, as vehicle mass increases, rolling resistance also increases.Therefore, increasing battery size can improve range, but the added mass also increases energy consumption. This demonstrates that range optimization is a nonlinear engineering problem [16].

$$Rr=Cr\ Xg$$

Aerodynamic drag $(A_d)=12\rho CdAv^2$ and the power required to overcome aerodynamic $(A_d)==21\rho CdAv^2$ are given. his relation is highly significant because it shows that the power required to overcome air resistance increases with the cube of vehicle speed. Therefore, at high speeds, driving range may decrease substantially even if the battery capacity is large. Low drag coefficients, optimized body geometry, smooth underbody design, active aerodynamic elements, and efficient wheel design are therefore critical for improving range. Internal battery losses can be expressed as;

$$P_{loss}=I^2R_j$$

Where, I is the current and R_j is the internal resistance of the battery. Since heat generation increases with the square of current, aggressive acceleration, high-speed

driving, heavy loads, and fast charging can significantly increase thermal losses. Reducing internal resistance through improved electrode design, stable interfaces, low-resistance current collectors, and effective thermal management increases usable energy and supports longer range [5,17-19]. Increasing the driving range of an electric vehicle requires the simultaneous optimization of battery chemistry, pack design, vehicle dynamics, thermal management, and control software. Simply increasing battery size is often insufficient because larger battery packs increase vehicle mass, cost, and thermal complexity [16, 18]. The battery management system is the electronic and software-based control unit responsible for ensuring safe, efficient, and durable operation of a battery pack. The BMS continuously monitors cell voltage, current, temperature, state of charge, state of health, cell imbalance, internal resistance, and safety limits [16,18]. In electric vehicles, the BMS is not merely a protection device; it is a core control system that affects range, performance, safety, and lifetime.One of the most important functions of BMS is state-of-charge estimation, which indicates the remaining usable energy in the battery. State-of-health estimation, on the other hand, evaluates how much the battery has degraded compared with its original condition. Incorrect SOC or SOH estimation can lead to inaccurate range prediction, excessive safety margins, premature power limitation, or unsafe operation [18]. Big data analytics and machine learning are transforming battery management from rule-based monitoring into predictive and adaptive control. Battery cycle life can be predicted from early-cycle data, providing an important methodology for accelerating battery testing and lifetime estimation [19-21].Future battery engineering wouldnt be limited to cell chemistry. It wouldnt require real-world usage data, digital twin models, predictive maintenance, rapid charging optimization, thermal event detection, recycling planning, and fleet-level energy analytics [18-21]. In Figure -2 sho that motion of Internal and ion transport pathways of sodium-based batteries.,

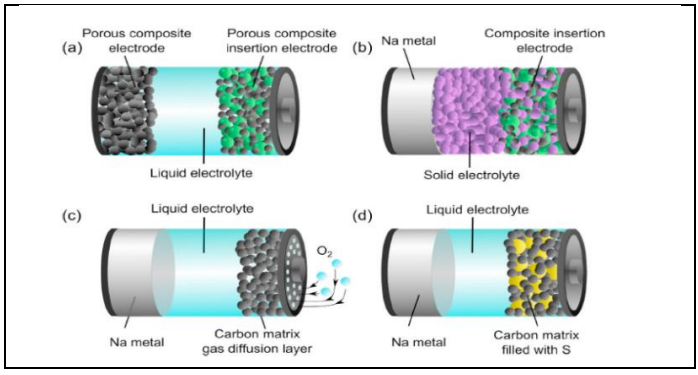

Figure 2. Internal and ion transport pathways of sodium batteries[18- 21].

(a) Liquid electrolyte porous additive electrode, there is a liquid electrolyte between two electrodes. Ions move within the liquid, similar to classic battery structure. (b) Solid electrolyte structureThere is a solid electrolyte in the middle. Sodium metal is used as the anode on the left side. It aims for a safer and higher energy density. (c) Na-O_2 (sodium-air) cell There is a carbon matrix and a gas diffusion layer. Oxygen comes from the external environment. A high theoretical energy density is aimed for. (d) Na-S (sodium-sulfur) cellThe carbon matrix is filled with sulfur. Sodium and sulfur react to store energy.

Table 1. Lithium-Ion, Sodium-Ion, and Solid-State Batteries[18- 21].

Criterion	Lithium-Ion	Sodium-Ion	Solid-State
Technology maturity	High	Developing / early commercial	Pilot / developing
Energy density	High	Medium	Very high potential
Raw material risk	Lithium, nickel, cobalt dependence	Lower critical metal pressure	Depends on materials
Safety	Chemistry-dependent	Good potential	Very high potential
Cold-weather performance	Variable	Strong potential	Electrolyte-dependent
Long-range EV suitability	Very suitable	Limited / medium	Highly promising
Stationary storage	Suitable	Very suitable	Limited by cost
Defense logistics	Suitable but critical-metal dependent	Strategically advantageous	Suitable for critical missions
Sustainability	Recycling-dependent	Strong potential	Material- and process-dependent
Criterion	Lithium-Ion	Sodium-Ion	Solid-State
Energy density	High	Medium	Very high potential
Cost	Medium to high	Low-cost potential	Currently high

In table-1 shows that the three technologies are not simple substitutes for one another. Instead, they offer complementary solutions for different mission profiles. Lithium-ion batteries will remain dominant in the short and medium term due to their high energy density and manufacturing maturity [1-4]. Sodium-ion batteries are expected to grow in low-cost mobility, stationary storage, and supply-secure applications [7-10]. Solid-state batteries are likely to become increasingly important for high-safety and high-energy strategic platforms [11-15]. Lithium-ion batteries will remain the dominant technology for long-range electric vehicles in the short and medium term because of their high energy density and commercial maturity [1-4].

4. CONCLUSION AND DISCUSSION

This technological race in the world of energy storage isn't actually a race to declare a single winner; rather, it's the beginning of a new era where each technology will find its own niche. While lithium-ion batteries are everywhere in our lives today, raw material costs and safety concerns are pushing us towards new solutions. In this context, sodium-ion batteries represent the power of what is "cheap and accessible," while solid-state batteries symbolize the safest and most powerful limit that technology can reach. Sodium-ion batteries have strategic importance for stationary energy storage, affordable electric vehicles, short-range platforms, and military logistics because of their potential for lower cost, abundant raw materials, and improved supply-chain security [7-10].Solid-state batteries are promising candidates for electric aircraft, UAVs, submarine auxiliary power systems, and high-value defense platforms because of their potential for high safety and high energy density [11-15].Increasing electric vehicle range requires more than increasing battery capacity. Aerodynamics, vehicle mass, rolling resistance, motor-inverter efficiency, thermal management, and BMS algorithms must be optimized together [16-18].SEI stability, internal resistance, thermal runaway behavior, and battery aging are critical factors that determine long-term range retention and operational safety [5-19].Big data analytics and machine learning will play a decisive role in battery lifetime prediction, fast-charging optimization, predictive maintenance, fault detection, and safety management [20-21].In defense systems, batteries should be regarded not only as energy storage devices but also as strategic components that enable silent mobility, low thermal signature, mission endurance, logistics independence, and operational superiority.Future energy architectures will not rely on a single battery chemistry. Platform-specific hybrid solutions involving lithium-ion, sodium-ion, solid-state batteries, fuel cells, and supercapacitors will provide more realistic and effective outcomes. Overall, sodium-ion and solid-state battery systems represent high-value strategic technologies for engineering, academia, education, industry, and defense. Future research and industrial development in this field will contribute not only to longer-range vehicles but also to safer, more sustainable, more economical, and more independent energy systems.Lithium-ion, sodium-ion, and solid-state batteries should be understood as complementary technologies for future electric platforms. Lithium-ion batteries will continue to dominate long-range electric vehicles because of their high energy density, manufacturing maturity, and established supply chains [1-4]. However, their dependence on critical materials and safety-related limitations create strong incentives for alternative battery development [5, 6, 19].Sodium-ion batteries are unlikely to replace high-energy lithium-ion batteries in long-range electric vehicles in the immediate future. Nevertheless, they can fill an important technological and economic gap in stationary energy storage, affordable urban mobility, short-range commercial vehicles, and military logistics applications [7-21].

5.REFERENCES

1 -Armand, M., & Tarascon, J. M. (2008). Building better batteries. *Nature, 451*, 652–657. https://doi.org/10.1038/451652a

2- Tarascon, J. M., & Armand, M. (2001). Issues and challenges facing rechargeable lithium batteries. *Nature, 414*, 359–367. https://doi.org/10.1038/35104644

3- Goodenough, J. B., & Kim, Y. (2010). Challenges for rechargeable Li batteries. *Chemistry of Materials, 22*(3), 587–603. https://doi.org/10.1021/cm901452z

4 -Dunn, B., Kamath, H., & Tarascon, J. M. (2011). Electrical energy storage for the grid: A battery of choices. *Science, 334*(6058), 928–935. https://doi.org/10.1126/science.1212741

5- Grey, C. P., & Tarascon, J. M. (2017). Sustainability and in situ monitoring in battery development. *Nature Materials, 16*, 45–56. https://doi.org/10.1038/nmat4777

6- Xu, C., Dai, Q., Gaines, L., Hu, M., Tukker, A., & Steubing, B. (2020). Future material demand for automotive lithium-based batteries. *Communications Materials, 1*, 99. https://doi.org/10.1038/s43246-020-00095-x

7- Yabuuchi, N., Kubota, K., Dahbi, M., & Komaba, S. (2014). Research development on sodium-ion batteries. *Chemical Reviews, 114*(23), 11636–11682. https://doi.org/10.1021/cr500192f

8- Hwang, J. Y., Myung, S. T., & Sun, Y. K. (2017). Sodium-ion batteries: Present and future. *Chemical Society Reviews, 46*, 3529–3614. https://doi.org/10.1039/C6CS00776G

9- Slater, M. D., Kim, D., Lee, E., & Johnson, C. S. (2013). Sodium-ion batteries. *Advanced Functional Materials, 23*(8), 947–958. https://doi.org/10.1002/adfm.201200691

10- Pan, H., Hu, Y. S., & Chen, L. (2013). Room-temperature stationary sodium-ion batteries for large-scale electric energy storage. *Energy & Environmental Science, 6*, 2338–2360. https://doi.org/10.1039/C3EE40847G

11- Janek, J., & Zeier, W. G. (2016). A solid future for battery development. *Nature Energy, 1*, 16141. https://doi.org/10.1038/nenergy.2016.141

12- Manthiram, A., Yu, X., & Wang, S. (2017). Lithium battery chemistries enabled by solid-state electrolytes. *Nature Reviews Materials, 2*, 16103. https://doi.org/10.1038/natrevmats.2016.103

13- Famprikis, T., Canepa, P., Dawson, J. A., Islam, M. S., & Masquelier, C. (2019). Fundamentals of inorganic solid-state electrolytes for batteries. *Nature Materials, 18*, 1278–1291. https://doi.org/10.1038/s41563-019-0431-3

14- Kato, Y., Hori, S., Saito, T., Suzuki, K., Hirayama, M., Mitsui, A., Yonemura, M., Iba, H., & Kanno, R. (2016). High-power all-solid-state batteries using

sulfide superionic conductors. *Nature Energy, 1*, 16030. https://doi.org/10.1038/nenergy.2016.30

15- Bachman, J. C., Muy, S., Grimaud, A., Chang, H. H., Pour, N., Lux, S. F., Paschos, O., Maglia, F., Lupart, S., Lamp, P., Giordano, L., & Shao-Horn, Y. (2016). Inorganic solid-state electrolytes for lithium batteries: Mechanisms and properties governing ion conduction. *Chemical Reviews, 116*(1), 140–162. https://doi.org/10.1021/acs.chemrev.5b00563

16- Lu, L., Han, X., Li, J., Hua, J., & Ouyang, M. (2013). A review on the key issues for lithium-ion battery management in electric vehicles. *Journal of Power Sources, 226*, 272–288. https://doi.org/10.1016/j.jpowsour.2012.10.060

17- Finegan, D. P., Scheel, M., Robinson, J. B., Tjaden, B., Di Michiel, M., Hinds, G., Brett, D. J. L., & Shearing, P. R. (2015). In-operando high-speed tomography of lithium-ion batteries during thermal runaway. *Nature Communications, 6*, 6924. https://doi.org/10.1038/ncomms7924

18- Xiong, R., Li, L., & Tian, J. (2018). Towards a smarter battery management system: A critical review on battery state of health monitoring methods. *Journal of Power Sources, 405*, 18–29. https://doi.org/10.1016/j.jpowsour.2018.10.019

19- Feng, X., Ouyang, M., Liu, X., Lu, L., Xia, Y., & He, X. (2018). Thermal runaway mechanism of lithium ion battery for electric vehicles: A review. *Energy Storage Materials, 10*, 246–267. https://doi.org/10.1016/j.ensm.2017.05.013

20- Severson, K. A., Attia, P. M., Jin, N., Perkins, N., Jiang, B., Yang, Z., Chen, M. H., Aykol, M., Herring, P. K., Fraggedakis, D., Bazant, M. Z., Harris, S. J., Chueh, W. C., & Braatz, R. D. (2019). Data-driven prediction of battery cycle life before capacity degradation. *Nature Energy, 4*, 383–391. https://doi.org/10.1038/s41560-019-0356-8

21- Attia, P. M., Grover, A., Jin, N., Severson, K. A., Markov, T. M., Liao, Y. H., Chen, M. H., Cheong, B., Perkins, N., Yang, Z., Herring, P. K., Aykol, M., Harris, S. J., Braatz, R. D., Ermon, S., & Chueh, W. C. (2020). Close

CHAPTER -3

BORON STRATEGY IN ENERGY TECHNOLOGIES: OPTIMIZATION AND SUSTAINABILITY OF PCM AND NANOFLUID HYBRID PV/T SYSTEMS

İlknur ŞAHİN[1]

1. INTRODUCTION

Optimization and sustainability processes of these boron-based hybrid systems hold an important place in new technological developments. Boron, one of the cornerstones of chemistry and materials science, offers a wide range of uses in the historical and modern world. This element, found in nature as borate and boric acid salts, has traditionally been used in glass, ceramics, and antiseptic products. However, in the modern era, boron is becoming a strategic material in many fields, from energy technologies to nanotechnology. In addition, the role of boron in the energy sector is quite significant, especially in renewable energy systems and battery technologies. In solar energy systems, boron stands out as a component that increases the energy density and lifespan of lithium-ion batteries while also increasing the efficiency of photovoltaic cells.noteknoloji gibi birçok alanda stratejik bir malzeme haline gelmektedir. Ayrıca, yenilenebilir enerji sistemleri ve pillerin enerji sektöründeki rolü de çok açıktır. Güneş enerjisi sisteminde bor, lityum iyon pillerin enerji yoğunluğunu ve ömrünü uzamasında önemli bir rol oynayan bir bileşendir. While boron hydrides are gaining importance in the field of hydrogen storage and release, boron carbide enhances safety in nuclear energy reactors by providing neutron control. Boron is also used in the production of lightweight and durable materials in the defense and aerospace industries. In nanotechnology, boron nanotubes and nanomaterials enable groundbreaking applications in energy storage, industrial catalysts, and sensor technologies. Furthermore, boron-based compounds are attracting attention in the biomedical field with their anti-cancer properties and wound-healing effects. The boron element also contributes to sustainable agricultural practices as a key component of fertilizers that promote plant growth and increase agricultural productivity. The versatile use of boron makes it an indispensable component in the energy, materials, and biotechnology fields of the

[1] PhD, Department of Mathematics and Science Education, Faculty of Graduate School of Natural and Applied Sciences, Middle East Technical University, Türkiye. ilknurs@metu.edu.tr, (0000-0002-4383-3817)

future. Boron-based nanofluids are used in contrast to traditional coolants (water or glycol) which have limited thermal conductivity.

2. PCM (PHASE CHANGE MATERIAL)

Phase change materials (PCMs) are substances that store a high amount of latent heat during solid-liquid phase change, providing energy efficiency in buildings and cooling systems. Boron compounds (borax decahydrate) are used as effective inorganic PCMs due to their high thermal storage capacity; a 1% borax solution can reduce energy consumption in cooling systems by 41.7%.Boron compounds, particularly hexagonal boron nitride (hBN) and boron carbide (B4C), overcome this limitation. Phase change materials (PCMs) and the properties of boron are based on the following basic working principle; PCMs absorb or release a large amount of heat energy (latent heat) while undergoing a phase change at their melting point. During this process, the ambient temperature remains constant. The Role of Boron: Borax decahydrate ($Na_2B_4O_7H_2O$) and other boron compounds, especially among inorganic PCMs, function as reliable heat batteries due to their high heat storage capacities. They can store 5 to 14 times more energy per volume than conventional materials. Nanofluids containing hBN, which have high heat transfer, rapidly reduce the operating temperature of PV/T panels, minimizing electrical efficiency loss and thermal degradation. In terms of volumetric absorption, boron carbide nanoparticles absorb solar radiation not only on the surface but throughout the entire volume of the fluid, increasing thermal efficiency. In terms of chemical stability, boron and boron-containing products maintain their structure even at high temperatures, reducing the risk of corrosion and extending the system's lifespan [3-6]. PCM (phase change material) is quite important in terms of thermal storage. Boron-doped PCMs integrated behind the PV/T system act as thermal buffers. In terms of thermal balance, boron-doped PCMs (boron-doped paraffins) trap excess heat during the day. It prevents overheating of PV/T cells while allowing the stored heat to be used even after sunset. In terms of optimization, boron's high thermal conductivity optimizes the heat absorption and release rate of the PCM (PCM) during the charge/discharge cycle. This increases the overall exergy efficiency of the system. The Role of Boron in Nanomaterials: Boron is a globally highly functional element. Located between metals and nonmetals in the periodic table, boron is a binary element that can interact with both metals and nonmetals thanks to its rich and multidimensional chemical structure. Due to these properties, boron, used in many industrial and scientific fields, is becoming an integral part of advanced technological applications such as nanotechnology. Nanomaterials are individual materials that can be manipulated at the nanoscale. The combination of boron with nanomaterials opens a brand new chapter for materials science. Due to its chemical properties, boron imparts extraordinary properties to nanomaterials, such as chemical stability, hardness, thermal

stability, and unique electronic properties. As a result, boron-doped nanomaterials are used efficiently in many applications, including electrical energy storage units and biotechnological applications. This study aims to address the mechanical, thermal, electrical, and chemical property improvements that boron imparts to nanomaterials. In addition, the importance and potential of boron nanomaterials in biotechnology are also highlighted [3-12,15]. Boron appears to be a timely element for advancements in materials science and nanotechnology. The use of boron technologies in these hybrid systems increases energy density while optimizing the economic lifespan of the system. This can be directly related to solar cell cooling strategies, especially in radiation tests or space applications you are working on. Table-1 shows the performance and technology difference between traditional solar energy systems and modern hybrid systems developed using boron technology. Essentially, unlike standard solar panels that only generate electricity, PV/T (Photovoltaic/Thermal) systems produce both electricity and hot water/heat. The use of boron and PCM (phase change material) makes this process much more efficient. As solar panels heat up, their electricity generation performance decreases. Table-1 shows that the boron-based nanofluid panel dissipates heat much faster than water, thus keeping the panel cool and operating with high efficiency. In terms of thermal efficiency, while standard systems can convert less than half of the solar energy into heat (40-50%), boron-based systems increase this rate to over 75% thanks to boron's high heat absorption capacity [9-18]. In photovoltaic/thermal (PV/T) systems, the integration of boron-doped phase change materials (PCMs) serves as a critical cooling and energy storage strategy [6-15,19].

Table 1. Comparison conventional refrigerant and boron-doped PCM [3-12,15].

Metric	Conventional PV/T (Water/Air)	Boron-doped PCM-enhanced PV/T	Thermodynamic Properties & Data
Cooling efficiency	Dependent on flow rate and pump power.	Passive cooling via latent heat absorption.	Maintains panel temperature 10-15 lower than standard modules.
Heat conductivity	High (water) or Low (air).	Significantly enhanced by Boron Nitride (BN) fillers.	BN increases PCM conductivity from 0.2 to over 1.5-2.5 W/mK
Electrical yield	Moderate; temperature fluctuations occur.	High; maintains cell temperature near PCM melting point.	Potential increase of 5-12 in electrical output due to reduced thermal degradation.
Thermal stoge	Requires large external tanks.	Built-in compact storage within the panel module.	Volumetric energy density is 3-4 times higher than water-based storage.

3. BIG DATA ANALYTICS (BDA) OPTIMIZATION

Big Data Analytics (BDA) optimization enhances organizational decision-making, efficiency, and competitiveness by processing high-volume, fast, and diverse data, often using artificial intelligence and machine learning. It reduces operational downtime and improves supply chain planning by transforming raw data into predictive insights. [1-8,15-20].Standard PV panels lose efficiency as their temperature rises; for each degree above 25°C, electrical efficiency typically decreases by approximately 0.4–0.5%. Using a boron-doped PCM solves this problem by absorbing excess heat from the solar cells and storing it for thermal applications (such as water heating), while simultaneously keeping the PV cells at a lower, more efficient operating temperature.PV/T (Photovoltaic Thermal) hybrid systems are systems that simultaneously generate both electrical and thermal energy from the sun. Big data analytics and phase-change materials (PCMs) are two fundamental elements used to increase the efficiency and lifespan of these systems. This study focuses on using big data analytics (BVA) and PCMs in PV/T hybrid systems to keep them cool and store energy optimally, thus managing and controlling this process in the smartest and most profitable way. The first fundamental element is the importance of phase-change materials (PCMs). As solar panels heat up, their electrical efficiency decreases. PCMs act as thermal batteries at this point. With the help of temperature control, the PCM placed behind the solar panel absorbs heat as it melts, keeping the panel temperature at ideal levels and increasing electrical efficiency. With energy storage, heat absorbed during the day is stored in the PCM and released after sunset, allowing it to continue being used for hot water production or space heating. Thermal stability helps extend the lifespan of the material by preventing the panel from being affected by sudden temperature changes. The second key element is the importance of big data analytics. Modern PV/T systems are equipped with sensors and continuously generate data. Big data analytics (BVA) manages this complexity, identifying problems such as contamination, cracks, or PCM leaks in panels before failure occurs, through anomalies in the data. BVA optimization analyzes weather forecasts and usage patterns to determine when to store or release energy to the grid, and improves system design by analyzing how the PCM and panel perform under different geographical conditions. Big data analytics (BDA) utilizes various data mining techniques to gain unique insights and transforms business functions by enhancing process-oriented dynamic capabilities, product innovation, and overall business value. Despite its advantages, the application of big data analytics faces challenges such as data fragmentation, integration difficulties, high costs, and security and privacy concerns.Figure - 1 shows the effect of UV radiation on a PV/T + PCM system. PV/T hybrid systems increase overall efficiency by generating both electrical and thermal energy. They

have low thermal conductivity. When PV panels and PCM materials are exposed to UV radiation, photochemical reactions, surface oxidation, and microcracks can occur[8-15,18].In the Table -2 show that mathematical modeling with energy relations For Photovoltaic (PV) Sytems ,electrıcal efficiency ,the electrical output of PV system is expressed as given by,

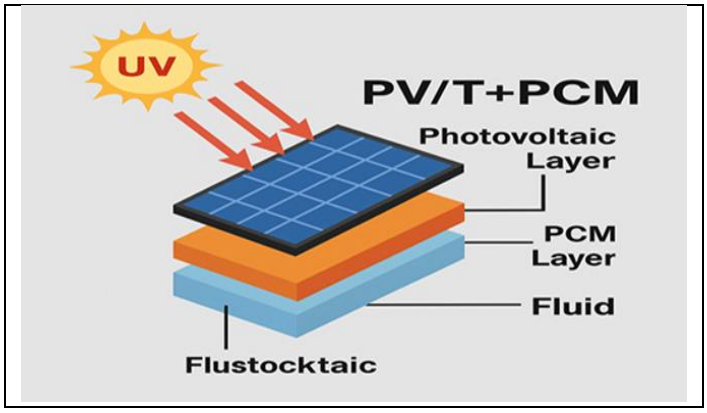

Figure 1. Radiation effect of PV/T + PCM system[3-8].

$$Pel=\eta PV \cdot G \cdot A \quad and \quad \eta PV=\eta ref[1-\beta(Tcell-Tref)]$$

For Photovoltaic/Thermal (PV/I), both electrical and thermal energy are produced simultaneously, for PV/T + Phase change material (PCM) model, energy storage in PCM and energy balance, the PCM absorbs excess heat during phase transition, stabilizing PV temperature and enhancing system reliability and efficiency.

$$Qabsorbed=Qelectric+Qthermal+Qstored+Qloss$$

Big data analytics (BDA) optimization model, BDA is used to optimize system performance under dynamic environmental conditions.Multi-objective optimization function and subject to constraints.The PCM absorbs excess heat during phase transition, stabilizing PV temperature and enhancing system reliability and efficiency.In PV/T + PCM systems, thermal energy storage is introduced using latent heat.

Table 2.Mathematical modeling in PV and PV/T systems [8-15,18].

PV Electrical Efficiency $\eta_{PV} = \frac{P_{el}}{G \cdot A}$ $\eta_{PV}(T) = \eta_{ref}[1 - \beta(T_{cell} - T_{ref})]$	**PV/T Hybrid Efficiency** $\eta_{PV/T} = \eta_{el} + \eta_{th}$ $\eta_{th} = \frac{\dot{m}C_p(T_{out} - T_{in})}{G \cdot A}$
PV/T + PCM Thermal Storage Model $Q_{PCM} = m_{PCM}L + m_{PCM}C_p(T - T_m)$ $Q_{stored} = Q_{absorbed} - Q_{loss}$	**BDA Multi-Objective Optimization Function** $\max F = w_1\eta_{el} + w_2\eta_{th} - w_3C_{total}$ $T_{cell} \leq T_{max}$

3.BORON CARBIDE (B_4C) MINERAL IN NUCLEAR SYSTEMS

Neutron absorption cross-section of B_4C, the neutron absorption mechanism mainly occurs via the (n,α) reaction, in which thermal neutrons are captured by the boron core and converted into lower-energy particles. This conversion reduces the free neutron population in the system, limiting the chain reaction rate. This property is vital and critical for controlling nuclear fission events in the reactor core.In nuclear reactor, energy is released through the nuclear chain reaction and its control mechanism, resulting from the bombardment and fission of uranium atoms with neutrons. Each fission releases new neutrons, which then break apart other atoms, creating a chain reaction. For the safe critical operation of the reactor, the energetic neutrons in the environment must be kept under control. In this respect, boron carbide (B4C) plays an important role in fission reactors as a good neutron absorber. As a neutron-absorbing material, the boron isotope is as important as cadmium in operating the reactor at a suitable critical power in the nuclear fuel cycle. Boron carbide (B4C), with both its industrial hardness and its critical role in nuclear physics, is one of the most strategic materials in modern engineering. Its role as brake Boron carbide, with its structure and properties, is the third hardest known material after belmas and cubic boron nitride. However, its value in the nuclear field is due more to its atomic structure than its hardness. In terms of neutron absorption capacity, the boron

atom, especially the 10B isotope, has a very high cross-section for capturing free neutrons. In terms of thermal stability, it can withstand the extreme temperatures in the reactor core thanks to its melting point of around 2450°C. Natural boron consists of two isotopes: 19.8% 10B with an absorption cross-section of 3900 barn and 80.2% 11B with an absorption cross-section of 0.5 barn. The decomposition of boron isotopes is an expensive process[1-8;15-20]. The decomposition process is possible through the stepwise distillation of $BF_4(CH_3)O$.In terms of chemical resistance, it maintains its structural integrity even under high radiation and is highly resistant to corrosion mechanism in nuclear reactors stems particularly from its unique relationship with neutrons

4. **RESULTS AND DISCUSSION**

This PCM and nanofluid combination, based on a boron strategy, successfully applies the low volume, high efficiency principle in solar energy technologies. Integrating boron as a strategic raw material into such advanced energy technologies is critically important for both energy supply security and technological independence. Future studies are recommended to focus on cost/benefit analyses of these systems in large-scale industrial facilities. The analysis of system performance revealed that hybrid PV/T systems integrating boron-based nanofluids and phase-change materials (PCMs) exhibited a significant increase in overall energy efficiency compared to conventional water-cooled systems. In terms of electrical efficiency, the heat absorption ability of the PCM layer prevented a 12-18% decrease in efficiency due to thermal losses by keeping the photovoltaic cell temperature within the operational limit. In terms of thermal efficiency, the use of boron nitride (BN) or boron carbide (B4C) doped nanofluids stabilized the collector outlet temperature by increasing the thermal conductivity of the fluid. The most critical point to highlight in the discussion section regarding the effect of boron doping on optimization is how boron transforms the thermo-physical properties of the material. The biggest disadvantage of pure PCMs, low thermal conductivity, was overcome by creating thermal bridges with boron nanoparticles. As a critical threshold, optimization studies showed that boron concentrations between 0.5% and 1.5% by volume yielded the highest performance; It has been determined that exceeding this ratio increases pumping costs due to the increase in fluid viscosity. In terms of sustainability,

the chemical stability of boron has ensured that there is no performance loss in long-term cyclical tests of the system[11-21] .This directly contributes to economic sustainability by reducing the maintenance costs of the system. In addition, the combined efficiency factor, which expresses the sum of thermal and electrical efficiency, has reached the 75-80% range in the hybrid system. This result proves that not only electricity generation but also the waste heat released is successfully recovered with boron-supported mechanisms. One of the most important factors is related to the environment and carbon emissions; from the perspective of carbon emissions, it has been calculated that these systems optimized with the boron strategy reduce the annual carbon footprint per square meter by 25% more compared to standard PV systems.

5.REFERENCE

1- Su et al., (2018).Experimental study of using phase change material cooling in a solar tracking concentrated photovoltaic-thermal system,Sol. Energy, 159 ,777-785.

2- Xiao et al., (2009).Analytical optimization of interior PCM for energy storage in a lightweight passive solar room,Appl. Energy, 86, 2013-2018.

3- Kośny et al., (2012).Field thermal performance of naturally ventilated solar roof with PCM heat sink,Sol. Energy, 86 , 2504-2514.

4- Regin et al., (2008).Heat transfer characteristics of thermal energy storage system using PCM capsules: a reviewRenew, Sustain. Energy Rev., 12 , 2438-2458.

5- Qiu et al., (2016).Experimental investigation of the energy performance of a novel Micro-encapsulated Phase Change Material (MPCM) slurry based PV/T system,Appl. Energy, 165 , 260-271.

6- Elarga et al., (2016).Thermal and electrical performance of an integrated PV-PCM system in double skin facades: a numerical study,Sol. Energy, 136 , 112-124.

7- Sardarabadi et al. (2017), Experimental study of using both ZnO/ water nanofluid and phase change material (PCM) in photovoltaic thermal systems,Sol. Energy Mater. Sol. Cells, 161 , 62-69

8- Chow, T. T., Pei, G., Fong, K. F., Lin, Z., Chan, A. L. S., & Ji, J. (2009). Energy and exergy analysis of photovoltaic-thermal collector with and without glass cover. Applied Energy

9- Cemal ,at al..(2022).The Relationship Between Big Data Analytics Capability and Firm Performance: The Moderating Role of Firm Size ,Yıldız Social Sciences Institute Journal (YSBED),6 (2), 62 – 73.

10- Ali et al. (2023). Energy Efficiency In Dome Structures: An Examination Of Thermal Performance İn Iranian Architecture,Building journal,13(9),2-21.

11-Steinbrück,M.,(2010).Degradation and oxidation of B_4C control rod segments at high temperatures., Journal of nuclear materials,400 (2) 15 ,138-150.

12-Nagase et al.,(1997).Chemical interactions between B_4C and stainless steel at hightemperatures , Journal of nuclear materials,245(1) ,52-59.

13-Dominguez et al., (2008). Investigation on boron carbide oxidation for nuclear reactor safety: Experiments in highly oxidising conditions,Journal of nuclear materials ,374(3)15, 473-481.

14-Steinbrück et al.,(2005). Oxidation of boron carbide at high temperatures,Journal of nuclear materials, 336 (2–3) , 185-193.

15-Adroguer,B.,at al.,(2005). Core loss during severe accident (Coloss), Nuclear engineering and design, 235(2–4),173-198.

16- Repetto,G.,at al., (2010). Experimental program on debris reflooding (PEARL) – Results on Prelude facility ,Nuclear engineering and design,264, 176-186.

17-Veshchunov,M.S., et al., (1996). Critical evaluation of uranium oxide dissolution by molten Zircaloy in different crucible tests,Journal of nuclear materials, 231(1–2), 1-19.

18- Veshchunov,M.S., et al., (1994). Dissolution of solid UO_2 by molten Zircaloy,Journal of nuclear materials,209(1) 27-40.

19- Xuesong .,B.,at al.,(2026). Eutectic melting characteristics in B_4C–316L stainless steel system under rapid heating,Journal of nuclear materials, 619-156259.

20- Hofmann,P., et al. ,(1997). Metallic fast reactor fuels , Progress in nuclear energy 31(1–2), 83-110.

21-Peipei W., et al.(2022) Oxidation protection of b_4c modified hfb_2-sic coating for C/C composites at 1073–1473K ,Ceramics Inte

CHAPTER-4

ELECTROCHEMICAL MATERIALS, ELECTRIC VEHICLE BATTERIES: ADVANCED CHEMISTRY- INDUSTRIAL TRANSFORMATION

Almusa ATAMALIYEV[1], Temel Kan BAKIR[2], Aybaba HANÇERLİOĞULLARI[3] Malahat BAGİYEVA[4] , Rezvan REZAEIZADEH[5]

1. INTRODUCTION

The transition toward sustainable energy systems has become one of the defining scientific and technological challenges of the twenty-first century. Growing concerns regarding climate change, environmental degradation, and energy security have accelerated global efforts to reduce greenhouse gas emissions and decrease dependence on fossil fuels. Within this framework, the transportation sector has attracted particular attention because it constitutes a significant source of global carbon dioxide emissions. Consequently, the electrification of transportation has emerged as a key strategy for achieving decarbonization targets and supporting long-term sustainable development goals [1-15]. Electric vehicles (EVs) have become a central component of this transformation due to their high energy efficiency, reduced direct emissions, and compatibility with renewable energy technologies. According to recent market analyses, global EV sales exceeded 14 million units in 2023, reflecting unprecedented growth in both consumer adoption and industrial investment [1]. This rapid expansion has substantially increased the demand for advanced electrochemical energy storage systems capable of meeting the performance, safety, and durability requirements of modern transportation.

[1] Kastamonu University, Faculty of Science, Department of Chemistry, Almusa, Azerbaijan, almusa.atamaliyev@adpu.edu.az orcid id: (0009-0009-8887-6149)
[2] Kastamonu University, Faculty of Science, Department of Chemistry, Kastamonu, Türkiye temelkan@kastamonu.edu.tr orcid id: (0000-0002-7447-1468)
[3] Kastamonu Universety, Faculty of Sience, Department of Physics, Kastamonu, Turkiye, aybaba@kastamonu.edu.tr, orcid id: (0000-0002-9830-4220
[4] Baku State Universty, Faculty of Chemistry, Malahat, Azerbaijan, malahatbagiyeva@bsu.edu.az orcid id :(0009-0001-8619-8059)
[5] Department of Enginering, Faculty of Basic Science, Universety of Applied Science, Ahwaz, Iran, r.rezaeizade@gmail.com, orcid id: (0000-0001-6219-6174)

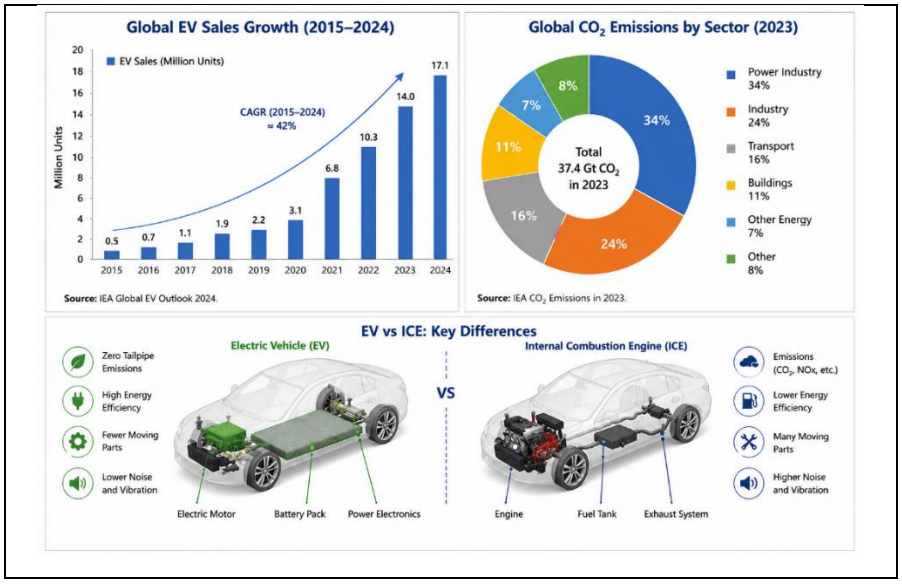

Figure 1. Global EV Market Expansion, Sectoral CO_2 Emissions, and Comparative Characteristics of Electric and Internal Combustion Vehicles

At the heart of EV technology lies the rechargeable battery, which functions as the primary energy storage and delivery system. Battery performance directly influences driving range, charging characteristics, vehicle safety, operational reliability, and overall economic viability. Among the various battery technologies developed to date, lithium-ion batteries (LIBs) remain the dominant technology owing to their high energy density, long cycle life, low self-discharge rates, and favorable electrochemical characteristics [2,3,4,7]. Since their commercialization, continuous advances in materials chemistry and electrochemical engineering have significantly improved battery performance while reducing manufacturing costs. From a chemical perspective, lithium-ion batteries operate through reversible electrochemical reactions involving lithium-ion migration between two electrodes. During charging, lithium ions are extracted from the cathode and intercalated into the anode, whereas the reverse process occurs during discharge. Simultaneously, electrons travel through the external circuit to maintain charge balance and provide electrical power. The efficiency and stability of these processes are strongly dependent on the physicochemical properties of electrode materials, electrolyte composition, ionic conductivity, and interfacial reaction mechanisms [3,4,14]. The electrochemical performance of EV batteries is commonly assessed through several key parameters, among which energy density is particularly important. Gravimetric energy density, which describes the amount of stored energy per unit mass, can be expressed as:

$$E_{density} = E/m \quad (1)$$

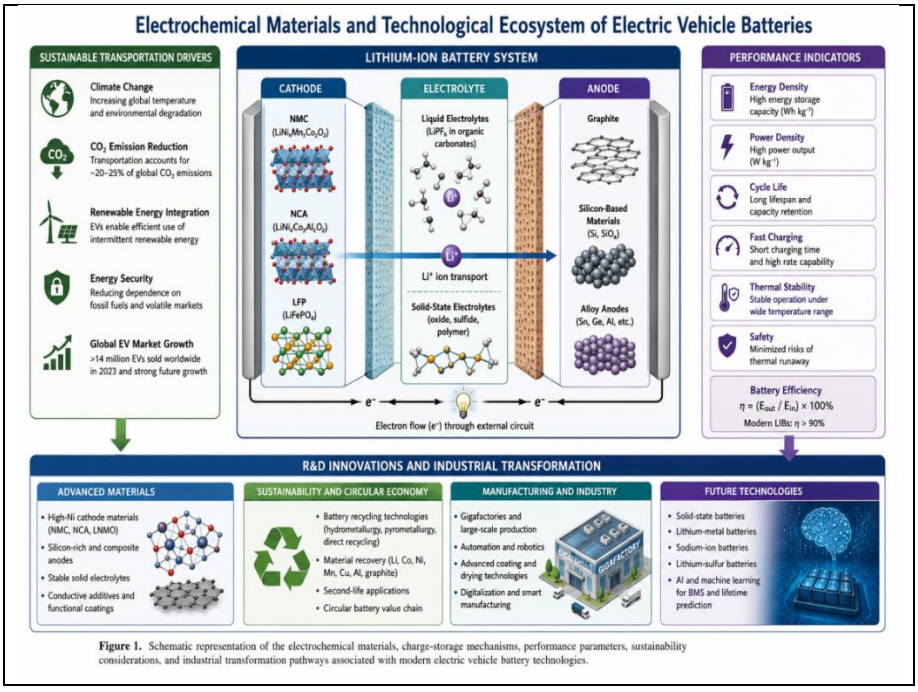

Figure 2. Schematic representation of the electrochemical materials, charge-storage mechanisms,and industrial transormation modern electric vehicle battery technologies.

Where; $E_{density}$ represents the specific energy density (Wh kg^{-1}), E denotes the stored electrical energy, and m corresponds to the total battery mass. Maximizing energy density while preserving safety, long cycle life, and cost-effectiveness remains one of the principal objectives of battery materials research [7,19]. Recent progress in EV battery development has largely been driven by innovations in electrochemical materials. Cathode materials such as lithium nickel manganese cobalt oxide (NMC), lithium nickel cobalt aluminum oxide (NCA), and lithium iron phosphate (LFP) have become essential components of commercial battery systems due to their favorable electrochemical properties and structural stability [8,12-26]. At the same time, significant efforts have been directed toward the development of advanced anode materials, including silicon-based composites, graphene-derived carbon structures, and alloy-forming materials that offer substantially higher theoretical capacities than conventional graphite electrodes [11,13,25]. In addition to bulk electrode materials, the chemistry occurring at electrode–electrolyte interfaces plays a crucial role in determining battery performance and longevity. The

formation of the solid electrolyte interphase (SEI) on the anode surface is particularly important because it governs lithium-ion transport, suppresses undesirable side reactions, and contributes to long-term electrochemical stability. However, continuous interfacial degradation may result in capacity loss, increased internal resistance, lithium plating, and thermal instability, all of which negatively affect battery lifespan and safety [9,25,27]. Consequently, understanding interfacial electrochemistry at both molecular and nanoscale levels has become a major focus of contemporary battery research.Despite remarkable technological progress, several challenges continue to limit the widespread deployment of advanced battery systems. One of the most significant concerns is the growing dependence on critical raw materials, including lithium, cobalt, nickel, and graphite. The increasing demand for these resources has generated concerns regarding supply-chain security, resource availability, geopolitical risks, and environmental impacts associated with mining and processing operations [15,22-30]. According to international projections, the demand for battery-related minerals is expected to increase substantially over the coming decades as electrification and renewable energy deployment continue to expand globally [15].The environmental dimension of battery technology extends beyond raw material extraction. Sustainable battery development increasingly requires the implementation of circular economy principles aimed at minimizing waste generation and maximizing resource recovery. Consequently, battery recycling technologies, material recovery processes, and second-life battery applications have become important research and industrial priorities. These approaches contribute to reducing environmental burdens while improving the long-term sustainability of battery value chains [6,18,23].Another critical aspect of battery performance is degradation behavior. Electrochemical aging is a complex phenomenon involving multiple interconnected mechanisms, including active material loss, electrolyte decomposition, structural instability of electrode materials, transition-metal dissolution, and continuous growth of interfacial layers. These processes gradually reduce battery capacity and power capability during long-term operation [9,27]. A simplified representation of capacity degradation can be expressed as:

$$C_t = C_0 e^{-kt} \tag{2}$$

where C_t denotes battery capacity at time t, C_0 represents the initial battery capacity, and k is the degradation coefficient influenced by temperature, charging conditions, cycling frequency, and material properties. Understanding these degradation mechanisms is essential for improving battery durability and economic feasibility.

Battery efficiency is another parameter of considerable importance because it directly affects energy utilization and vehicle performance. The energy efficiency of a battery system can be expressed as:

$$\eta = (E_{out} / E_{in}) \times 100\% \quad (3)$$

where η represents battery efficiency, Eout is the usable output energy, and Ein corresponds to the supplied charging energy. Modern lithium-ion batteries generally achieve efficiencies exceeding 90%, significantly outperforming conventional internal combustion systems in terms of energy conversion effectiveness [2,7].Beyond scientific advancements, battery technologies have become a major catalyst for industrial transformation. The establishment of large-scale battery manufacturing facilities, widespread automation, and continuous improvements in production technologies have substantially lowered battery costs while increasing manufacturing capacity [5,20,24]. The emergence of gigafactory-scale production has reshaped global supply chains, stimulated investments in advanced manufacturing infrastructure, and strengthened the strategic importance of battery technologies within the global economy.Simultaneously, ongoing research into solid-state batteries, lithium-metal systems, sodium-ion batteries, advanced battery management systems, and artificial intelligence-assisted battery optimization is expected to redefine the future of electrochemical energy storage [10,21,28]. These emerging technologies aim to achieve higher energy densities, improved safety profiles, faster charging capabilities, and greater sustainability compared with conventional lithium-ion systems. Given the pivotal role of electrochemical energy storage in the transition toward sustainable transportation, a comprehensive understanding of battery chemistry, materials design, electrochemical processes, and industrial development has become increasingly important. Therefore, this chapter examines the fundamental electrochemical principles governing EV batteries, explores recent advances in battery materials and emerging technologies, and evaluates the industrial transformation driven by developments in electrochemical energy storage systems. Particular emphasis is placed on the relationships between materials chemistry, battery performance, sustainability, and future technological innovations that are expected to shape the next generation of electric vehicle batteries.

2. Fundamental Electrochemical Principles and Battery Technologies

Electric vehicle (EV) batteries represent advanced electrochemical energy storage systems that integrate principles of electrochemistry, materials science, and solid-state chemistry. Their operation relies on reversible redox reactions, through

which electrical energy is stored and released via the transport of lithium ions between the cathode and anode. Consequently, battery performance is strongly influenced by electrode materials, electrolyte composition, interfacial chemistry, and cell architecture [2,3,4].

2.1 Electrochemical Fundamentals of Energy Storage

The operation of lithium-based batteries is governed by ion migration through the electrolyte and electron transfer through the external circuit.

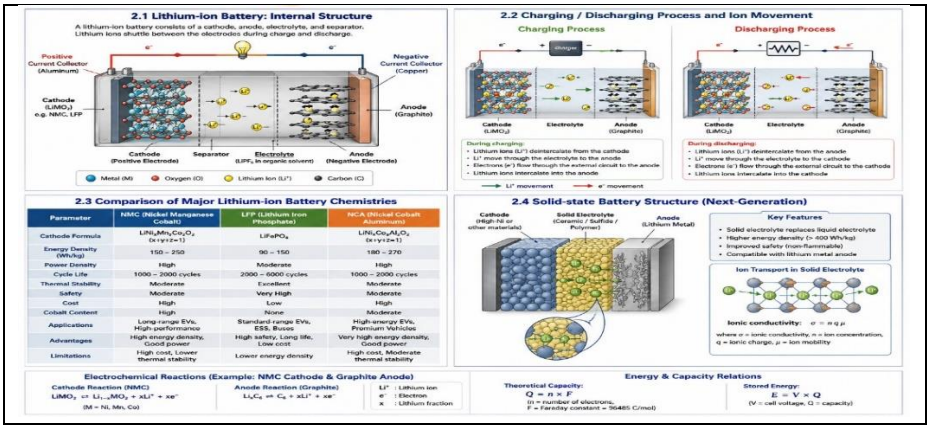

Figure 3. Internal structure, charge-storage mechanisms, battery chemistries,

During charging, lithium ions are extracted from the cathode and inserted into the anode, while the reverse process occurs during discharge. This reversible intercalation mechanism forms the basis of modern rechargeable battery technologies [3,14].The theoretical charge capacity of an electrochemical cell can be expressed

$$Q = nF \tag{4}$$

where Q is the electrical charge capacity (C), n is the number of transferred electrons, and F is Faraday's constant (96,485 C mol^{-1}).

Similarly, the stored electrochemical energy is given by,

$$E = VQ \tag{5}$$

where E is the stored energy, V is the cell voltage, and Q is the charge capacity. These relationships demonstrate the direct connection between electrochemical reactions and battery performance.

2.2 Major Battery Technologies for Electric Vehicles

Among currently available energy-storage systems, lithium-ion batteries dominate the EV sector due to their high energy density, long cycle life, and excellent charge-discharge efficiency [2,7]. Commercial EV batteries are primarily based on three major electrochemical systems;Nickel Manganese Cobalt (NMC) batteries,Lithium Iron Phosphate (LFP) batteries,Emerging Solid-State Batteries

Nickel Manganese Cobalt (NMC) Batteries;NMC cathodes are widely employed in long-range electric vehicles because of their high energy density and favorable electrochemical performance. Their electrochemical reaction can be simplified as,

$$LiMO_2 \rightleftharpoons Li_{1-x}MO_2 + xLi^+ + xe^- \quad (6)$$

where M represents transition metals such as nickel, manganese, and cobalt. Increasing nickel content generally enhances energy density but may reduce thermal stability and accelerate degradation processes [7,8,12].

Lithium Iron Phosphate (LFP) Batteries;LFP batteries have gained significant industrial importance owing to their superior thermal stability, extended cycle life, and improved safety characteristics. Their charge-storage mechanism is represented by:

$$LiFePO_4 \rightleftharpoons FePO_4 + Li^+ + e^- \quad (7)$$

Although LFP systems exhibit lower energy densities than NMC batteries, their lower cost, reduced cobalt dependency, and high operational safety have promoted widespread adoption in commercial EV production [12,26].

Solid-State Batteries;Solid-state batteries are considered one of the most promising next-generation technologies. By replacing flammable liquid electrolytes with solid ionic conductors, these systems offer enhanced safety and potentially higher energy densities [10,25]. The ionic conductivity of solid electrolytes can be expressed as:$\sigma = nq\mu$ (8) Where σ is ionic conductivity, n is ion concentration, q is ionic charge, and μ is ion mobility. Improving ionic conductivity while maintaining interfacial stability remains one of the primary scientific challenges in solid-state battery development [10]

2.3 Thermal Management and Battery Stability

Temperature significantly influences battery performance, aging, and safety. Elevated temperatures accelerate electrolyte decomposition, side reactions, and electrode degradation, whereas low temperatures reduce ionic mobility and increase

internal resistance [27]. The temperature dependence of degradation processes is commonly described using the Arrhenius relationship:

$$k = Ae\ (-Ea/RT) \tag{9}$$

where k is the degradation rate constant, A is the pre-exponential factor, Ea is activation energy, R is the gas constant, and T is absolute temperature. To mitigate thermal risks and maintain stable operation, modern EV battery packs incorporate advanced Battery Management Systems (BMS), liquid-cooling technologies, and intelligent monitoring systems capable of controlling temperature, voltage, and state-of-charge conditions in real time [20,21]. Overall, the technological foundation of modern EV batteries is based on the interaction between electrochemical materials, ion transport mechanisms, and advanced battery-management technologies. Continuous research efforts focus on improving energy density, safety, durability, and sustainability through innovations in cathode materials, anode design, electrolytes, and next-generation battery architectures [7,10,18].

3. Advanced Electrochemical - Chemistry in Electric Vehicle Batteries

The continuous advancement of electric vehicle (EV) batteries is fundamentally dependent on a comprehensive understanding of electrochemical thermodynamics, interfacial phenomena, ion transport mechanisms, crystal chemistry, and degradation processes. Although lithium-ion batteries have achieved remarkable commercial success, further improvements in energy density, safety, durability, and sustainability require deeper insights into the physicochemical principles governing battery operation. Consequently, modern battery research increasingly focuses on the relationship between material structure, electrochemical behavior, and long-term performance [3,4,7].

3.1 Electrochemical Thermodynamics and the Nernst Equation

The operation of rechargeable batteries is governed by the principles of electrochemical thermodynamics, which determine the feasibility and efficiency of energy conversion processes. The electrochemical potential difference between the cathode and anode provides the driving force for electron transfer and lithium-ion migration during battery operation. One of the most important relationships describing this behavior is the Nernst equation:

$$E = Ex - (RT/nF)\ lnQ \tag{10}$$

where E is the cell potential under non-standard conditions, Ex is the standard electrode potential, R is the universal gas constant, T is the absolute temperature, n is the number of transferred electrons, F is Faraday's constant, and Q represents the reaction quotient. The Nernst equation demonstrates that battery voltage is not constant but varies with lithium concentration, temperature, and state of charge. During charging and discharging, changes in lithium-ion activity alter the chemical potential of electrode materials, resulting in variations in cell voltage. This thermodynamic relationship is essential for predicting battery behavior, optimizing charging protocols, and improving energy efficiency [3,14].Furthermore, the maximum electrical work obtainable from a battery is directly related to the Gibbs free energy change of the electrochemical reaction:

$$\Delta G = -nFE \tag{11}$$

where ΔG represents the Gibbs free energy change. This relationship establishes a direct connection between battery chemistry and energy storage capability, emphasizing the importance of material selection in achieving high-performance electrochemical systems [4,14].

3.2 Solid Electrolyte Interphase (SEI) and Interfacial Chemistry

Among the most critical phenomena affecting lithium-ion battery performance is the formation of the Solid Electrolyte Interphase (SEI), a passivation layer generated on the anode surface during the initial charging cycles. The SEI originates from the reductive decomposition of electrolyte components at potentials below their thermodynamic stability limits [9,25].Although electrolyte decomposition appears undesirable, the resulting SEI layer plays a beneficial role by preventing continuous electrolyte degradation while allowing lithium-ion transport through the interface. An ideal SEI exhibits high ionic conductivity, low electronic conductivity, chemical stability, and mechanical integrity. Typical SEI components include lithium fluoride (LiF), lithium carbonate (Li_2CO_3), lithium alkyl carbonates, and various inorganic lithium salts [25]. The electrochemical properties of the SEI strongly influence battery lifetime and Coulombic efficiency. Unstable or continuously growing SEI layers consume active lithium and increase internal resistance, ultimately leading to capacity loss and reduced power performance. Consequently, considerable research efforts focus on electrolyte additives, artificial interfacial coatings, and surface engineering strategies aimed at stabilizing electrode–electrolyte interfaces [9,25]. In addition to anode interfaces, cathode-electrolyte interactions also contribute significantly to battery degradation. High-voltage cathode materials may promote electrolyte oxidation, transition-metal dissolution, and structural instability,

emphasizing the importance of interfacial chemistry throughout the entire battery system [12].

3.3 Lithium-Ion Diffusion Mechanisms

The transport of lithium ions within electrode materials represents a fundamental process controlling battery capacity, rate capability, and charging performance. During operation, lithium ions migrate through the electrolyte and diffuse into the crystal lattice of active electrode materials. The kinetics of this diffusion process largely determine how rapidly a battery can be charged or discharged [2,7].Lithium-ion transport is commonly described by Fick's First Law:

$$J = -D(dC/dx) \tag{12}$$

where J is the diffusion flux, D is the diffusion coefficient, and dC/dx represents the concentration gradient. According to this relationship, ion transport occurs from regions of higher lithium concentration toward regions of lower concentration. Materials possessing high lithium diffusion coefficients generally exhibit superior rate performance and faster charging capabilities. Consequently, significant research has focused on nanostructured materials, particle-size reduction, and surface modification techniques to shorten diffusion pathways and enhance ionic transport [2,8]. Diffusion behavior is strongly influenced by crystal structure, defect concentration, particle morphology, and operating temperature. Therefore, understanding lithium-ion migration at the atomic level remains essential for the rational design of next-generation electrode materials.

CONCLUSION

Electric vehicle batteries represent one of the most significant technological achievements in contemporary electrochemical energy storage, serving as a fundamental enabler of transportation electrification and sustainable energy transition. The analysis presented in this chapter highlights that the performance of modern battery systems is intrinsically linked to the principles of electrochemical thermodynamics, charge-transfer reactions, and lithium-ion transport processes.The operation of rechargeable batteries is governed by reversible redox reactions and ion migration mechanisms that collectively determine energy storage capability, power delivery, and overall system efficiency. In particular, electrochemical thermodynamics provides the theoretical framework for understanding voltage generation and energy conversion, while lithium-ion diffusion kinetics directly influence charge–discharge behavior and rate performance. These fundamental processes establish the scientific basis for the design and optimization of advanced

battery systems.Furthermore, continuous progress in electrochemical materials and battery technologies remains essential for improving energy density, operational efficiency, and long-term reliability. A deeper understanding of ion transport phenomena and electrode reactions will support the development of next-generation energy storage systems capable of meeting the growing demands of electric mobility. Consequently, sustained research efforts in electrochemistry and materials science will play a decisive role in shaping the future of electric vehicle battery technologies and accelerating the global transition toward low-carbon transportation.

REFERENCES

1.International Energy Agency. (2024). *Global EV Outlook 2024*. Paris: IEA Publications.

2.Nitta, N., Wu, F., Lee, J. T., & Yushin, G. (2021). Li-ion battery materials: Present and future. *Materials Today, 18*(5), 252–264. https://doi.org/10.1016/j.mattod.2020.10.021

3.Tarascon, J. M., & Armand, M. (2001). Issues and challenges facing rechargeable lithium batteries. *Nature, 414*(6861), 359–367. https://doi.org/10.1038/35104644

4.Goodenough, J. B., & Park, K. S. (2013). The Li-ion rechargeable battery: A perspective. *Journal of the American Chemical Society, 135*(4), 1167–1176. https://doi.org/10.1021/ja3091438

5.BloombergNEF. (2023). *Battery Price Survey 2023*. New York: Bloomberg Finance L.P.

6.Gaines, L. (2022). Lithium-ion battery recycling processes: Research towards a sustainable course. *Sustainable Materials and Technologies, 17*, e00068. https://doi.org/10.1016/j.susmat.2021.e00068

7.Li, M., Lu, J., Chen, Z., & Amine, K. (2022). 30 years of lithium-ion batteries. *Advanced Materials, 30*(33), 1800561. https://doi.org/10.1002/adma.201800561

8.Xu, B., Qian, D., Wang, Z., & Meng, Y. S. (2021). Recent progress in cathode materials research for advanced lithium ion batteries. *Materials Science and Engineering: R: Reports, 73*(5–6), 51–65. https://doi.org/10.1016/j.mser.2020.11.003

9.Zhang, S. S. (2020). The effect of the charging protocol on battery capacity fading. *Journal of Power Sources, 161*(2), 1385–1391. https://doi.org/10.1016/j.jpowsour.2020.06.040

10.Janek, J., & Zeier, W. G. (2023). A solid future for battery development. *Nature Energy, 1*(9), 16141. https://doi.org/10.1038/nenergy.2016.141

11.Obrovac, M. N., & Chevrier, V. L. (2021). Alloy negative electrodes for Li-ion batteries. *Chemical Reviews, 114*(23), 11444–11502. https://doi.org/10.1021/cr500207g

12.Manthiram, A. (2020). A reflection on lithium-ion battery cathode chemistry. *Nature Communications, 11*, 1550. https://doi.org/10.1038/s41467-020-15355-0

13.Novoselov, K. S., Geim, A. K., Morozov, S. V., et al. (2020). Electric field effect in atomically thin carbon films. *Science, 306*(5696), 666–669. https://doi.org/10.1126/science.1102896

14.Armand, M., & Tarascon, J. M. (2021). Building better batteries. *Nature, 451*(7179), 652–657. https://doi.org/10.1038/451652aWorld Bank. (2020). *Minerals for Climate Action: The Mineral Intensity of the Clean Energy Transition*. Washington, DC: World Bank Group.
15.Dunn, J. B., Gaines, L., Kelly, J. C., James, C., & Gallagher, K. G. (2021). The significance of Li-ion batteries in electric vehicle life-cycle energy and emissions. *Energy & Environmental Science, 8*(1), 158–168. https://doi.org/10.1039/C4EE03029J
16.Ellingsen, L. A. W., Singh, B., & Strømman, A. H. (2020). The size and range effect: Lifecycle greenhouse gas emissions of electric vehicles. *Environmental Research Letters, 11*(5), 054010. https://doi.org/10.1088/1748-9326/11/5/054010
17.Harper, G., Sommerville, R., Kendrick, E., et al. (2021). Recycling lithium-ion batteries from electric vehicles. *Nature, 575*(7781), 75–86. https://doi.org/10.1038/s41586-019-1682-5
18.Schmuch, R., Wagner, R., Hörpel, G., Placke, T., & Winter, M. (2020). Performance and cost of materials for lithium-based rechargeable automotive batteries. *Nature Energy, 3*(4), 267–278. https://doi.org/10.1038/s41560-018-0107-2
19.Tesla. (2023). *Battery Day Technical Report*. Palo Alto, CA: Tesla Inc.
20.International Renewable Energy Agency. (2023). *Electric Vehicle Charging Infrastructure and Smart Grids*. Abu Dhabi: IRENA.
20.European Commission. (2023). *EU Battery Regulation and Sustainable Battery Value Chains*. Brussels: European Union Publications Office.
21.United Nations Environment Programme. (2022). *Sustainability and Circularity of Electric Vehicle Batteries*. Nairobi: UNEP.
22.Wood, D. L., Li, J., & Daniel, C. (2021). Prospects for reducing the processing cost of lithium ion batteries. *Journal of Power Sources, 275*, 234–242. https://doi.org/10.1016/j.jpowsour.2020.11.019
23.Cheng, X. B., Zhang, R., Zhao, C. Z., & Zhang, Q. (2021). Toward safe lithium metal anode in rechargeable batteries. *Chemical Reviews, 117*(15), 10403–10473. https://doi.org/10.1021/acs.chemrev.7b00115
24.Sun, Y. K., Myung, S. T., Park, B. C., Prakash, J., Belharouak, I., & Amine, K. (2020). High-energy cathode material for long-life and safe lithium batteries. *Nature Materials, 8*(4), 320–324. https://doi.org/10.1038/nmat2418
25.Wang, Q., Ping, P., Zhao, X., Chu, G., Sun, J., & Chen, C. (2021). Thermal runaway caused fire and explosion of lithium ion battery. *Journal of Power Sources, 208*, 210–224. https://doi.org/10.1016/j.jpowsour.2020.02.038

26.Cano, Z. P., Banham, D., Ye, S., et al. (2021). Batteries and fuel cells for emerging electric vehicle markets. *Nature Energy, 3*(4), 279–289. https://doi.org/10.1038/s41560-018-0108-1
27.Agency for the Cooperation of Energy Regulators. (2023). *Smart Grid and Vehicle-to-Grid Integration Report*. Brussels: ACER Publications.
28.McKinsey & Company. (2024). *The Future of Battery Supply Chains 2030*. New York: McKinsey Sustainability Reports.

CHAPTER-5

MONITORING LITTER QUANTITY AND DECOMPOSITION IN FOREST ECOSYSTEMS USING HYPERSPECTRAL SATELLITE IMAGES

Gamze SAVACI SELAMET[1]

1. INTRODUCTION

Nutrients play a crucial role in the productivity, sustainability, and health of forest ecosystems, and trees are largely dependent on natural nutrient sources to meet these needs [1]. In this context, leaf litter in forest ecosystems plays a significant role in returning nutrients to the soil. The amount of needle/leaf litter produced by a tree and its root mass are ecological factors that significantly influence stand productivity, and they provide information specifically about the plant nutrients transferred from the aboveground to the soil through annual needle/leaf litter [2]. Through litter decomposition, nutrients taken up by plants return to the soil, enriching it with organic matter and mineral nutrients. In contrast, undecomposed litter accumulates on the soil surface, becoming an important nutrient reserve [3].

The decomposition of leaf litter involves the extensive breakdown of organic matter into CO_2 and nutrients through physical, biological, and chemical processes [4]. In terrestrial ecosystems, more than 50% of net primary production is returned to the soil each year through the decomposition of leaf litter [5]. The amount of litter on the forest soil surface is significantly influenced by site, climatic characteristics, topography, elevation, aspect, tree species, tree age, canopy cover, density, and the physical and chemical properties of the soil, as well as by the microorganisms and soil fauna living in the soil. In most ecosystems, leaf litter decomposition is largely influenced by climate, litter quality, and soil fauna [6, 7]. A schematic representation of leaf litter decomposition is provided in Figure 1.

[1] Assoc. Prof. Dr., Department of Forest Engineering/Faculty of Forestry, Kastamonu University, Türkiye, gsavaci@kastamonu.edu.tr, (ORCID: 0000-0003-4685-2797)

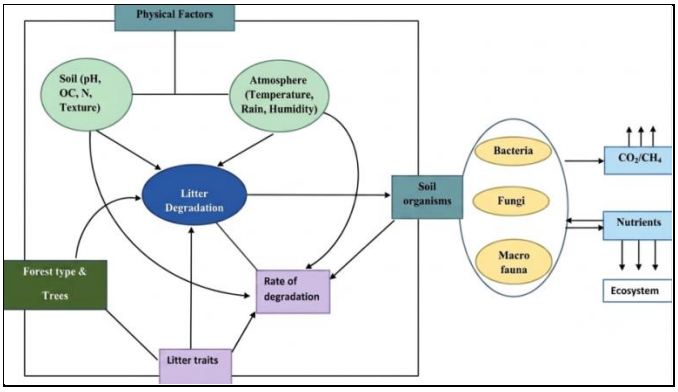

Figure 1. Diagrammatic representation of factors affecting litter decomposition [8].

Litter decomposition is a biological process encompassing complex interactions among insects, earthworms, bacteria, and fungi on the soil surface and within the soil, involving chemical, physical, and biological factors [9, 10]. The decomposition of organic matter plays a significant role as an energy source for soil organisms and as a nutrient reservoir in the cycling processes within natural ecosystems [11].

The main stages of leaf litter decomposition are shown in Figure 2. The decomposition cycle begins with the leaching phase, an abiotic process; during this stage, water-soluble polar compounds in the cell walls are removed from the matrix by hydrospheric effects. Microbial colonization (bacteria and fungi), which begins simultaneously, takes over the chemical modification of the substrate. While microorganisms rapidly mineralize labile carbon sources (cellulose and hemicellulose) through the exoenzymes they secrete, the degradation of lignin, a recalcitrant (resistant) hydrophobic polymer, constitutes the rate-limiting step of the process. In this process, the organic residues that mix into the mineral soil layer undergo mineralization (release of ammonium, nitrate, and phosphate), which meets the ecosystem's nutrient needs, and humification, which ensures the system's physico-chemical stability (Figure 2). Consequently, at this stage, a delicate ecological balance is established between the nutrient cycle and long-term soil carbon storage.

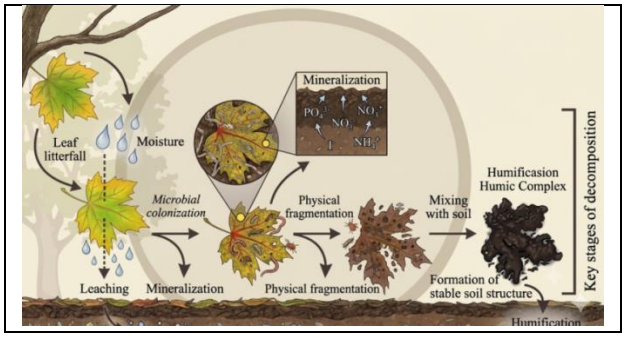

Figure 2. The main stages of leaf litter decomposition [12].

The decomposition of the leaf litter consists of two main processes occurring simultaneously: (a) the mineralization and humification of lignin, cellulose, and other compounds mediated by microorganisms; (b) the leaching into the soil of soluble compounds that gradually mineralize carbon, nitrogen, and other elements [13, 14]. The nutrients released into the soil through the leaf litter decomposition process are recycled as a nutrient source by trees and other plants growing on the soil surface. In particular, these nutrients include micro- and macroelements essential for plant and animal growth [14]. Therefore, litter decomposition is a highly significant natural process in forest ecosystems because it recycles important components back into the environment [14–16]. The rates of litter decomposition and the release of nutrient elements are influenced by environmental conditions, the nature of microorganisms and soil fauna within the decomposition process, and the composition or quality of the litter. The decomposition of litter, as it mixes into the soil as humus or decomposition products, not only affects the soil's physical and chemical properties but also plays a significant role in plant growth and nutrition [17].

While lignin and cellulose account for a significant portion of the litter composition, the composition also includes hemicellulose, proteins, tannins, cutin, suberin, oils, waxes, ash (mineral matter), and other organic compounds [18]. With the continuous advancement of chemical analysis methods targeting the components of the cell walls of needles and leaves, which are key components of the litter layer (total C and N content, lignin, cellulose, hemicellulose), it has become possible to conduct faster analyses, easily track the decomposition process, and achieve more accurate results [19]. Some of these structural components either accelerate or slow down the decomposition rate. Protein, Ca, Mg, $O_8P_2^{-4}$, K, N, C/N, sugars, starch, hemicellulose, pectin, fragrant aromatic compounds, and water-soluble substances, as well as all variants of COOH and CHO, such as oxalic acid ($COOH_2$), acetic acid, colorless organic acids such as lactic acid

($CH_3CHOHCOOH$), and saccharic acid ($C_7H_5O_3NS$), are compounds that increase the decomposition rate of the organic matter; lignin, resin, alkaloids, glycosides, fats, tannins, and wood tissues with high lignin content, as well as xylem in roots, epidermis, and leaf veins, are compounds that hinder decomposition [20].

In forest ecosystems, the chemical composition of the litter layer (particularly lignin and cellulose) exhibits specific absorption features in the Short-Wave Infrared (SWIR) region due to molecular bond vibrations (C-H, O-H, N-H). As decomposition progresses, cellulose is rapidly consumed while lignin structure is preserved, directly altering the shape of the spectral curve. Among the physical properties of the forest floor, litter amount (g/m^2) and decomposition degree directly affect surface roughness, thereby altering electromagnetic wave scattering. However, the most critical physical parameter affecting remote sensing is the litter moisture content. High moisture creates strong water-absorption bands at 1450 nm and 1940 nm in the spectrum, masking the characteristic spectral signals of organic components (lignin and cellulose). Distinguishing the weak absorption features suppressed by moisture is only possible with hyperspectral satellite data comprising hundreds of consecutive narrow bands. Nutrient elements (N, P, K) released into the soil through decomposition do not directly provide spectral signals. However, the dynamics of carbon (C) bound to organic matter can be tracked. While conventional satellites can only measure chlorophyll in living leaves (VNIR region), hyperspectral satellites are the only tool capable of monitoring the non-photosynthetic carbon cycle (Non-Photosynthetic Vegetation - NPV) in forest litter.

Consequently, the physical (moisture, degree of decomposition) and chemical (lignin, cellulose, C/N ratio) heterogeneity of the litter layer directly determines the spectral characteristics of the electromagnetic radiation reflected from the forest floor. Hyperspectral remote sensing technology, with its hundreds of narrow and continuous bands, offers the potential to continuously monitor litter quantity and decomposition rate spatially by analyzing absorption depths, particularly in the Short-Wave Infrared (SWIR) region.

2. LITTER DECOMPOSITION EXPERIMENT METHODOLOGY

The stages of the litter decomposition experiment, a classic method conducted in field and laboratory studies, include the following methodological steps.

2.1. Material Collection and Stabilization

Fresh leaf/needle samples are collected using litter traps from the dominant tree species representing the forest ecosystem where the study will be conducted. This fresh material, which has not come into contact with soil, is brought to the

laboratory and cleaned of foreign matter. For soluble carbohydrates and polyphenols, it has been determined that drying the litter samples in paper bags in an oven at 30-40°C is the most suitable method [21, 22]. For the analysis of structural components (lignin, cellulose, and hemicellulose), the samples are dried in an oven at 60–85°C until a constant weight is reached [23, 24].

Figure 3. Annual leaf litter falling from trees; examples of systems that collect it using litter traps [24-25].

2.2. Selection of Decomposition Litterbags and Optimization of Mesh Size

The bags used to hold dried litter samples should be made of polyethylene, nylon, or fiberglass, materials that are resistant to abiotic conditions and decay. Decomposition bag sizes are typically standardized at 10 x 10 cm or 20 x 20 cm. During the experimental phase, mesh size is the most critical parameter determining which biotic components will dominate the process.

- **Fine-Mesh Bags (0.1 mm):** Physically prevent the entry of soil macro- and mesofauna (mites, collembola, nematodes, etc.) into the bag. This stage is preferred to measure the isolated aspect of decomposition occurring solely through fungal and bacterial (microbial) activities.
- **Wide-Pore Bags (1–2 mm):** These allow the fauna found in natural forest litter to penetrate the bag freely. Because this pore structure fully simulates real ecosystem dynamics and physical decomposition processes, it is preferred in hyperspectral modeling studies.

2.3. Weighing and Field Placement

Litter samples with a constant dry weight are weighed to exactly 5–10 grams (±0.01 g) on a precision scale, placed in decomposition bags, and the bag openings are sealed using a heat sealer or corrosion-resistant staples. Each bag has a unique label containing a number. In the field, the living vegetation (the layer of live grass and shrubs) in the designated sampling areas is gently scraped away. The

decomposition bags are laid horizontally at the exact interface between the mineral soil (A horizon) and the existing organic litter layer, ensuring maximum surface contact with the soil. To prevent them from being displaced by wildlife or wind, they are secured to the ground with stainless steel nails (Figure 4). Olson's model first describes a rapidly declining curve, followed by a decline that closely mirrors the mass loss commonly observed in aging leaves. This characteristic of decomposition has been described as a process in which compounds that decompose more easily and rapidly are initially broken down, followed by particles that are more resistant and decompose less readily. In the litter decomposition experiment, leaves and needles that have fallen to the forest floor within a year are collected. The initial chemical composition of the leaves and needles brought to the laboratory is determined; they are then placed into fiberglass bags measuring 20x20 cm with mesh sizes smaller than 1 mm and returned to the site where they were originally collected. At different time intervals, these bags are collected, and both mass losses and their chemical compositions are determined. The decomposition rates and the most influential component in decomposition are then determined through statistical analyses of the relationship between mass loss rates and chemical components [19].

Figure 4. Step-by-step demonstration of litter decomposition experiment [26]

2.4. Collection of Field Decomposition Samples

After litterbags are placed in the field, they are typically retrieved from the site at successive intervals covering the 6th, 12th, 18th, and 24th months. To statistically balance climatic anomalies and microscopic heterogeneity, at least 5

replicates from each forest type are removed from the field during each collection period. The decomposition bags collected from the field are placed in separate, sealed polyethylene bags to prevent sudden moisture loss or debris shedding, and transported to the laboratory under a cold chain (+4°C). In the laboratory, mineral soil particles adhering to the outer surface of the bags, algae, and living plant roots that have grown into the bag pores are carefully cleaned using tweezers and fine brushes. The cleaned internal material is stored until the analysis phase.

2.5. Calculations of Mass Loss and Decay Rate (*k* constant)

A After determining the fresh weights of the needles in the field-collected decomposition bags, they are placed in an oven at 85°C for 2 hours. The percentage moisture content is calculated using the difference between the fresh weight and the oven-dry weight [27-28]. Subsequently, the mass loss of the needles relative to their initial weights is calculated [29]. The mass losses of the samples in the decomposition bags are calculated using the following formula.

$$RM\% = (W_t/W_0)\times 100 \quad (1)$$

RM% = Percentage of residual dry weight, W_t = Weight during the sampling period, W_0 = Initial weight

To better monitor and determine how litter decomposition occurs in different ecosystems, the litter cover experiment, a traditional method for measuring litter type and condition, comparing decomposition rates across species, estimating decomposition rates (decomposition rate constant and k-value), and measuring mass loss, the litter bag experiment, a traditional method, has gained importance since the 1960s [30]. The litter decomposition rate constant was first introduced by Jenny et al. [31] and later developed by Olson [32], providing a robust general concept and analytical approach for subsequent litter decomposition studies (Equation 2). Olson's simple negative-exponential model, presented below, is frequently used today.

$$W_t/W_0 = e^{-kt} \quad (2)$$

where, the annual decomposition rate constant (*k*-value) of the forest stand is calculated. In this formula, t represents time, and k represents the decomposition rate constant.

Experimental methodologies applied in the field or the laboratory to determine spatial variations in litter quantity and decomposition rate (*k*-value) enable direct, precise measurement of ecosystem dynamics. However, since these conventional

techniques produce point-scale data, they are insufficient to fully represent the temporal and spatial heterogeneity of large forest ecosystems. In this context, experimental methodologies serve as indispensable ground-truth references for remote sensing-based models. Time-series data on mass loss and biogeochemical analysis obtained from the field are matched with pixel-based spectral reflectance values derived from hyperspectral satellite imagery. Thus, experimental findings conducted at the local scale are calibrated using advanced spectral analysis methods, such as narrow-band absorption depths and continuum removal, to develop predictive models at regional and global scales.

3. PRINCIPLES OF HYPERSPECTRAL REMOTE SENSING AND SPECTRAL ABSORPTION BANDS OF LITTER

Imaging spectroscopy, also known as hyperspectral imaging, is a passive remote sensing technology that simultaneously acquires images across many spectrally adjacent narrow bands to obtain a reflectance spectrum for each pixel [33–34]. Thanks to the successful launches of the PRISMA satellite (PRecursore IperSpettrale della Missione Operative) [35] by the Italian Space Agency (ASI) in 2019 and the EnMAP (Environmental Mapping and Analysis Program) [36] launched by the German Aerospace Center (DLR) in 2022, the availability of space-based hyperspectral data has increased significantly in recent years.

In general, the spectral characteristics of vegetation exhibit strong pigment absorptions in the visible (VIS: 400 nm–700 nm) region of the spectrum (Figure 5). The near-infrared (NIR: 700–1400 nm) region, however, is characterized by a sharp increase in reflectance associated with the biomass, cellular structure, type, density, geometry, and water content of the vegetation layer. The shift of the red edge toward shorter wavelengths between 680 nm and 780 nm is associated with a decrease in chlorophyll; this may indicate heavy metal, water, or nutrient stress. Aging leaves are also characterized by a decrease in chlorophyll, followed by the loss of other pigments and leaf water content [37]. The biochemical composition of leaves and vegetation, including nitrogen-containing compounds and lignin, typically absorbs radiation at fundamental stretching frequencies in the near-infrared (NIR) and short-wave infrared (SWIR) regions [37].

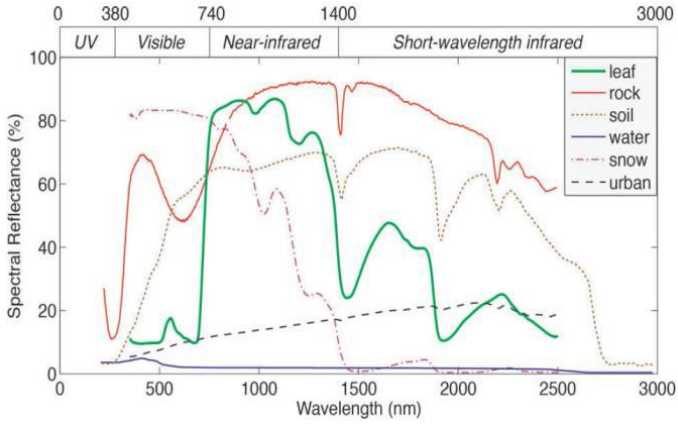

Fig 5. Reflectance spectra of selected Earth's surface [36].

During the decomposition of litter, cellulose and hemicellulose, which are readily consumed by microorganisms, rapidly decrease. In contrast, lignin, which is resistant to decomposition, begins to accumulate in the environment [38–39]. This biochemical transformation directly alters the depth ratios of absorption bands in the SWIR region. Consequently, NIRS technology, used to determine the chemical composition and degree of decomposition of litter organic matter in a laboratory setting, derives its power from these sensitive molecular resonances in the SWIR region [40]. Analysis of the spectral depths of these bands enables remote sensing monitoring of carbon cycles and organic matter dynamics in ecosystems [37]. The main chemical components of litter, namely cellulose, hemicellulose, and lignin polymers, exhibit characteristic spectral absorption features in the Short-Wave Infrared (SWIR: 1300–2500 nm) region [41, 42].

4. SPECTRAL INDICES USED TO MONITOR LITTER DYNAMICS

The narrow-band data from hyperspectral satellites enable quantitative modeling of dry biomass, lignin, and cellulose in forest soils by comparing reflectance and absorption rates across specific spectral regions. The most critical indices developed for this purpose are as follows:

-Cellulose Absorption Index (CAI) is specifically designed to measure the depth of the cellulose and hemicellulose absorption dip at a wavelength of 2100 nm. This index is one of the parameters that most clearly distinguishes between living vegetation (chlorophyll) and litter (NPV). It is calculated using a linear combination of three consecutive bands in hyperspectral data [43, 44].

$$CAI = 0.5(R_{2.0} + R_{2.2}) - R_{2.1} \quad (3)$$

Here, $R_{2.0}$, $R_{2.1}$, and $R_{2.2}$ are the reflectance coefficients in the 2.00–2.05, 2.08–2.13, and 2.19–2.24 μm bands, respectively.

In the early stages of decomposition, CAI values are high and positive because the litter contains a high amount of cellulose. As decomposition progresses and microorganisms consume cellulose, the CAI value decreases linearly.

- Normalized Difference Lignin Index (NDLI): Tracking lignin, which is released into the soil later than cellulose and retains its structure for a long time, is essential for the temporal modeling of the carbon cycle. It estimates the relative lignin concentration in leaves and the total canopy leaf biomass to determine reflectance spectra in the 1754 nm range [38, 45, 46]. NDLI is a hyperspectral vegetation index used to estimate lignin content in plant tissue. Lignin is an important structural component of plant cell walls, and its content can vary among different plant species, tissues, and growth stages. In hyperspectral data, NDLI is calculated using Formula 4.

$$NDLI = \frac{\log\left(\frac{1}{\rho_{1754}}\right) - \log\left(\frac{1}{\rho_{1680}}\right)}{\log\left(\frac{1}{\rho_{1754}}\right) + \log\left(\frac{1}{\rho_{1680}}\right)} \quad (4)$$

NDLI shows a high correlation in estimating lignin density under the forest canopy and, consequently, the chemical quality of litter (as indicated by the C/N ratio).

4.3. Dead Fuel Index (DFI)

The DFI algorithm, which combines the SWIR-1 and SWIR-2 bands, is used to comprehensively monitor both the quantity (g/m²) and moisture content of litter. This index determines the accumulation of combustible material (dead fuel) on the forest floor and its dryness level, thereby providing a basis for both decomposition gradients and forest fire risk analyses. The DFI is determined according to the following formula [47].

$$DFI = \left(1 - \frac{B_7}{B_6}\right) \times \frac{B_1}{B_2} \times 100 \quad (5)$$

Here, B_1, B_2, B_6, and B_7 are the average values of MODIS bands 1, 2, 6, and 7, respectively. 100 is the scale factor.

5. CONCLUSION AND DISCUSSION

In this section, the potential for monitoring litter volume and decomposition processes, vital to the carbon budget and nutrient cycling of forest ecosystems, using hyperspectral remote sensing technologies is examined within a theoretical and methodological framework. The following key findings were obtained:

a) The narrow-band structure of hyperspectral sensors enables the quantitative differentiation of chemical bond vibrations in organic polymers within the SWIR region.

b) Specific indices such as CAI and NDLI possess the ability to linearly track chemical transformation stages, such as cellulose loss and lignin accumulation, in forest soils.

c) Traditional experimental methodologies (litterbag) serve as an indispensable data source for the calibration and validation processes of remote sensing-based prediction models (ground-based measurements).

The role of hyperspectral remote sensing technologies in monitoring litter quantity and decomposition dynamics in forest ecosystems necessitates a multifaceted discussion that considers both their technical advantages and operational limitations. The greatest signal limitation in modeling litter using satellite data is canopy closure. Even advanced hyperspectral satellites (PRISMA, EnMAP), which rely on optical sensors, struggle to directly capture ground signals in closed forest formations with high leaf area index (LAI). In this context, the potential for data fusion between hyperspectral satellite data and LIDAR (Light Detection and Ranging) or active microwave SAR (Synthetic Aperture Radar) systems, which can determine the three-dimensional structure of the tree canopy, will usher in a new era in forest floor monitoring studies. This integration will enable the real-time, high-precision mapping of forest ecosystem capacities under global climate change scenarios.

REFERENCES

1-Sarıyıldız, T., & Savacı, G. (2024). Bursa, Karacabey Subasar ormanı dişbudak (*Fraxinus angustifolia* Vahl.) meşcerelerinin ölü örtü ve toprakta depolanan organik karbon ve besin elementlerinin belirlenmesi. Turkish Journal of Forest Science, 8(2), 177-200.

2-Tüfekçioğlu, A., Sarıyıldız, T., Güner, S., & Küçük, M. (2005). Artvin Genya dağı doğu ladini meşcerelerinde kök kütlesi, yıllık ibre dökümü ve toprak solunumu miktarlarının değişimleri. Ladin Sempozyumu, I. Cilt, 123-129, Trabzon.

3-Pang Y., Tian J., Zhao X., Chao Z., Wang Y., Zhang X., et al., (2020). The linkages of plant, litter and soil C:N:P stoichiometry and nutrient stock in different secondary mixed forest types in the Qinling Mountains, China. Peer J, 8, e9274.

4-Aerts, R. (1997). Climate, leaf litter chemistry and leaf litter decomposition in terrestrial ecosystems: A triangular relationship. *Oikos*, 439-449.

5-Garcia-Palacios, P., Maestre, F. T., Kattge, J., & Wall, D. H. (2013). Climate and litter quality differently modulate the effects of soil fauna on litter decomposition across biomes. Ecology Letters, 16(11), 1418-1418.

6-Hättenschwiler, S., & Gasser, P. (2005). Soil animals alter plant litter diversity effects on decomposition. Proceedings of the National Academy of Sciences, 102(5), 1519-1524.

7-McCay, T. S., Cardelús, C. L., & Neatrour, M. A. (2013). Rate of litter decay and litter macroinvertebrates in limed and unlimed forests of the Adirondack Mountains, USA. Forest Ecology and Management, 304, 254-260.

8-Krishna, M. P., & Mohan, M. (2017). Litter decomposition in forest ecosystems: a review. Energy, Ecology and Environment, 2(4), 236-249.

9-Graça, M. A. (2001). The role of invertebrates on leaf litter decomposition in streams–a review. International Review of Hydrobiology: A Journal Covering all Aspects of Limnology and Marine Biology, 86(4-5), 383-393.

10-Hasanuzzaman, M., & Hossain, M. (2014). Leaf litter decomposition and nutrient dynamics associated with common horticultural cropland agroforest tree species of Bangladesh. International Journal of Forestry Research, 2014(1), 805940.

11-Swift, M. J., Heal, O. W., Anderson, J. M., & Anderson, J. M. (1979). Decomposition in terrestrial ecosystems (Vol. 5). Univ of California Press.

12-Tennakoon, D. S., Gentekaki, E., Jeewon, R., Kuo, C. H., Promputtha, I., & Hyde, K. D. (2021). Life in leaf litter: fungal community succession during decomposition.

13-Dechaine, J., Ruan, H., Sanchez-de Leon, Y., & Zou, X. (2005). Correlation between earthworms and plant litter decomposition in a tropical wet forest of Puerto Rico. Pedobiologia, 49(6), 601-607.

14-Sayer, E. J., Rodtassana, C., Sheldrake, M., Brechet, L. M., Ashford, O. S., Lopez-Sangil, L., ... & Tanner, E. V. (2020). Revisiting nutrient cycling by litterfall—Insights from 15 years of litter manipulation in old-growth lowland tropical forest. In Advances in ecological research (Vol. 62, pp. 173-223). Academic Press.

15-Leppert, K. N., Niklaus, P. A., & Scherer-Lorenzen, M. (2017). Does species richness of subtropical tree leaf litter affect decomposition, nutrient release, transfer and subsequent uptake by plants?. Soil Biology and Biochemistry, 115, 44-53.

16-Froufe, L. C. M., Schwiderke, D. K., Castilhano, A. C., Cezar, R. M., Steenbock, W., Seoane, C. E. S., ... & Vezzani, F. M. (2020). Nutrient cycling from leaf litter in multistrata successional agroforestry systems and natural regeneration at Brazilian Atlantic Rainforest Biome. Agroforestry systems, 94(1), 159-171.

17-Kantarcı, M. (2000). Toprak İlmi. İstanbul Ün. Orman Fak. Yayınları No:462, s:420, İstanbul.

18- Sariyildiz, T. (2000). Biochemical and Environmental Controls of Litter Decomposition. PhD thesis.

19-Sariyildiz, T. (2003). Litter decomposition of Pic*ea orientalis*, *Pinus sylvestris* and *Castanea sativa* trees grown in Artvin in relation to their initial litter quality variables. Turkish J. Agric. For., 27, 237- 243.

20-Çepel, N. (1996). Toprak İlmi Ders Kitabı -Orman topraklarının karakteristikleri, toprakların oluşumu, özellikleri ve ekolojik bakımdan değerlendirilmesi. İstanbul Üniversitesi Yayın No, 3945, Orman Fakültesi Yayın No, 438, İstanbul.

21-Allen, S. E., Grimshaw, H. M., Parkinson, J. A., & Quarmby, C. (1974). Chemical analysis of ecological materials (pp. xii+-565).

22-Gupta, S. R., & Malik, V. (1999). Measurement of leaf litter decomposition. In Analysis of Plant Waste Materials (pp. 181-207). Berlin, Heidelberg: Springer Berlin Heidelberg.

22-Marstorp, H. (1996). Influence of soluble carbohydrates, free amino acids, and protein content on the decomposition of Lolium multiflorum shoots. Biology and Fertility of Soils, 21(4), 257-263.

24-Mjöfors, K., Johansson, M. B., Nilsson, Å., & Hyvönen, R. (2007). Input and turnover of forest tree litter in the Forsmark and Oskarshamn areas (No.

SKB-R--07-23). Swedish Nuclear Fuel and Waste Management Co., Stockholm (Sweden).

25-Seta, T., Demissew, S., & Woldu, Z. (2018). Litterfall dynamics in boter-becho forest: moist evergreen montane forest of Southwestern Ethiopia. *Journal of Ecology and The Natural Environment*, *10*(1), 13-21.

26-Savacı, G., 2017. Farklı arazi kullanım türleri ve ağaç yaşının bazı toprak özellikleri, karbon ve azot depolamasına etkileri. Doktora Tezi, Kastamonu Üniversitesi, Fen Bilimleri Enstitüsü, s.179. Kastamonu, Türkiye.

27-Berg, B., Erhagen, B., Johansson, M., Vesterdal, L., Faituri, M., Sanborn, P., & Nilsson, M. (2013). Manganese Dynamics in decomposing needle and leaf litter a synthesis. *Canadian Journal of Forest Research*., 43(12),1127-1136.

28-Enez, K., Aricak, B., & Sariyildiz, T. (2015). Effects of harvesting activities on litter decomposition rates of scots pine, trojan fir, and sweet chestnut. Šumarski list. 139(7-8), 361-367.

29-Sariyildiz, T., & Anderson, J. M. (2003a). Interactions between litter quality, decomposition and soil fertility: a laboratory study. Soil Biol. Biochem., 35, 391-399.

30-Prescott, C. E. (2010). Litter decomposition: what controls it and how can we alter it to sequester more carbon in forest soils? Biogeochemistry, 101(1-3), 133- 149.

31-Jenny, H., Gessel, S. P., & Bingham, F. T. (1949). Comparative study of decomposition rates of organic matter in temperate and tropical regions. Soil Science, 68(6), 419-432.

32-Olson, J. S. (1963). Energy storage and the balance of producers and decomposers in ecological systems. Ecology, 14, 322-331.

33-Goetz, A. F., Vane, G., Solomon, J. E., & Rock, B. N. (1985). Imaging spectrometry for earth remote sensing. science, 228(4704), 1147-1153.

34- Schaepman, M. E. (2007). Spectrodirectional remote sensing: From pixels to processes. International Journal of Applied Earth Observation and Geoinformation, 9(2), 204-223.

35-Pignatti, S., Palombo, A., Pascucci, S., Romano, F., Santini, F., Simoniello, T., Umberto, A., Vincenzo, C., Acito, N., Diani, M., Matteoli, S., 2013. The PRISMA hyperspectral mission: Science activities and opportunities for agriculture and land monitoring. In 2013 IEEE International Geoscience and Remote Sensing Symposium-IGARSS, pp. 4558-4561, IEEE.

36-Chabrillat, S; Guanter, L.; Kaufmann, H.; Foerster, S.; Beamish, A. et al. (2022) EnMAP Science Plan. EnMAP Technical Report, GFZ Data Services. DOI: http://doi.org/10.48440/enmap.2022.001

37-Ustin, S. L., Roberts, D. A., Gamon, J. A., Asner, G. P., & Green, R. O. (2004). Using imaging spectroscopy to study ecosystem processes and properties. BioScience, 54(6), 523-534.

38-Melillo, J. M., Aber, J. D., & Muratore, J. F. (1982). Nitrogen and lignin control of hardwood leaf litter decomposition dynamics. Ecology, 63(3), 621-626.

39-Aber, J. D., Melillo, J. M., & McClaugherty, C. A. (1990). Predicting long-term patterns of mass loss, nitrogen dynamics, and soil organic matter formation from initial fine litter chemistry in temperate forest ecosystems. Canadian Journal of Botany, 68(10), 2201-2208.

40-McLellan, T. M., Martin, M. E., Aber, J. D., Melillo, J. M., Nadelhoffer, K. J., & Dewey, B. (1991). Comparison of wet chemistry and near infrared reflectance measurements of carbon-fraction chemistry and nitrogen concentration of forest foliage. Canadian Journal of Forest Research, 21(11), 1689-1693.

41-Curran, P. J. (1989). Remote sensing of foliar chemistry. Remote sensing of environment, 30(3), 271-278.

42-Ono, K., Hiraide, M., & Amari, M. (2003). Determination of lignin, holocellulose, and organic solvent extractives in fresh leaf, litterfall, and organic material on forest floor using near-infrared reflectance spectroscopy. Journal of Forest Research, 8(3), 191-198.

43-Daughtry, C. S. T., McMurtrey Iii, J. E., Nagler, P. L., Kim, M. S., & Chappelle, E. W. (1996). Spectral reflectance of soils and crop residues. Near infrared spectroscopy: The future waves, 505-510.

44-Daughtry, C. S. (2001). Discriminating crop residues from soil by shortwave infrared reflectance. Agronomy Journal, 93(1), 125-131.

45-Fourty, T., Baret, F., Jacquemoud, S., Schmuck, G., & Verdebout, J. (1996). Leaf optical properties with explicit description of its biochemical composition: direct and inverse problems. Remote sensing of Environment, 56(2), 104-117.

46- Serrano, L., Peñuelas, J., & Ustin, S. L. (2002). Remote sensing of nitrogen and lignin in Mediterranean vegetation from AVIRIS data: Decomposing biochemical from structural signals. Remote sensing of Environment, 81(2-3), 355-364.

47- Cao, X., Chen, J., Matsushita, B., & Imura, H. (2010). Developing a MODIS-based index to discriminate dead fuel from photosynthetic vegetation and soil background in the Asian steppe area. International Journal of Remote Sensing, 31(6), 1589-1604.

CHAPTER -6

IRON OXIDE NANOPARTICLES IN ANTIBACTERIAL APPLICATIONS

Selin ÇETER[1], Şuheda BOLAT[2], İdris YAZGAN[3]

1. INTRODUCTION

Nanotechnology has emerged as a transformative field with the potential to address challenges that cannot be effectively solved using conventional bulk materials, particularly in biomedical sciences [1]. At the heart of nanotechnology are nanomaterials, whose utilization can be traced back thousands of years, long before the concept itself was formally recognized. Historical evidence suggests that ancient civilizations inadvertently exploited nanoscale materials in various applications. For example, asbestos nanofibers were used to reinforce ceramic materials as early as 2500 BCE, while ancient Egyptians employed lead sulfide-based hair dyes and metallic nanoparticle-containing pigments for cosmetic and decorative purposes. Similarly, Roman and Egyptian artisans utilized colloidal metallic particles in glassmaking and coloration processes, unknowingly benefiting from nanoscale phenomena [2].The modern scientific development of nanotechnology began in the nineteenth century with the pioneering work of Michael Faraday, who reported the synthesis and optical properties of colloidal gold nanoparticles in 1857. Subsequent investigations into the size-dependent optical behavior of gold colloids at the beginning of the twentieth century provided early insights into the unique properties of nanomaterials and stimulated growing interest in the field [2]. However, the conceptual foundation of contemporary nanotechnology is generally attributed to Richard Feynman, whose visionary 1959 lecture, “There's Plenty of Room at the Bottom,” proposed the possibility of manipulating matter at the atomic and molecular scales. The term “nanotechnology” was later introduced by Norio Taniguchi in 1974 to describe precision manufacturing processes at the nanometer level [3].Significant

[1] MSc, Department of Biology, Faculty of Science, Kastamonu University, Turkiye, akdoganselin@gmail.com, (ORCID: 0000-0003-4379-7411)
[2] MSc, Department of Biology, Faculty of Science, Kastamonu University, Türkiye, suheda.bolat@outlook.com, (ORCID: 0009–0003-6414–9699)
[3] Prof. Dr., Department of Biology, Faculty of Science, Kastamonu University, Turkiye, iyazgan@kastamonu.edu.tr, (ORCID: 0000-0002-0264-1253)

technological advances during the late twentieth century accelerated the development of nanoscience and nanotechnology. The invention of scanning tunneling microscopy by researchers at IBM in 1981 enabled the direct visualization and manipulation of individual atoms, providing an unprecedented understanding of nanoscale structures. One of the most iconic demonstrations of atomic manipulation was achieved in 1989 when scientists arranged individual xenon atoms to create the IBM logo, illustrating the feasibility of constructing structures atom-by-atom [4]. These breakthroughs, together with the publication of the first dedicated books on nanotechnology and nanomedicine in the 1980s and 1990s, laid the foundation for the rapid expansion of nanotechnology into diverse scientific disciplines, including medicine, biotechnology, materials science, and environmental engineering.Nanomaterials are now essential to many technological fields, including materials science and biomedicine. They are commonly classified into carbon-based, organic, inorganic, and composite nanomaterials. Inorganic nanomaterials, particularly metal and metal oxide nanomaterials, are among the most widely utilized [5]. Metal oxide nanomaterials have gained significant interest because of their catalytic, sensing [6], and biological functions [7]. Among them, iron oxide nanoparticles (IONPs) are especially attractive owing to their biocompatibility, magnetic manipulability, ease of surface modification, Lewis acidic iron centers, and low cost [3]. These features have made IONPs promising candidates for biomedical applications, including the treatment of multidrug-resistant bacterial infections and the development of sensitive biosensors [8]. Iron oxide nanoparticles (IONPs) are generally categorized into three major forms: magnetite (Fe_3O_4), maghemite (γ-Fe_2O_3), and wüstite (FeO). Among these, magnetite and maghemite have attracted considerable attention owing to their excellent magnetic properties, biocompatibility, and broad applicability in antimicrobial research and biosensor development [8]. Numerous synthetic strategies have been employed for the preparation of IONPs, including sol–gel methods, microwave-assisted synthesis, chemical co-precipitation, hydrothermal, sonochemical, and biological approaches. Each method offers distinct advantages in terms of particle size control, morphology, crystallinity, scalability, and cost-effectiveness, making them suitable for specific applications [9]. This review focuses primarily on the magnetic characteristics and surface chemistry of IONPs, with particular emphasis on their emerging roles in antimicrobial applications.

2. ANTIMICROBIAL APPLICATIONS OF IRON OXIDE NANOPARTICLES

Antimicrobial resistance (AMR) has emerged as one of the most pressing global public health challenges since the widespread development and use of antibiotics. It is estimated that AMR-associated infections could account for more than 10 million deaths annually by 2050 if effective intervention strategies are not implemented [8]. Consequently, there is an urgent need for rapid, reliable, and innovative approaches to prevent and combat resistant microbial infections. Among the various alternatives under investigation, iron oxide nanoparticles (IONPs) have attracted considerable attention owing to their excellent biocompatibility, tunable surface properties, controllable crystalline structures, capacity to catalyze Fenton-like reactions, generation of reactive oxygen species (ROS), adaptability to photodynamic and photothermal therapeutic approaches, and ability to release bioactive iron ions. These unique physicochemical characteristics make IONPs promising candidates for the development of next-generation antimicrobial strategies. Before discussing the potential antibacterial applications and mechanisms of IONPs, the significance and global impact of AMR are briefly outlined below.

2.1 The Importance of Antimicrobial Resistance

Although bacterial infections are thought to be as old as human civilization itself, our scientific understanding of bacteria began much later. The first direct observations of bacteria were made by Anton van Leeuwenhoek in 1683 using a microscope. Subsequently, in 1854, John Snow demonstrated the relationship between contaminated drinking water and the spread of cholera, and in 1876, Robert Koch established the microbial basis of infectious diseases through his pioneering work on germ theory. Numerous studies conducted in the following decades facilitated the identification and characterization of bacterial species, while the discovery of penicillin by Alexander Fleming in 1929 marked the beginning of the antibiotic era [10]. Earlier antimicrobial approaches, including the use of pyocins and the development of sulfonamides, emerged during the early twentieth century and represented some of the first targeted strategies against bacterial infections [11]. The widespread development and extensive use of antibiotics have dramatically improved the treatment of bacterial infections; however, they have also contributed to the emergence and dissemination of antibiotic-resistant bacterial strains. Although bacterial resistance was recognized as early as the 1910s [11], the first documented reports describing multidrug-resistant (MDR) bacteria appeared in the 1960s [12]. For many decades, the primary strategy to combat MDR bacterial infections relied on the continuous development of novel and more potent antibiotics. Nevertheless, the remarkable diversity of bacterial resistance mechanisms and the ability of

resistance determinants to spread between bacterial species have significantly undermined the long-term effectiveness of these drugs. As a result, antibiotics considered highly effective today may rapidly become less potent or even obsolete in the future. Multidrug resistance is commonly defined as the ability of a bacterial strain to resist three or more classes of antimicrobial agents, although the term is also frequently applied to pathogens that exhibit resistance to the most effective antibiotics available in clinical [13]. According to the World Health Organization (WHO), the spread of MDR bacteria is among the ten most significant threats to global public health [14]. WHO estimates indicate that approximately 50 million cases of sepsis were reported worldwide in 2017, resulting in nearly 11 million deaths [15]. In addition to the substantial human toll, MDR infections impose a considerable economic burden, with treatment costs reaching approximately USD 50,000 per patient in some cases [16]. Failure to develop effective therapies against resistant bacterial infections is projected to result in millions of additional deaths and an estimated cumulative economic loss of nearly USD 100 trillion by 2050 [17]. In the United States alone, healthcare expenditures associated with MDR infections were estimated at USD 4.6 billion in 2017, with the highest per-patient treatment costs attributed to infections caused by carbapenem-resistant *Acinetobacter baumannii* (CRAB) strains [18].

2.2. Current Status and Challenges of Using IONPs as AMR-Targeting Agents

The growing prevalence of multidrug-resistant (MDR) bacterial infections has intensified the search for alternative antimicrobial strategies beyond conventional antibiotics. Among the various nanomaterials investigated, iron oxide nanoparticles (IONPs) have emerged as promising candidates owing to their intrinsic antimicrobial properties, biocompatibility, magnetic responsiveness, and ease of surface functionalization. Similar to many inorganic nanomaterials, IONPs can exert antibacterial effects through both passive and active targeting mechanisms. Passive targeting refers to the ability of nanoparticles to accumulate and interact with bacterial cells through their physicochemical properties, including size, surface charge, hydrophobicity, and permeability within biological environments. In contrast, active targeting involves the selective recognition of bacterial cells or tissues through specific ligand–receptor interactions [19].

For in situ applications such as wound dressings, catheters, and implant coatings, active targeting may also be achieved through the application of external magnetic fields when magnetic IONPs are employed. This strategy enables localized accumulation of nanoparticles at infection sites, thereby enhancing therapeutic efficacy while minimizing systemic exposure [20]. Both superparamagnetic iron

oxide nanoparticles (SPIONs) and wüstite iron oxide nanostructures have demonstrated significant antibacterial potential through distinct mechanisms [21,22]. Gao *et al* (2020) showed that alternating the external magnetic field applied to the IONPs on wounded area of mice brought out strong antibacterial activity [23]. One of the earliest demonstrations of magnetically guided antibacterial therapy was reported by Subbiahdoss *et al.* (2012), who synthesized bare SPIONs as well as surface-functionalized derivatives coated with carboxyethylsilanetriol (CES), aminopropyltriethoxysilane (APTES), and o-(2-aminoethyl)-o′-methylpolyethylene glycol (PEG). Following gentamicin conjugation, all nanoparticle formulations exhibited antibacterial activity against bacterial biofilms under magnetic guidance. Notably, CES-coated SPIONs achieved approximately eightfold greater antibacterial efficacy than free gentamicin. Interestingly, despite possessing comparable particle sizes (~14 nm), bare SPIONs exhibited a positive zeta potential of approximately +43 mV, whereas CES-coated particles displayed a negative zeta potential of approximately –15 mV [24]. The superior antibacterial activity of CES-coated particles suggests that surface chemistry may play a more significant role than electrostatic interactions alone, challenging the common assumption that higher positive surface charge necessarily correlates with enhanced antibacterial activity [25,26]. Besides, Shoudho *et al* (2024) reviewed the physicochemical characteristics role in the antibacterial activity of IONPs, which clearly shows that it is not easily possible to attain the observed antibacterial activity to a specific parameter since size, shape, morphology, surface chemistry and synthesis procedure including the precursors play role for the observed activity [27]. The importance of surface chemistry has been further highlighted by several subsequent studies [28]. Ismail *et al.* (2015) synthesized SPIONs via laser ablation in different media and demonstrated that variations in synthesis conditions significantly affected antibacterial performance. Nanoparticles prepared in dimethylformamide (DMF) exhibited stronger antibacterial activity against both Gram-positive *Staphylococcus aureus* and Gram-negative *Escherichia coli* compared with particles synthesized in distilled water or aqueous sodium dodecyl sulfate solutions [29]. Similarly, Tedjani *et al.* (2022) synthesized IONPs using *Moringa oleifera* leaf extracts and reported that antibacterial efficacy varied with extract concentration, despite the presence of chemically similar phytochemical constituents on the nanoparticle surface [30]. These observations suggest that differences in surface ligand density, oxidation state, molecular orientation, or accessibility may substantially influence antibacterial performance.Green synthesis approaches have also produced highly active antibacterial IONPs despite of the fact that Ali *et al.* (2025) compared chemically synthesized and green-synthesized IONPs and concluded that chemically synthesized nanoparticles exhibited superior antibacterial efficacy while maintaining

acceptable in vivo biocompatibility [31]. However, the literature also shows that green IONPs could show higher antibacterial activity compared to chemically synthesized IONPs, which can be related to the selection of the plant species or bio-component. Also, it should be mentioned that green IONPs provide better biocompatibility for living cells [32]. Zakariya *et al.* (2022) employed *Penicillium* spp. filtrates to synthesize IONPs with diameters ranging from approximately 3–10 nm and a zeta potential of +33.9 mV. These nanoparticles exhibited antibacterial activities comparable to those of ciprofloxacin and gentamicin against *Staphylococcus aureus*, *Escherichia coli*, *Klebsiella pneumoniae*, *Pseudomonas aeruginosa*, and *Shigella sonnei*. However, detailed surface characterization was not performed, making it difficult to identify the specific surface-associated compounds responsible for the observed activity [33]. Likewise, Madubuonu *et al*. (2020) demonstrated concentration-dependent antibacterial effects of *Psidium guajava* extract-mediated IONPs against both *E. coli* and *S. aureus* [34].In addition to their intrinsic antibacterial activity, IONPs have shown considerable promise as drug delivery vehicles. Caamaño *et al.* (2016) reported that erythromycin-loaded IONPs exhibited enhanced antibacterial activity relative to free erythromycin, primarily because nanoparticle-mediated delivery facilitated antibiotic penetration through bacterial capsules. Such findings highlight the dual functionality of IONPs as both antimicrobial agents and antibiotic delivery platforms [35]. It is critical to bear in mind that the components of IONPs can interact with bacterial cell membrane, proteins in cytoplasm, DNA and interfere with nuclear material of the bacteria [36,37]. Therefore, IONPs synergistically improve the antibacterial activity of the carried drug. Compositional modifications have also been explored to improve antibacterial efficacy. Abdelghany *et al.* (2025) demonstrated that silver-doped IONPs synthesized using *Pseudomonas aeruginosa* KB1 supernatants exhibited superior antibacterial activity against *E. coli* and *K. pneumoniae* compared with non-doped IONPs. The enhancement was attributed to the well-established antimicrobial properties of silver ions acting synergistically with iron oxide-mediated mechanisms [37]. Similarly, Situ *et al* (2014) reported Iron oxide/nanocarbon chain particles using paramagnetic wüstite precursors, which reduced the treatment time for the removal of bacterial viability [38]. Actually, this is the first study using paramagnetic IONPs to develop antibacterial IONPs (the final form is magnetic). Later on, Abid *et al* (2022) developed a wüstite phase IONPs synthesized with trigonella extract, that showed stronger antibacterial activity against *E. coli* and *S. aureus* [22].

Surface functionalization with biologically relevant ligands offers another strategy to improve bacterial targeting. Saladino *et al.* (2021) coated microwave-synthesized SPIONs with carbohydrate derivatives and demonstrated that carbohydrate–lectin interactions could selectively direct nanoparticles toward

specific bacterial strains. Such targeting strategies are particularly attractive because they exploit naturally occurring recognition pathways while potentially reducing off-target effects [39]. The study can be placed into *active targeting* approach since it relies on carbohydrate-lectin interaction. In this manner, Vignesh *et al* (2015) reported the coating of IONPs with bacterial exopolysaccharides, which improved the antibacterial activity for *Aeromonas* spp. [40]. It is known that exopolysaccharides are composed of repeating sugar residues and non-sugar compounds [41] and carbohydrate-carbohydrate interaction plays role in ligand-receptor interaction in addition to the ligand-lectin interactions [42]. In addition to carbohydrates, aptamers were shown to be used for active targeting. Kang *et al* (2023) reported the development of aptamer-gold coated IONPs that can selectively recognize bacterial species (e.g. *S. aureus*) and effectively kill them under photodynamic therapy [43]. Recent studies have also explored the use of iron oxide-based nanostructures in combination with photodynamic therapies. Hammad *et al.* (2025) compared iron oxide supraparticles (IOSPs) with conventional IONPs and found that IOSPs possessed enhanced peroxidase-like catalytic activity, stronger antibacterial effects, and improved biocompatibility [44]. These findings suggest that hierarchical iron oxide architectures may offer advantages over conventional nanoparticles in reactive oxygen species-mediated antibacterial applications.Further enhancement of bacterial interactions has been achieved through surface engineering strategies. Daramola *et al.* (2025) modified gold-decorated IONPs with positively charged olyethyleneimine/polyethylene glycol coatings to strengthen electrostatic interactions with bacterial membranes [45]. While this approach demonstrated enhanced bacterial binding, its clinical applicability may be more suitable for localized wound-healing applications rather than systemic antimicrobial therapies due to concerns regarding polymer-associated toxicity and biodistribution. It is also noteworthy to mention that surface coating must be optimized not to prevent possible Fenton reaction formation (for example excess oleic acid decreases the Fenton reaction rate [46]), which enhances the antibacterial activity. Fenton reactions triggered by IONPs can also indirectly enhance the antibacterial activity, which was shown by stimulation of macrophage's ability to capture bacterial cells in an in vitro model study [47]. Fenton reactions elevates the production of ROS that is critical for the antibacterial activity [48]. Recently, Huang *et al* (2026) reported heme containing IONPs showing excellent antibacterial activity, tested for *S. aureus* persister cells, through release of heme group and Fe^{2+} ions that turn into elevation of reactive oxygen species resulted from Fenton reaction [49]. The incorporation of additional antimicrobial agents onto IONPs has also yielded promising results. Panigrahi *et al.* (2023) developed nisin-loaded chitosan-coated IONPs and demonstrated enhanced reactive oxygen species production, membrane disruption, and cytoplasmic leakage

compared with free nisin or unmodified IONPs. Consequently, the composite nanoparticles exhibited superior antibacterial activity against both Gram-positive and Gram-negative bacteria [50]. In this manner, Zhang *et al* (2012) reported conjugation of Bacitracin to SPIONs elevated the antibacterial activity compared to free Bacitracin for both gram (+) and gram (-) bacterial species [51]. Likewise, Sharaf *et al.* (2022) reported that rhamnolipid-coated IONPs loaded with coumaric acid and gallic acid strongly interacted with bacterial cells, inducing genetic alterations that suppressed biofilm formation and promoted bacterial cell death [52]. Surprisingly, conjugation/loading of the potent antibacterial agents including antibiotics to the IONPs lessen their cytotoxicity, which is a push to implement these particles for real applications. The coatings, also, improve the stability, surface characteristics and delivery [27].

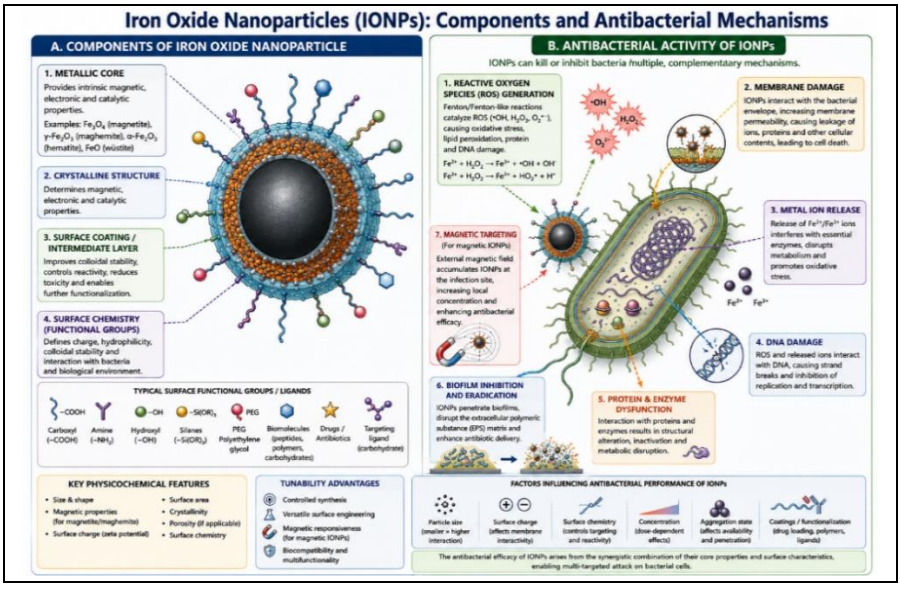

Figure 1: Schematic Representation of Iron Oxide Nanoparticle Architecture and Their Antibacterial Modes of Action. *Created with AI-assisted graphic generation (OpenAI ChatGPT) and adapted by the authors*.

Collectively, these studies demonstrate that the antibacterial efficacy of IONPs is strongly influenced by multiple parameters, including particle size, morphology, magnetic properties, surface chemistry, coating composition, and functional cargo at figure -1. Among these factors, surface chemistry appears to play a particularly critical role, often outweighing the influence of particle charge alone. Despite the encouraging progress achieved thus far, substantial challenges remain regarding mechanistic understanding, standardization of synthesis

methods, comprehensive surface characterization, long-term biosafety assessment, and translation from laboratory-scale studies to clinically relevant applications. Addressing these challenges will be essential for realizing the full potential of IONPs as next-generation antimicrobial agents against MDR bacterial infections.

3. CONCLUSION

The growing burden of antimicrobial resistance demands the development of innovative therapeutic approaches capable of complementing or replacing conventional antibiotics. Iron oxide nanoparticles have emerged as highly promising antimicrobial platforms owing to their multifunctional properties, including magnetic responsiveness, biocompatibility, catalytic activity, and versatile surface chemistry. The studies discussed in this review demonstrate that IONPs can inhibit bacterial growth through multiple mechanisms, including ROS generation, membrane disruption, biofilm eradication, targeted drug delivery, and magnetic-field-assisted localization. Importantly, antibacterial performance is not determined solely by particle size or surface charge but is strongly influenced by surface functionalization, coating composition, and nanoparticle architecture. Advances in green synthesis, hybrid nanocomposites, metal doping, and ligand-mediated targeting have further expanded the antimicrobial potential of IONPs against a broad range of clinically relevant pathogens.Despite encouraging laboratory-scale results, several challenges must be addressed before widespread clinical implementation can be achieved. Standardization of synthesis procedures, comprehensive characterization of surface properties, long-term biosafety studies, and detailed investigations of antibacterial mechanisms remain critical research priorities. Future efforts should also focus on improving targeting specificity, minimizing host toxicity, and evaluating efficacy in clinically relevant infection models. With continued interdisciplinary research, IONPs hold substantial promise as next-generation antimicrobial agents capable of contributing to the global fight against multidrug-resistant bacterial infections.

While current antibacterial IONP research has predominantly focused on ROS generation, membrane disruption, and antibiotic delivery, emerging evidence suggests that glycan-functionalized IONPs may provide a more selective approach toward bacterial targeting. By exploiting carbohydrate–lectin interactions, these systems may enhance bacterial recognition, improve local nanoparticle accumulation, reduce off-target effects, and potentially interfere with bacterial adhesion and biofilm formation. Future research should therefore focus on understanding how glycan structure, density, presentation, and multivalency influence the antibacterial performance of IONP-based nanoplatforms.

REFERENCES

[1] H.F. Hetta, Y.N. Ramadan, A.I. Al-Harbi, E. A. Ahmed, B. Battah, N.H. Abd Ellah, S. Zanetti, M.G. Donadu, Nanotechnology as a Promising Approach to Combat Multidrug Resistant Bacteria: A Comprehensive Review and Future Perspectives, Biomedicines 11 (2023) 413. https://doi.org/10.3390/biomedicines11020413.

[2] S. Khan, S. Mansoor, Z. Rafi, B. Kumari, A. Shoaib, M. Saeed, S. Alshehri, M.M. Ghoneim, M. Rahamathulla, U. Hani, F. Shakeel, A review on nanotechnology : Properties , applications , and mechanistic insights of cellular uptake mechanisms, J. Mol. Liq. 348 (2022) 118008. https://doi.org/10.1016/j.molliq.2021.118008.

[3] M. Schneider, J. Otarola, E. Vakarelska, V. Simeonov, M. Nedyalkova, Biomedical Applications of Iron Oxide Nanoparticles : Current Insights Progress and Perspectives, Pharmaceutics 14 (2022) 204.

[4] A.P. Nikalje, Nanotechnology and its Applications in Medicine, Med. Chem. (Los. Angeles). 5 (2015) 81–89. https://doi.org/10.4172/2161-0444.1000247.

[5] B. Mekuye, Nanomaterials : An overview of synthesis , classification , characterization , and applications, Nano Sel. 4 (2023) 486–501. https://doi.org/10.1002/nano.202300038.

[6] P. Kannan, G. Maduraiveeran, Metal Oxides Nanomaterials and Nanocomposite-Based Electrochemical Sensors for Healthcare Applications, Biosens 13 (2023) 542.

[7] J. Prakash, S. Babu, N. Krishna, P. Kumar, V. Kumar, K.S. Ghosh, H.C. Swart, S. Bellucci, J. Cho, Recent Advances on Metal Oxide Based Nano-Photocatalysts as Potential Antibacterial and Antiviral Agents, Catalysts 12 (2022) 1047.

[8] N.T. Tasnim, N. Ferdous, M.H. Rumon, S. Shakil, The Promise of Metal-Doped Iron Oxide Nanoparticles as Antimicrobial Agent, ACS Omega 9 (2024) 16–32. https://doi.org/10.1021/acsomega.3c06323.

[9] A. Ali, H. Zafar, M. Zia, I. Haq, A.R. Phull, J.S. Ali, A. Hussain, Synthesis, characterization, applications, and challenges of iron oxide nanoparticles, Nanotechnol. Sci. Appl. 6 (2016) 49–67. https://doi.org/10.2147/NSA.S99986.

[10] J. Lederberg, Infectious History, Science (80-.). 288 (2000) 287–293. https://doi.org/10.1126/science.288.5464.287.

[11] S. Walesch, J. Birkelbach, G. Jézéquel, F.P.J. Haeckl, J.D. Hegemann, T. Hesterkamp, A.K.H. Hirsch, P. Hammann, R. Müller, Fighting antibiotic resistance—strategies and (pre)clinical developments to find new

antibacterials, EMBO Rep. 24 (2023) e56033. https://doi.org/10.15252/embr.202256033.

[12] E.J. Klemm, V.K. Wong, G. Dougan, Emergence of dominant multidrug-resistant bacterial clades: Lessons from history and whole-genome sequencing, Proc. Natl. Acad. Sci. U. S. A. 115 (2018) 12872–12877. https://doi.org/10.1073/pnas.1717162115.

[13] A.P. Magiorakos, A. Srinivasan, R.B. Carey, Y. Carmeli, M.E. Falagas, C.G. Giske, S. Harbarth, J.F. Hindler, G. Kahlmeter, B. Olsson-Liljequist, D.L. Paterson, L.B. Rice, J. Stelling, M.J. Struelens, A. Vatopoulos, J.T. Weber, D.L. Monnet, Multidrug-resistant, extensively drug-resistant and pandrug-resistant bacteria: An international expert proposal for interim standard definitions for acquired resistance, Clin. Microbiol. Infect. 18 (2012) 268–281. https://doi.org/10.1111/j.1469-0691.2011.03570.x.

[14] A. Algammal, H.F. Hetta, M. Mabrok, P. Behzadi, Editorial: Emerging multidrug-resistant bacterial pathogens "superbugs": A rising public health threat, Front. Microbiol. 14 (2023). https://doi.org/10.3389/fmicb.2023.1135614.

[15] N. Osman, N. Devnarain, C.A. Omolo, V. Fasiku, Y. Jaglal, T. Govender, Surface modification of nano-drug delivery systems for enhancing antibiotic delivery and activity, Wiley Interdiscip. Rev. Nanomedicine Nanobiotechnology 14 (2022) 1–24. https://doi.org/10.1002/wnan.1758.

[16] J.M. V. Makabenta, A. Nabawy, C.H. Li, S. Schmidt-Malan, R. Patel, V.M. Rotello, Nanomaterial-based therapeutics for antibiotic-resistant bacterial infections, Nat. Rev. Microbiol. 19 (2021) 23–36. https://doi.org/10.1038/s41579-020-0420-1.

[17] T. Kebede, E. Gadisa, A. Tufa, Antimicrobial activities evaluation and phytochemical screening of some selected medicinal plants: A possible alternative in the treatment of multidrug-resistant microbes, PLoS One 16 (2021) 1–16. https://doi.org/10.1371/journal.pone.0249253.

[18] R.E. Nelson, K.M. Hatfield, H. Wolford, M.H. Samore, R.D. Scott, S.C. Reddy, B. Olubajo, P. Paul, J.A. Jernigan, J. Baggs, National estimates of healthcare costs associated with multidrug-resistant bacterial infections among hospitalized patients in the United States, Clin. Infect. Dis. 72 (2021) S17–S26. https://doi.org/10.1093/cid/ciaa1581.

[19] N. Schleich, C. Po, D. Jacobs, B. Ucakar, B. Gallez, F. Danhier, V. Préat, Comparison of active , passive and magnetic targeting to tumors of multifunctional paclitaxel / SPIO-loaded nanoparticles for tumor imaging and therapy, J. Control. Release 194 (2014) 82–91. https://doi.org/10.1016/j.jconrel.2014.07.059.

[20] Z. Lu, D. Yu, F. Nie, Y. Wang, Iron Nanoparticles Open Up New Directions for Promoting Healing in Chronic Wounds in the Context of Bacterial Infection, Pharmaceutics 15 (2023) 2327.

[21] R. Prucek, L. Kvítek, J. Filip, M. Kolá, R. Zbo, The targeted antibacterial and antifungal properties of magnetic nanocomposite of iron oxide and silver nanoparticles s Paná, Biomaterials 32 (2011) 4704–4713. https://doi.org/10.1016/j.biomaterials.2011.03.039.

[22] M.A. Abid, D.A. Kadhim, W.J. Aziz, Iron oxide nanoparticle synthesis using trigonella and tomato extracts and their antibacterial activity, Mater. Technol. 37 (2022) 547–554. https://doi.org/10.1080/10667857.2020.1863572.

[23] F. Gao, X. Li, T. Zhang, A. Ghosal, G. Zhang, H. Ming, Iron nanoparticles augmented chemodynamic e ff ect by alternative magnetic fi eld for wound disinfection and healing, J. Control. Release 324 (2020) 598–609. https://doi.org/10.1016/j.jconrel.2020.06.003.

[24] G. Subbiahdoss, S. Sharifi, D.W. Grijpma, S. Laurent, H.C. Van Der Mei, M. Mahmoudi, H.J. Busscher, Magnetic targeting of surface-modified superparamagnetic iron oxide nanoparticles yields antibacterial efficacy against biofilms of gentamicin-resistant staphylococci, Acta Biomater. 8 (2012) 2047–2055. https://doi.org/10.1016/j.actbio.2012.03.002.

[25] S. Vihodceva, A. Šutka, M. Sihtmäe, M. Rosenberg, M. Otsus, I. Kurvet, K. Smits, L. Bikse, A. Kahru, K. Kasemets, Antibacterial Activity of Positively and Negatively Charged Hematite (α -Fe2O3) Nanoparticles to Escherichia coli , Staphylococcus aureus and Vibrio fischeri, Nanomaterials 11 (2021) 652.

[26] W. Du, S. Niu, Y. Xu, Z. Xu, C. Fan, Antibacterial activity of chitosan tripolyphosphate nanoparticles loaded with various metal ions, Carbohydr. Polym. 75 (2009) 385–389. https://doi.org/10.1016/j.carbpol.2008.07.039.

[27] K.N. Shoudho, S. Uddin, M.H. Rumon, S. Shakil, Influence of Physicochemical Properties of Iron Oxide Nanoparticles on Their Antibacterial Activity, ACS Omega 9 (2024) 33303−33334. https://doi.org/10.1021/acsomega.4c02822.

[28] X. Li, J. Niu, L. Deng, Y. Yu, L. Zhang, Q. Chen, J. Zhao, B. Wang, H. Gao, Amphiphilic polymeric nanodrug integrated with superparamagnetic iron oxide nanoparticles for synergistic antibacterial and antitumor therapy of colorectal cancer, Acta Biomater. 173 (2024) 432–441. https://doi.org/10.1016/j.actbio.2023.11.019.

[29] R.A. Ismail, G.M. Sulaiman, S.A. Abdulrahman, T.R. Marzoog, Antibacterial activity of magnetic iron oxide nanoparticles synthesized by

laser ablation in liquid, Mater. Sci. Eng. C 53 (2015) 286–297. https://doi.org/10.1016/j.msec.2015.04.047.

[30] M.L. Tedjani, A. Khelef, S.E. Laouini, A. Bouafia, Optimizing the Antibacterial Activity of Iron Oxide Nanoparticles Using Central Composite Design, J. Inorg. Organomet. Polym. Mater. 32 (2022) 3564–3584. https://doi.org/10.1007/s10904-022-02367-0.

[31] A.M. Ali, H.J. Hill, G.E. Elkhouly, N.R. Raya, N.F. Tawfik, M.R. Bakkar, A.B. El-basaty, Z. Stamataki, Y. Abo-zeid, Green and chemical synthesis of iron oxide nanoparticles : Comparative study for antimicrobial activity and toxicity concerns, J. Drug Deliv. Sci. Technol. 103 (2025) 106434.

[32] M. Junaid, H. Dowlath, S. Anjum, S.B.M. Khalith, S. Varjani, S. Kumar, G. Munuswamy, S. Woong, W. Jin, B. Ravindran, Comparison of characteristics and biocompatibility of green synthesized iron oxide nanoparticles with chemical synthesized nanoparticles, Environ. Res. 201 (2021) 111585. https://doi.org/10.1016/j.envres.2021.111585.

[33] N.A. Zakariya, S. Majeed, W. Ha, Investigation of antioxidant and antibacterial activity of iron oxide nanoparticles (IONPS) synthesized from the aqueous extract of, Sensors Int. 3 (2022) 100164. https://doi.org/10.1016/j.sintl.2022.100164.

[34] N. Madubuonu, S.O. Aisida, I. Ahmad, S.B. Ting, M. Maaza, Bio-inspired iron oxide nanoparticles using Psidium guajava aqueous extract for antibacterial activity, Appl. Phys. A 126 (2020) 72. https://doi.org/10.1007/s00339-019-3249-6.

[35] M.A. Caamaño, M. Carrillo-morales, J.D.J. Olivares-trejo, Iron Oxide Nanoparticle Improves the Antibacterial Activity of Erythromycin, J. Bacteriol. Parasitol. 7 (2016) 1000267. https://doi.org/10.4172/2155-9597.1000267.

[36] S. Sinha, R. Sharma, R. Ansari, R. Singh, Multifunctional oleic acid functionalized iron oxide nanoparticles for antibacterial and dye, Mater. Adv. 6 (2025) 2253–2268. https://doi.org/10.1039/d5ma00036j.

[37] S. Abdelghany, A. Elsayed, H. Kabary, H. Salaheldin, Iron oxide/silver-doped iron oxide nanoparticles : facile synthesis, characterization, antibacterial activity, genotoxicity and anticancer evaluation, Sci. Rep. 15 (2025) 29593.

[38] S.F. Situ, A.C.S. Samia, Highly Efficient Antibacterial Iron Oxide@Carbon Nanochains from Wüstite Precursor Nanoparticles, ACS Appl. Mater. Interfaces 6 (2014) 20154−20163.

[39] G.M. Saladino, B. Hamawandi, M.A. Demir, I. Yazgan, M.S. Toprak, A versatile strategy to synthesize sugar ligand coated superparamagnetic iron

oxide nanoparticles and investigation of their antibacterial activity, Colloids Surfaces A Physicochem. Eng. Asp. 613 (2021) 126086. https://doi.org/10.1016/j.colsurfa.2020.126086.

[40] V. Vignesh, G. Sathiyanarayanan, G. Sathishkumar, K. Parthiban, K. Sathish-kumar, R. Thirumurugan, Formulation of iron oxide nanoparticles using exopolysaccharide : evaluation of their antibacterial and anticancer activities †, RSC Adv. 5 (2015) 27794–27804. https://doi.org/10.1039/c5ra03134f.

[41] H. Li, Y. Jin, H. Li, J. Zhao, C. Stanton, R.P. Ross, W. Chen, B. Yang, Understanding Exopolysaccharides from Lactic Acid Bacteria: Synthesis, Functions, and Applications, J. Agric. Food Chem. 73 (2025) 22110−22132. https://doi.org/10.1021/acs.jafc.5c04613.

[42] A. Chandra, A. Gimeno, M. Pay, P. Ravindra, V. Mahida, J. Jim, European Journal of Medicinal Chemistry Rational design of heparin antagonist : Guanidine-based mimetics unveil key carbohydrate-carbohydrate interactions, Eur. J. Med. Chem. 305 (2026) 118551. https://doi.org/10.1016/j.ejmech.2025.118551.

[43] Q. Kang, X. Xing, S. Zhang, L. He, J. Li, J. Jiao, S. Wang, A novel Aptamer-induced CHA amplification strategy for ultrasensitive detection of Staphylococcus aureus and NIR-triggered photothermal bactericidal Activity based on aptamer-modified magnetic Fe 3 O 4 @ AuNRs, Sensors Actuators B. Chem. 382 (2023) 133554. https://doi.org/10.1016/j.snb.2023.133554.

[44] M. Hammad, A. Amin, C. Ursu, I. Rosca, D. Peptanariu, L. Qian, V. Nica, S. Hardt, H. Wiggers, D. Segets, Hierarchical assembly of iron-oxide supraparticles for enhanced photothermal antibacterial activity, Colloid Interface Sci. Commun. 67 (2025) 100843.

[45] O.B. Daramola, N. Torimiro, R. Chinedu, Affinity Capture Using Ligand and Polymer - Functionalized Iron Oxide , Gold and Iron - Gold Nanocomposites to Target Enteric Bacteria, Bionanoscience 15 (2025) 8. https://doi.org/10.1007/s12668-024-01682-9.

[46] W. Aadinath, V. Muthuvijayan, Influence of oleic acid coating on the magnetic susceptibility and Fenton reaction-mediated ROS generation by the iron oxide nanoparticles In fl uence of oleic acid coating on the magnetic susceptibility and Fenton reaction-mediated ROS generation by the, Nano Express 5 (2024) 015017.

[47] B. Yu, Z. Wang, L. Almutairi, S. Huang, M. Kim, Harnessing iron-oxide nanoparticles towards the improved bactericidal activity of macrophage against Staphylococcus aureus, Nanomedicine Nanotechnology, Biol.

Med. 24 (2020) 102158. https://doi.org/10.1016/j.nano.2020.102158.
[48] F. Batool, M.S. Iqbal, S.U.D. Khan, J. Khan, B. Ahmed, M.I. Qadir, Biologically synthesized iron nanoparticles (FeNPs) from Phoenix dactylifera have anti-bacterial activities, Sci. Rep. 11 (2021) 22132. https://doi.org/10.1038/s41598-021-01374-4.
[49] M. Huang, Q. Li, H. Du, Heme-loaded iron oxide nanoparticles synergistically eradicate Staphylococcus aureus Persister cells via activating Persister metabolism and Fenton reaction, Mater. Lett. 412 (2026) 140388. https://doi.org/10.1016/j.matlet.2026.140388.
[50] L.L. Panigrahi, S. Shekhar, B. Sahoo, M. Arakha, RSC Advances coated iron oxide nanoparticles fosters oxidative stress triggering bacterial cell death †, RSC Adv. 13 (2023) 25497–25507. https://doi.org/10.1039/d3ra04070d.
[51] W. Zhang, X. Shi, J. Huang, Y. Zhang, Z. Wu, Bacitracin-Conjugated Superparamagnetic Iron Oxide Nanoparticles : Synthesis , Characterization and Antibacterial Activity, ChemPhysChem 13 (2012) 3388–3396. https://doi.org/10.1002/cphc.201200161.
[52] M. Sharaf, A.H. Sewid, H.I. Hamouda, M.G. Elharrif, A.S. El-Demerdash, A. Alharthi, NadaHashim, A.A. Hamad, S. Selim, D.H.M. Alkhalifah, W.N. Hozzein, M. Abdalla, T. Saber, Rhamnolipid-Coated Iron Oxide Nanoparticles as a Novel Multitarget Candidate against Major Foodborne E. coli Serotypes and Methicillin-Resistant S. aureus, Microbiol. Spectr. 10 (2022) e00250-22.

CHAPTER -7

FOOD CHEMISTRY ASPECTS OF BEE POLLEN

Serhat KARABICAK[1], Oktay BIYIKLIOĞLU[2]

1. INTRODUCTION

Pollen grains, which carry the male reproductive material of flowering plants, can travel across continents after being released from the anther due to the influence of various abiotic factors. Each pollen grain is a gametophyte consisting of a few cells, including an exine (formed with the participation of the sporophyte), an intine (of gametophyte origin), and shared cell walls. While pollen development begins within the anther, it can continue until the formation of the pollen tube as the pollen grain adheres to the stigma. Although this varies among species, the full development of pollen grains can take anywhere from a few days to several months. The ability of pollen grains to remain viable during this long journey can be explained by the complex structure of their physicochemical properties [1].

The robust structure of pollen grains makes them an important food source for many organisms. Pollen can be collected from plants in various ways. Generally, it can be collected directly from trees with high pollen production, such as those in the Pinaceae family, or through traps placed in beehives (bee pollen) [2].

Pollen is the male reproductive unit of seed plants and is produced within the anthers of flowering plants and gymnosperms. Each pollen grain is surrounded by a highly specialized wall composed of an inner layer (intine), primarily consisting of cellulose and pectin, and an outer layer (exine), which is largely formed from sporopollenin, one of the most chemically resistant biopolymers found in nature [3]. This multilayered structure protects the cellular contents of pollen against environmental stresses such as ultraviolet radiation, temperature fluctuations, dehydration, and microbial attack, enabling pollen grains to remain viable during dispersal and reproduction [4]. Following release from the anther, pollen grains can be transported over short or long distances by wind, water, insects, and other vectors. The remarkable durability of pollen is largely attributed to its unique physicochemical characteristics and the protective

[1] PhD, Department of Biology, Faculty of Science, Kastamonu University, Turkiye, serhatkarabicak@gmail.com, (ORCID: 0009-0004-7404-6471)

[2] PhD, Department of Biology, Faculty of Science, Kastamonu University, Turkiye, oktayman@gmail.com, (ORCID: 0000-0003-4238-931X)

properties of the exine layer. These structural features not only ensure reproductive success in plants but also contribute to the preservation of the diverse nutrients and bioactive compounds contained within pollen grains [1].

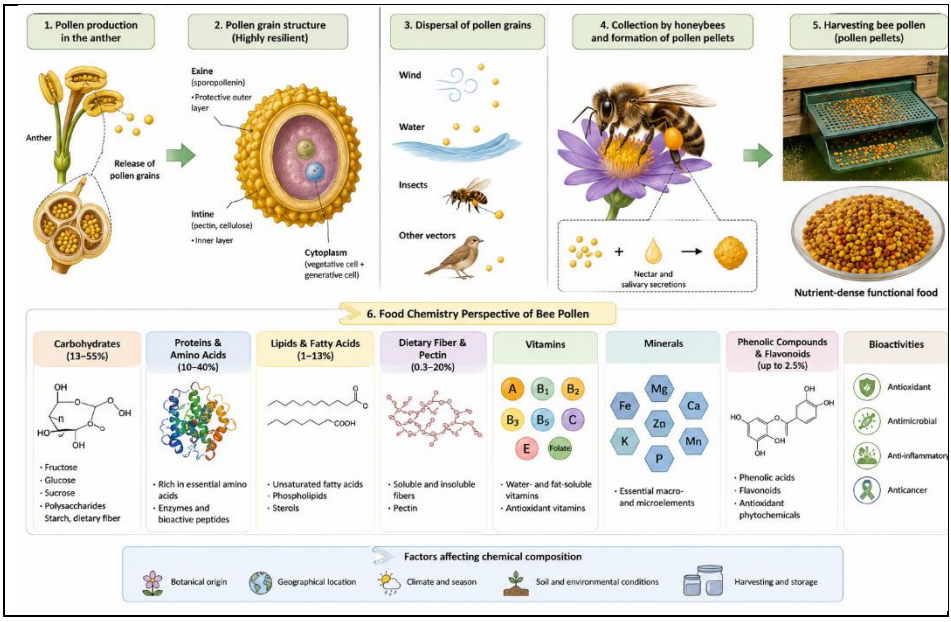

Figure1. From pollen grain to bee pollen: Structure, collection and food chemistry perspective

Due to its rich nutritional composition and resilience, pollen serves as an important food source for numerous organisms. Pollen intended for human consumption can be collected directly from highly productive plant species, such as members of the Pinaceae family, or more commonly as bee pollen through traps installed at the entrances of beehives. During collection, honeybees agglomerate pollen grains with nectar and salivary secretions, producing pollen pellets that are subsequently harvested and utilized as a nutrient-dense functional food [2].

2. BEE POLLEN

The use of bee pollen by humankind dates back thousands of years. This natural product, which has been an integral part of traditional medical practices across various civilizations for centuries, has long been recognized for its nutritional and health-promoting benefits. Indeed, the consumption of pollen is praised in the Bible (Genesis 1:29), and pollen has emerged as a fundamental component in the dietary cultures of leading civilizations such as Ancient China

and Egypt [5]. Essentially the reproductive cell of flowering plants, pollen transforms into a natural, bioactive substance of extremely high nutritional value after being collected by bees, playing a critical role in the colony's nutrition [6]. Upon examination of its chemical composition, it is reported to contain macro- and micronutrients such as protein, essential amino acids, carbohydrates, lipids, and vitamins [7]. Additionally, due to the high levels of phenolic compounds and flavonoids in its composition, it exhibits multifaceted biological activities such as antimicrobial, antioxidant, anti-inflammatory, and anticancer properties [8]. Today, bee pollen is classified as a food product for human consumption, and accordingly, its physicochemical properties and nutritional profile are standardized in accordance with national regulations. On the other hand, while bee pollen is officially recognized as a medicinal product (drug) in Germany, its use is also recommended in clinical Chinese medicine for the treatment of various pathophysiological conditions [5].The use of pollen as a food source is largely derived from bee pollen obtained from beehives. Bee pollen consists of 10–40% protein, 13–55% carbohydrates, 1–13% lipids, 0.3–20% dietary fiber and pectin, and up to 2.5% phenolic compounds by dry weight. Additionally, they contain minerals such as Fe, Mg, Cu, Mn, Ca, K, P, and Zn, as well as vitamins including β-carotene, B1, B2, B3, B5, B6, C, biotin, folic acid, and tocopherol, along with phenolic compounds [9]. Pollen is generally very rich in nutrients such as polysaccharides, proteins, lipids, minerals, and phenolics. While the chemical composition of pollen is generally similar, it can vary depending on the species and may also change based on abiotic conditions [2].

2.1 Carbohydrates

A large portion of the carbohydrates in pollen consists of fructose, glucose, and sucrose. Although the general composition of pollen is similar, its content may vary depending on botanical and geographical origin. The dietary fiber and starch in pollen also highlight its nutritional value [10]. Studies on pine pollen have indicated that it contains polysaccharides such as mannose, ribose, xylose, glucuronic acid, galacturonic acid, glucose, galactose, rhamnose, ribose, fucose, and arabinose [2]. FT-IR and Raman analyses have reported high starch content in Poaceae and Cyperaceae pollen, while Iridaceae, Xanthorrhoeaceae, Liliaceae, and Arecaceae pollen are largely starch-deficient. It has also been shown that anemophilous species have higher carbohydrate content than other species [11].

The total sugar content (Glucose + Fructose + Maltose + Sucrose + Melezitose) in Slovenian bee pollen has been reported to range from 24.71 to

54.19 (g per 100 g dry weight). Total dietary fiber was determined to be 11.90–20.20% (dry matter). This highlights pollen as a nutritious dietary product [10].

2.2 Proteins and amino acids

Studies on pine pollen report a total protein content of approximately 10%, with glutenin constituting the majority of this content. Similarly, the average amino acid content is reported to be around 10%, with the most abundant amino acids being glutamic acid, arginine, aspartic acid, and proline. The most common fatty acids are oleic acid, linoleic acid, and palmitic acid [2]. FT-IR and Raman analyses have shown that entomophilous species have a higher protein content. This is associated with entomophilous species producing higher levels of protein to attract insects. This finding is consistent with a similar distribution observed not only in pollen grains but also in the plant stem [11].

In a study on bee pollen, the total protein content ranged from a low of 15.58 ± 0.22 in *Zea mays* to a high of 26.86 ± 0.95 in the *Quercus spp.* taxon. In other polyfloral species, it was determined to be 23.06 ± 1.35%. In a sample dominated by the Pinaceae taxon, this ratio was determined to be 23.09 ± 2.48%. Similarly, the highest amino acid content was found in the Pinaceae taxon at 31.40 μg/mg, while the lowest amino acid content was found in the *Robinia pseudoacacia* taxon at 8.84 μg/mg. Glutamic acid, proline, and aspartic acid stand out as the most abundant amino acids [12].

2.3 Fatty Acids

Studies on pine pollen indicate that approximately 2% of all fatty acids are unsaturated fatty acids, while the remainder consists of saturated fatty acids [2]. In palm pollen, the following fatty acids have been identified: capric acid, lauric acid, myristic acid, palmitic acid, stearic acid, arachidic acid, palmitoleic acid, oleic acid, and linolenic acid [13]. When comparing the lipid content of bee pollen across dominant taxa, the lowest value of 2.2% was found in the Zea mays taxon, while the highest value of 6.05% was found in the Pinaceae spp. taxon [12]. Palmitic acid, stearic acid, α-linolenic acid, linoleic acid, eicosenoic acid, and erucic acid are among the most commonly detected fatty acids in bee pollen. The fatty acids and their quantities in bee pollen vary significantly depending on the botanical source. For example, the highest palmitic acid content was found in *Papaver rhoeas* pollen, which was approximately 7 times higher than that in *Dendranthema indicum* pollen. Similarly, α-linolenic acid was reported to be approximately 8 times higher in *Taraxacum mongolicum* pollen compared to *Nelumbo nucifera* pollen [14]. Studies on various types of bee pollen also indicate that the ratio of saturated to unsaturated fats can vary. This may be due to

producers conducting selective harvesting during periods when certain pollen types are dominant [15,16].Seasonal changes in botanical sources can also cause variations in the fatty acid composition of bee pollen depending on the harvest date. Behenic acid (C22:0), lignoceric acid (C24:0), and saturated fatty acids (SFAs) are most commonly detected in bee pollen harvested during the winter months, while linoleic acid (C18:3), stearic acid (C18:0), linoleic acid (C18:2), arachidic acid (C20:0), the total concentration of C18:0, C18:1, C18:2, and C18:3, and essential fatty acids are most commonly reported in bee pollen harvested in the fall. In general, it is considered that bee pollen harvested in the spring and summer months has higher nutritional value [15]. The lipid content also varies significantly under the influence of abiotic factors. The total oil content in monofloral *Cistus creticus* bee pollen collected from 14 different regions was found to range from 2.50–3.24% (dry matter), while the oil content in monofloral Sinapis arvensis bee pollen ranged from 7.64–9.06% (dry matter). It has been reported that the differences between regions within both taxa are significant [17]. The most common saturated fatty acids identified in bee pollen are arachidic acid, behenic acid, capric acid, caproic acid, caprylic acid, lauric acid, lignoceric acid, myristic acid, nonanoic acid, palmitic acid, pentadecanoic acid, stearic acid, tridecanoic acid, and undecanoic acid, while the most common unsaturated fatty acids are arachidonic acid, docosadienoic acid, eicosadienoic acid, eicosatrienoic acid, eicosenoic acid, erucic acid, heptadecenoic acid, linoleic acid, nervonic acid, oleic acid, palmitoleic acid, and α-linolenic acid [14,16].

2.4 Mineral content

Studies on pine pollen have identified K as the most abundant mineral, followed by P, Mg, and Na. Pine pollen is also quite rich in secondary metabolites [2]. Numerous studies have shown that the dominant mineral in anemophilous plants is K. However, the elemental composition of pollen can vary depending on environmental conditions. This suggests that pollen can serve as a useful tool for investigating environmental pollution (Sénéchal et al., 2015). When the mineral content of date palm (*Phoenix dactylifera*) pollen was analyzed, the highest concentration was found to be Cu (319.6 mg/100 g). This was followed by minerals such as B, Co, Se, Ni, Mn, and Mo [13].

In studies on bee pollen, the element K stands out as the most abundant. Ca, Mg, Na, Fe, Mn, and P are reported as the other minerals most commonly found in bee pollen. However, mineral levels show a wide range in the literature. This is attributed to plant diversity as well as geographic location and soil structure [18–20]. For example, in a study conducted in Turkey, K levels ranged from

7,032.00 to 4,741.33 mg/kg, while Ca levels were measured at 2,821.67 to 1,052.67 mg/kg [19]. Mineral content can vary significantly depending on botanical origin. P, K, and Ca have been reported to be the minerals most affected by this variation. Additionally, it has been demonstrated that mineral level variation in monofloral bee pollen is greater than in polyfloral bee pollen. This finding may contribute to better standardization of mineral content in polyfloral bee pollen. Furthermore, even when derived from the same botanical source, pollen samples collected from different regions may exhibit statistically significant differences in mineral content [17].

2.5 Phenolic compounds and vitamins

Pine pollen contains *p*-hydroxybenzoic acid, protocatechuic acid, gallic acid, vanillic acid, cis- and trans-*p* -coumaric acid, cis- and trans-ferulic acid, and 4-glucosyloxybenzoic acid, as well as flavonoids such as dihydrocempferol and dihydroquercetin, naringin, and p-coumaric acid esters. They also contain various compounds such as carotenoids and terpenoids [2]. p-Coumaric acid was predominantly detected in Cyperaceae and Poaceae pollen grains. Furthermore, while sinapic acid was found in high concentrations in the Cyperaceae family, ferulic acid was detected in the Poaceae family [11]. Pollen contains significant amounts of vitamins.

A study on palm pollen identified vitamins A (7,708.33 IU/100 g), E (3,030.92 IU/100 g), and C (89.09 mg/100 g) [13]. Bee pollen also stands out as a food that is quite rich in phenolic acids. In a study conducted in Turkey, 23 types of phenolic compounds potentially present in bee pollen were examined, and 18 of these were detected in the samples analyzed. These compounds include 2,5-dihydroxybenzoic acid, 2-Hydroxy-trans-cinnamic acid, caffeic acid, catechin, chlorogenic acid, ethyl gallate, gallic acid, isorhamnetin, kaempferol, luteolin, myricetin, naringin, p-coumaric acid, phlorizin, propyl gallate, protocatechuic acid, quercetin, resveratrol, rutin, salicylic acid, sinapic acid, syringic acid, and trans-ferulic acid [9].

Tablo 1: Common Phenolic compounds in Pollen extracts

Referances	[9]	[21]						[22]	[19]					
Dominant taxon	not specified	Cistus type	Brassica type	Pimpinella anisum	Erica sp	Aster type	Polyfloral	not specified	Castanea sativa	Fagus esculentum	Hedera helix spp.	Rhododendron spp.	Rosa spp.	Polyfloral
Unit of measurement	mg/100 g	µg/g	µg/g	µg/g	µg/g	µg/g	µg/g	µ/g	µg/100 g	µg/100 g	µg/100 g	µg/100 g	µg/100 g	µg/100 g
2,5-Dihydroxybenzoic Acid	2.69-9.85	--	--	--	--	--	--	--	1860-2400	230	1240	413	nd	nd-312
2-Hydroxy-trans-Cinnamic Acid	nd	--	--	--	--	--	--	--	1063-1136	6800	1891	570	5976	560-4147
Caffeic Acid	12.46-56.17	--	--	--	--	--	--	--	2460	nd	nd	nd	nd	--
Chlorogenic Acid	4.37-36.09	--	--	--	--	--	--	nd – 334.83	nd	3187	nd	nd	nd	nd
Ethyl Gallate	0.04-3.14	--	--	--	--	--	--	--	--	--	--	--	--	--
Gallic Acid	35.31-157.84	--	--	--	--	--	--	7.27 – 648.56	--	--	--	--	--	--
Isorhamnetin	238.42-775.16	--	--	--	--	--	--	--	--	--	--	--	--	--
Kaempferol	112.94-768.04	6.6-62.0	4.6-347.6	172.4	46255	46070	11.5-90.8	--	--	--	--	--	--	--
Luteolin	21.91-3325.73	--	--	--	--	--	--	--	--	--	--	--	--	--
Myricetine	20.46-244.78	10.5-2081.7	89.9-977.2	2062.1	52.8	163.2	26.7-696.2	--	--	--	--	--	--	--
Naringin	nd	7.6-705.9	102.1-205.6	1418.1	220.8	192.5	97.8-625.9	nd – 4485.02	--	--	--	--	--	--
p-Coumaric Acid	36.28-83.67	nd	nd-130.3	32.8	64.8	46268	23.2-77.6	8.15 – 9312.07	nd-2675	1476	1554	nd	nd	nd-2398
Fluorinine (Phlorizin)	nd-78.6	--	--	--	--	--	--	--	--	--	--	--	--	--
Propyl Gallate	nd	--	--	--	--	--	--	--	--	--	--	--	--	--
Protocatechuic Acid	nd-61.3	--	--	--	--	--	--	--	--	--	--	--	--	--
Quercetin	381.10-3631.93	--	--	--	--	--	--	186.31 – 20749.05	--	--	--	--	--	--
Resveratrol	nd-122.81	8.4-377.7	69.7-413.1	48.4	156.3	122.7	149.2-453.4	--	--	--	--	--	--	--
Rutin	1728.76-12613.49	32.2-488.1	48.1-613.1	1052.7	46257	71.1	11.4-361.2	nd – 6751.00	13204-16008	1807	24378	1500	3508	nd-7830
Salicylic Acid	19.27-65.20	--	--	--	--	--	--	--	--	--	--	--	--	--
Trans-Ferulic Acid	23.23--107.86	--	--	--	--	--	--	--	nd	nd	nd	nd	nd	nd-4938
Vanillic acid	--	--	--	--	--	--	--	nd – 145.88	--	--	--	--	--	--
Caffeic acid	--	--	--	--	--	--	--	nd – 247.86	--	--	--	--	--	--
Vanillin	--	--	--	--	--	--	--	nd – 10488.72	--	--	--	--	--	--
Chrysin	--	--	--	--	--	--	--	--	287-1773	977	362	366	280	177-1761
Apigenin	--	--	--	--	--	--	--	--	nd	nd	nd	nd	nd	791-62141
Pinosembrin	--	--	--	--	--	--	--	--	304-330	656	1493	250	215	184-2083
Hesperidin	--	--	--	--	--	--	--	--	--	nd	1196	nd	nd	410-720

nd: not detected

3.Biological Properties of Bee Pollen

In addition to their nutritional value, the health benefits of pollen—which are even more significant—primarily stem from the bioactive compounds they contain. Pollen exhibits strong bioactivity due to the phenolic compounds it contains.

Studies have reported that the total phenolic content (TPC) in pine pollen consumed as food ranges from 1.92 to 3.52 g AEmg/g dw, while the total flavonoid content (TFC) ranges from 2.09 to 6.10 mg RE/g dw [2]. However, pollen consumption generally takes the form of bee pollen. The amounts of phenolic acids and flavonoids contained in bee pollen may vary depending on their botanical and geographical origins. Although it varies depending on the extraction method and the samples studied, in general, studies on bee pollen report TPC ranging from 6.08 to 31.13 mg GAE/g pollen and TFC ranging from 1.48 to 11.89 mg QE/g pollen [19,21,23].The DPPH radical scavenging activity, a measure of antioxidant power, has been reported with an IC50 value ranging from 3.04 to 0.13 mg/mL.Pollen is commonly obtained both by collecting it directly from trees and in the form of bee pollen, and considered a complete food due to its high content of essential compounds such as carbohydrates, proteins, and fats, as well as numerous minerals and phenolic compounds. For this reason, pollen can serve as a food source for many organisms other than pollinators. Due to its high nutritional value and bioactive properties, pollen can be incorporated into human diets to help prevent the development of diseases and strengthen the immune system. However, despite its exceptionally high nutritional value, there are serious allergic risks that must be carefully considered when consuming it. Pollen grains from plants carried by wind or insects can trigger immunoglobulin E (IgE)-mediated hypersensitivity reactions in humans, which can range up to anaphylaxis. In particular, highly active and well-known allergenic proteins (compounds) such as Ole e 1, Cup a 3, Bet v 1, and Lol p 1 are present within and on the surface of pollen grains [24]. Additionally, pollen may be contaminated with heavy metals and harmful gases. This contamination can directly harm humans or contribute to an increase in allergic symptoms [25,26].

3.1 Antibacterial and antifungal effects

The antimicrobial activity exhibited by bee pollen is highly dependent on environmental and natural parameters such as botanical and geographical origin, seasonal variations, and beekeeping practices. However, the findings of analyses conducted in a laboratory setting (in vitro) may vary significantly depending on the extraction procedures used, the preferred solvent systems, the targeted microbial strains, and the methodological approaches employed to assess

antimicrobial capacity. One of the primary barriers limiting bioavailability in this field is the outer layer of pollen, known as the "exine," which exhibits extraordinary resistance to biochemical degradation; this structure significantly limits the cellular bioavailability of bioactive components within the pollen matrix. This resistant cellular barrier can only be partially broken down through various technological processing and modification methods aimed at disrupting the wall structure to maximize the nutritional value and functional bio-capacity of pollen [27]. The antimicrobial activity of bee pollen extracts varies depending on the specific type of target microorganism. Gram-positive bacteria are generally much more susceptible than Gram-negative bacteria, which possess complex lipopolysaccharide membranes that confer structural resistance. Among the most commonly tested bacterial species, *S. aureus* is the pathogen exhibiting the highest sensitivity [28]. The antimicrobial activity against *E. coli*, a Gram-negative species, varies widely from strong to weak depending on the botanical origin of the bee pollen: Extracts from Poaceae and *Trifolium* monofloral bee pollen exhibit quite pronounced effects, whereas extracts derived from pollen of the Asteraceae and Rosaceae families were found to have relatively weaker effects [29] [27].

The antifungal activity of bee pollen is primarily due to the rich content of phenolic compounds and flavonoids in its composition. The primary mechanism of action of these bioactive compounds on fungal cells is based on the disruption of the cytoplasmic membrane, loss of intracellular potassium ions, and ultimately the induction of autolysis (self-digestion) [30]. Although antifungal research in the literature has primarily focused on fungal species belonging to the *Candida* genus (*Candida albicans, Candida glabrata,* etc.) [31], it has been reported that pollen extracts exhibit significant inhibitory effects on various yeast species other than *Aspergillus* (*A. niger*, *A. ochraceus*) and the *Candida* genus (non-Candida) [32].

3.2 Anticarcinogenic effects

Recent scientific findings indicate that natural bee products induce apoptosis (programmed cell death) in cancer cells by inhibiting the proliferation of tumor cells and their spread to other tissues (metastasis), thereby demonstrating that these bioactive compounds hold potential as an alternative therapeutic approach in the clinical treatment of human tumors. When traditional chemotherapy and radiation therapy methods are administered systemically or over a wide area to destroy cancerous tissue, they also damage healthy cells, leading to serious side effects that limit the treatment's efficacy and the tolerable dose—and in some cases, these side effects can be even more deadly than the disease itself. In this context, interest in research on safer alternative anticancer drugs, particularly those derived from natural products, is growing within the scientific community [33].Extensive in vitro and in

vivo studies on bee pollen have shown that this natural bee product successfully inhibits tumor proliferation by inducing apoptosis (programmed cell death) in cancer cells. This anticancer activity is primarily based on its strong antioxidant potential, which suppresses and inactivates reactive oxygen species that trigger cancer formation [34]. Furthermore, it has been reported that phenolic acids present in high concentrations in the pollen matrix, and specifically flavonoids such as kaempferol and apigenin, suppress the uncontrolled growth of neoplastic cells by modulating it. Indeed, specific laboratory analyses confirm that bee pollen extracts exhibit a strong inhibitory (cytotoxic) effect on human prostate cancer PC-3 cell lines and K-562 leukemia cell lines [5,35]. It has been reported that bee pollen, which has a very high nutritional value, holds potential as a complementary alternative to mitigate the adverse side effects of modern chemotherapy and radiation therapy treatments.

3.3 Anti-inflammatory effects

One of the most notable properties of pollen is its potent free radical scavenging (antioxidant) effect, which is mediated by the antioxidant enzymes (catalase, superoxide dismutase) and flavonoids (quercetin, kaempferol, etc.) present in its composition [5]. This antioxidant capacity, which suppresses oxidative stress, plays a critical role in preventing pathological processes such as chronic inflammation by inhibiting damage to cell membranes and cellular DNA [36].

In studies regarding its anti-inflammatory effect, it has been reported that structures such as polyphenols and flavonoids found in the compounds of bee pollen exert significant effects on cell types—including macrophages, T-B cells, mast cells, basophils, eosinophils, and neutrophils—that play a critical role in defense against pathogenic agents and in inflammatory processes [34]. When examined at the cellular level in the context of anti-inflammatory activity, the bioactive flavonoids in pollen significantly reduce the synthesis of pro-inflammatory prostaglandins in tissues by inhibiting arachidonic acid metabolism, thereby providing an anti-inflammatory effect [5]. Consequently, positive effects are observed regarding the relief of local pain and the prevention of platelet aggregation following bee pollen administration [37]. Additionally, it has been reported that bee pollen is beneficial in the resolution of kidney-related edema [38].

3. POLLEN GRAINS AS FOOD SUPPLEMENTS

According to current estimates, annual pollen production in the European Union is approximately 971 tons, while global production is estimated at around 17,500 tons based on managed honeybee colonies worldwide, although these figures remain highly uncertain. Bee pollen represents the primary natural protein source for

honeybees and contains a rich array of amino acids, lipids, vitamins, minerals, and bioactive compounds. Bee bread (perga), produced through the fermentation of pollen within the hive, possesses an extended shelf life and enhanced nutritional properties. Consequently, both bee pollen and bee bread have gained considerable attention as functional foods and dietary supplements for human consumption due to their nutritional and health-promoting characteristics [39].

The incorporation of bee pollen into food products has attracted increasing interest because of its antioxidant, antimicrobial, and sensory-enhancing properties. Novaković et al. (2021) demonstrated that the addition of bee pollen to frankfurters improved flavor characteristics and provided antioxidant protection throughout a 60-day storage period [40]. These effects are largely attributed to the high polyphenol content of bee pollen, which can exceed 8 mg/g and contributes substantial antioxidant and free-radical scavenging capacity [41]. The botanical origin of pollen plays a critical role not only in determining its antioxidant potential but also in influencing the sensory properties of food products. For example, Khider et al. (2013) reported that maize-derived bee pollen improved the taste and texture of yogurt, whereas clover and date palm pollens imparted a sweeter taste and a characteristic bean-like aroma. Similarly, Karabagias et al. (2018) showed that the incorporation of a mixed pollen preparation containing *Papaver rhoeas, Eucalyptus camaldulensis*, *Trifolium spp.,* and several additional plant species enhanced the taste, appearance, flavor, and texture of yogurt [42].Beyond dairy products, bee pollen has been successfully incorporated into a variety of functional foods. Tirla et al. (2023) developed a personalized natural sports food supplement by combining bee pollen with Aronia melanocarpa, thereby optimizing protein, fatty acid, polyphenol, carbohydrate, and antioxidant contents [43]. Likewise, Turhan et al. (2014) formulated meatballs supplemented with bee pollen and demonstrated that pollen addition reduced microbial growth while providing antioxidant protection without adversely affecting sensory characteristics [25].Despite its widespread reputation as a highly nutritious “superfood,” bee pollen may pose health risks depending on its floral origin. Allergic and immunological reactions have been reported following pollen consumption [44]. A case study by Martín-Muñoz et al. (2010) revealed that severe allergic reactions associated with bee pollen consumption were primarily linked to pollens originating from the Asteraceae (Compositae) family. The highest levels of pollen-specific IgE were detected against *Artemisia vulgaris* and *Taraxacum officinale*, while immunoblot inhibition analyses identified Asteraceae pollens as the most probable allergenic source [45]. Furthermore, Matuszewska et al. (2022) reported the presence of several allergenic proteins in bee pollen, including pollen-specific protein Bnm1 from *Brassica napus* and Sal k 2/Sal k 3 proteins from Salsola kali. Such allergenic proteins may trigger severe reactions, including

anaphylactic shock, in susceptible individuals [46].The allergenic potential of pollen is not restricted to proteinaceous components. Gilles-Stein et al. (2016) demonstrated for the first time that aqueous non-protein extracts of *Betula pendula* and *Phleum pratense* pollen could enhance allergic responses in the skin and nasal mucosa of sensitized patients [47]. In addition to allergenic compounds, bee pollen may also contain undesirable contaminants, including pesticides and mycotoxins. Carrera et al. (2024) analyzed 34 bee pollen samples collected from Spain and Slovenia and found that more than 23% contained detectable levels of mycotoxins, while only three samples were free of pesticide residues [48].

Storage conditions represent another critical factor affecting the quality and nutritional value of bee pollen. Braciuliene et al. (2026) reported that storage at room temperature resulted in a significant decline in total amino acid content, whereas storage at −20 °C or −80 °C substantially slowed degradation, although complete preservation was not achieved [49]. Similarly, Fernández et al. (2021) observed reductions in carbohydrate content after 12 months of storage, even when samples were maintained at 4 °C [50]. Recent findings indicate that ozone treatment and gamma irradiation may mitigate losses of total amino acids, proteins, and essential amino acids during room-temperature storage [51]. Lipid composition is also affected by storage duration and conditions, leading to reductions in fatty acid content [52]. Drying is commonly employed to extend shelf life and improve product stability; however, processing conditions can significantly influence pollen quality. Wang et al. (2022) demonstrated that conventional drying may reduce total lipid content and induce structural alterations in triglycerides and fatty acids through oxidative processes [53]. In a comparative study using rape bee pollen, Bi et al. (2024) reported that freeze-drying and pulsed vacuum drying effectively preserved free amino acids and carbohydrates while minimizing undesirable changes in volatile compounds [54].

Microbiological quality is likewise strongly influenced by storage conditions. Fernández et al. (2021) found that microbial populations increased during nine months of room-temperature storage, whereas no significant microbiological changes were observed in samples stored at 4 °C for up to 12 months [50].

In addition to post-harvest processing and storage conditions, the harvesting season significantly affects the chemical composition of bee pollen. Variations in floral availability throughout the year influence both the quantity and profile of fatty acids present in pollen. Al-Kahtani et al. (2021) reported that pollen collected during spring and summer contained the highest levels of fatty acids, particularly linoleic, oleic, and palmitic acids, which are among the predominant fatty acids found in bee pollen [15].

4. CONCLUSION

Bee pollen is a unique natural product that combines exceptional nutritional value with a diverse array of bioactive compounds. Its chemical composition includes carbohydrates, proteins, essential amino acids, lipids, dietary fiber, vitamins, minerals, and numerous phenolic compounds, making it one of the most nutritionally complex products of the beehive. However, the composition of bee pollen is highly dependent on botanical origin, geographical location, environmental conditions, harvesting season, and post-harvest processing, resulting in considerable variability among commercial products.From a food chemistry perspective, the nutritional and functional properties of bee pollen are closely linked to its unique physicochemical structure and rich phytochemical profile. The presence of phenolic acids, flavonoids, unsaturated fatty acids, vitamins, and minerals contributes not only to its nutritional quality but also to its antioxidant, antimicrobial, anti-inflammatory, and other health-promoting activities. These characteristics have stimulated increasing interest in the incorporation of bee pollen into functional foods, dietary supplements, and nutraceutical formulations.

Despite its considerable potential, several challenges remain regarding the standardization, quality control, processing, storage, and safety of bee pollen products. Variations in composition, susceptibility to degradation during storage, contamination by environmental pollutants, pesticides, or mycotoxins, and the presence of allergenic compounds may significantly influence product quality and consumer safety. Therefore, establishing reliable analytical methods and harmonized quality standards is essential for ensuring the authenticity, stability, and safety of bee pollen-based products.Future research should focus on improving the bioavailability of pollen nutrients through innovative processing technologies, elucidating the mechanisms underlying its biological activities, and developing standardized products with consistent chemical composition and functional properties. Such advances will further support the utilization of bee pollen as a valuable functional food ingredient and contribute to the growing demand for natural products that promote human health and well-being.

REFERENCES

1-M.B.H. Almosawi, A review in pollen grains for plants, GSC Biol. Pharm. Sci. 30 (2025) 20–30. https://doi.org/10.30574/gscbps.2025.30.1.0495.

2-Y. Cheng, Z. Wang, W. Quan, C. Xue, T. Qu, T. Wang, Q. Chen, Z. Wang, M. Zeng, F. Qin, J. Chen, Z. He, Pine pollen: A review of its chemical composition, health effects, processing, and food applications, Trends Food Sci. Technol. 138 (2023) 599–614. https://doi.org/10.1016/j.tifs.2023.07.004.

3-E. Pacini, G.G. Franchi, Pollen biodiversity - Why are pollen grains different despite having the same function? A review, Bot. J. Linn. Soc. 193 (2020) 141–164. https://doi.org/10.1093/botlinnean/boaa014.

4-J. Shi, M. Cui, L. Yang, Y.J. Kim, D. Zhang, Genetic and Biochemical Mechanisms of Pollen Wall Development, Trends Plant Sci. 20 (2015) 741–753. https://doi.org/10.1016/j.tplants.2015.07.010.

5-B. Denisow, M. Denisow-Pietrzyk, Biological and therapeutic properties of bee pollen: a review, J. Sci. Food Agric. 96 (2016) 4303–4309. https://doi.org/10.1002/jsfa.7729.

6-Y. ERDOĞAN, A. DODOLOĞLU, BAL ARISI (Apis mellifera L.) KOLONİLERİNİN YAŞAMINDA POLENİN ÖNEMİ, Uludag Bee J. 5 (2005) 79–84. http://www.culturaapicola.com.ar/apuntes/revistaselectronicas/Urludag/15.pdf.

7-S. Doreswamy, A. Bashir, J.E. Guarecuco, S. Lahori, A. Baig, L.R. Narra, P. Patel, S.E. Heindl, Effects of Diet, Nutrition, and Exercise in Children With Autism and Autism Spectrum Disorder: A Literature Review, Cureus 12 (2020) e12222. https://doi.org/10.7759/cureus.12222.

8-D. ONBAŞLI, Apiterapi ve İnsan Sağlığı Üzerine Etkileri, Erciyes Üniversitesi Vet. Fakültesi Derg. 16 (2019) 49–56. https://doi.org/10.32707/ercivet.538001.

9-N.E. Bayram, Y.C. Gercek, S. Çelik, N. Mayda, A.Ž. Kostić, A.M. Dramićanin, A. Özkök, Phenolic and free amino acid profiles of bee bread and bee pollen with the same botanical origin – similarities and differences, Arab. J. Chem. 14 (2021) 103004. https://doi.org/10.1016/j.arabjc.2021.103004.

10-J. Bertoncelj, T. Polak, T. Pucihar, N. Lilek, A.K. Borovšak, M. Korošec, Carbohydrate composition of Slovenian bee pollens, Int. J. Food Sci. Technol. 53 (2018) 1880–1888. https://doi.org/10.1111/ijfs.13773.

11-A. Kenđel, B. Zimmermann, Chemical Analysis of Pollen by FT-Raman and FTIR Spectroscopies, Front. Plant Sci. 11 (2020) 352. https://doi.org/10.3389/fpls.2020.00352.

12-M. Oroian, F. Dranca, F. Ursachi, Characterization of Romanian Bee Pollen—An Important Nutritional Source, Foods 11 (2022) 2633. https://doi.org/10.3390/foods11172633.
13-H.M.M. Hassan, Chemical Composition and Nutritional Value of Palm Pollen Grains, Glob. J. Biotechnol. Biochem. 6 (2011) 1–7.
14-J. Dong, Y. Yang, X. Wang, H. Zhang, Fatty acid profiles of 20 species of monofloral bee pollen from China, J. Apic. Res. 54 (2015) 503–511. https://doi.org/10.1080/00218839.2016.1173427.
15-S.N. Al-Kahtani, E.-K.A. Taha, S.A. Farag, R.A. Taha, E.A. Abdou, H.M. Mahfouz, Harvest season significantly influences the fatty acid composition of bee pollen, Biology (Basel). 10 (2021) 495. https://doi.org/10.3390/biology10060495.
16-D.H. Markowicz Bastos, O. Monika Barth, C. Isabel Rocha, I.B. da Silva Cunha, P. de Oliveira Carvalho, E.A.S. Torres, M. Michelan, Fatty acid composition and palynological analysis of bee (*Apis*) pollen loads in the states of São Paulo and Minas Gerais, Brazil, J. Apic. Res. 43 (2004) 35–39. https://doi.org/10.1080/00218839.2004.11101107.
17-V. Liolios, C. Tananaki, A. Papaioannou, D. Kanelis, M.-A. Rodopoulou, N. Argena, Mineral content in monofloral bee pollen: investigation of the effect of the botanical and geographical origin, J. Food Meas. Charact. 13 (2019) 1674–1682. https://doi.org/10.1007/s11694-019-00084-w.
18-D. Domínguez-Valhondo, D. Bohoyo Gil, M.T. Hernández, D. González-Gómez, Influence of the commercial processing and floral origin on bioactive and nutritional properties of honeybee-collected pollen, Int. J. Food Sci. Technol. 46 (2011) 2204–2211. https://doi.org/10.1111/j.1365-2621.2011.02738.x.
19-S. Kolayli, C. Birinci, E.D. Kanbur, O. Ucurum, Y. Kara, C. Takma, Comparison of biochemical and nutritional properties of bee pollen samples according to botanical differences, Eur. Food Res. Technol. 250 (2023) 799–810. https://doi.org/10.1007/s00217-023-04428-1.
20-M.A. Morgano, M.C.T. Martins, L.C. Rabonato, R.F. Milani, K. Yotsuyanagi, D.B. Rodriguez-Amaya, A comprehensive investigation of the mineral composition of brazilian bee pollen: geographic and seasonal variations and contribution to human diet, J. Braz. Chem. Soc. (2012). https://doi.org/10.1590/s0103-50532012000400019.
21-N. Boulfous, H. Belattar, R. Ambra, G. Pastore, A. Ghorab, Botanical Origin, Phytochemical Profile, and Antioxidant Activity of Bee Pollen from the Mila Region, Algeria, Antioxidants 14 (2025) 291. https://doi.org/10.3390/antiox14030291.

22-H. Hemmami, B. Ben Seghir, M. Ben Ali, A. Rebiai, S. Zeghoud, F. Brahmia, Phenolic profile and antioxidant activity of bee pollen extracts from different regions of Algeria, Ovidius Univ. Ann. Chem. 31 (2020) 93–98. https://doi.org/10.2478/auoc-2020-0017.

23-G. Alimoglu, E. Guzelmeric, P.I. Yuksel, C. Celik, I. Deniz, E. Yesilada, Monofloral and polyfloral bee pollens: Comparative evaluation of their phenolics and bioactivity profiles, LWT 142 (2021) 110973. https://doi.org/10.1016/j.lwt.2021.110973.

24-M. Thakur, V. Nanda, Composition and functionality of bee pollen: A review, Trends Food Sci. Technol. 98 (2020) 82–106. https://doi.org/10.1016/j.tifs.2020.02.001.

25-S. Turhan, F. Yazici, T. Saricaoglu, M. Mortas, H. Genccelep, Evaluation of the nutritional and storage quality of meatballs formulated with bee pollen, Korean J. Food Sci. Anim. Resour. 34 (2014) 423–433. https://doi.org/10.5851/kosfa.2014.34.4.423.

26-H. Sénéchal, N. Visez, D. Charpin, Y. Shahali, G. Peltre, J.-P. Biolley, F. Lhuissier, R. Couderc, O. Yamada, A. Malrat-Domenge, N. Pham-Thi, P. Poncet, J.-P. Sutra, A Review of the Effects of Major Atmospheric Pollutants on Pollen Grains, Pollen Content, and Allergenicity, Sci. World J. 2015 (2015) 1–29. https://doi.org/10.1155/2015/940243.

27-T. Lukman, S. Smole Možina, Antimicrobial Activity of Bee Pollen: Influence of Botanical Origin and Processing, Food Technol. Biotechnol. 64 (2026) 67–80. https://doi.org/10.17113/ftb.64.01.26.9421.

28-A.A.A. Mohdaly, A.A. Mahmoud, M.H.H. Roby, I. Smetanska, M.F. Ramadan, Phenolic Extract from Propolis and Bee Pollen: Composition, Antioxidant and Antibacterial Activities, J. Food Biochem. 39 (2015) 538–547. https://doi.org/10.1111/jfbc.12160.

29-K. Fatrcová-Šramková, J. Nôžková, M. Máriássyová, M. Kačániová, Biologically active antimicrobial and antioxidant substances in the Helianthus annuus L. bee pollen, J. Environ. Sci. Heal. - Part B Pestic. Food Contam. Agric. Wastes 51 (2016) 176–181. https://doi.org/10.1080/03601234.2015.1108811.

30-K. Komosinska-vassev, P. Olczyk, J. Ka, L. Mencner, K. Olczyk, Bee Pollen: Chemical Composition and Therapeutic Application KatarzynaKomosinska-Vassev,1, Evidence-Based Complement. Altern. Med. 2015 (2015) 6. http://www.nafsa.org/_/File/_/2015_state_by_state.pdf.

31-S. Gavanji, B. Larki, Comparative effect of propolis of honey bee and some herbal extracts on Candida albicans, Chin. J. Integr. Med. 23 (2017) 201–207. https://doi.org/10.1007/s11655-015-2074-9.

32-M. Kacániová, N. Vuković, R. Chlebo, P. Haščík, K. Rovná, J. Cubon, M. Dzugan, A. Pasternakiewicz, The antimicrobial activity of honey, bee pollen loads and beeswax from Slovakia, Arch. Biol. Sci. 64 (2012) 927–934. https://doi.org/10.2298/ABS1203927K.

33-P. Premratanachai, C. Chanchao, Review of the anticancer activities of bee products, Asian Pac. J. Trop. Biomed. 4 (2014) 337–344. https://doi.org/10.12980/APJTB.4.2014C1262.

34-A. Pascoal, S. Rodrigues, A. Teixeira, X. Feás, L.M. Estevinho, Biological activities of commercial bee pollens: Antimicrobial, antimutagenic, antioxidant and anti-inflammatory, Food Chem. Toxicol. 63 (2014) 233–239. https://doi.org/10.1016/j.fct.2013.11.010.

35-M.H. Jang, X.L. Piao, J.M. Kim, S.W. Kwon, J.H. Park, Inhibition of cholinesterase and amyloid-&bgr; aggregation by resveratrol oligomers from Vitis amurensis, Phyther. Res. 22 (2008) 544–549. https://doi.org/10.1002/ptr.

36-Y. Nakajima, K. Tsuruma, M. Shimazawa, S. Mishima, H. Hara, Comparison of bee products based on assays of antioxidant capacities, BMC Complement. Altern. Med. 9 (2009) 1–9. https://doi.org/10.1186/1472-6882-9-4.

37-J. Salles, N. Cardinault, V. Patrac, A. Berry, C. Giraudet, M.L. Collin, A. Chanet, C. Tagliaferri, P. Denis, C. Pouyet, Y. Boirie, S. Walrand, Bee pollen improves muscle protein and energy metabolism in malnourished old rats through interfering with the mtor signaling pathway and mitochondrial activity, Nutrients 6 (2014) 5500–5516. https://doi.org/10.3390/nu6125500.

38-A. Elghouizi, N. Al-Waili, N. Elmenyiy, S. Elfetri, A. Aboulghazi, A. Al-Waili, B. Lyoussi, Protective effect of bee pollen in acute kidney injury, proteinuria, and crystalluria induced by ethylene glycol ingestion in rats, Sci. Rep. 12 (2022) 8351. https://doi.org/10.1038/s41598-022-12086-8.

39-W. Haefeker, Pollen supplements and substitutes in the EU feed market : a product / market survey for bees and other animal species, EFSA Support. Publ. 18 (2021) EN-6461. https://doi.org/10.2903/sp.efsa.2021.EN-6461.

40-S. Novaković, I. Djekic, M. Pešić, A. Kostić, D. Milinčić, N. Stanisavljević, A. Radojević, I. Tomasevic, Bee pollen powder as a functional ingredient in frankfurters, Meat Sci. 182 (2021) 108621. https://doi.org/10.1016/j.meatsci.2021.108621.

41-G.U. Kroyer, N. Hegedus, Evaluation of bioactive properties of pollen extracts as functional dietary food supplement, Innov. Food Sci. Emerg. Technol. 2 (2001) 1999–2002.

42-M. Khider, K. Elbanna, A. Mahmoud, A.A. Owayss, Egyptian Honeybee Pollen as Antimicrobial , Antioxidant Agents , and Dietary Food Supplements, Food Sci. Biotechnol. 22 (2013) 1461–1469. https://doi.org/10.1007/s10068-013-0238-y.

43-A. Tirla, A.V. Timar, A. Becze, A.R. Memete, S.I. Vicas, M.S. Popoviciu, S. Cavalu, Designing New Sport Supplements Based on Aronia melanocarpa and Bee Pollen to Enhance Antioxidant Capacity and Nutritional Value, Molecules 28 (2023) 6944.

44-V. Aylanc, S. Ertosun, M. Estravís, I. Dávila, Investigating human IgE antibody interactions with pollen-derived sporopollenin biopolymers : immunoreactivity profiling for the rational design of structurally robust and biocompatible biomaterials Investigating human IgE antibody interactions with polle, Biomed. Mater. 21 (2026) 015009.

45-M.F. Martín-Muñoza, B. Bartolome, M. Caminoaa, I. Bobolea, M.C.G. Ara, S. Quirce, Bee pollen: a dangerous food for allergic children . Identification of responsible allergens, Allergol. Immunopathol. (Madr). 38 (2010) 263–265. https://doi.org/10.1016/j.aller.2009.12.003.

46-E. Matuszewska, S. Plewa, D. Pietkiewicz, K. Kossakowski, J. Matysiak, Mass Spectrometry-Based Identification of Bioactive Bee Pollen Proteins : Evaluation of Allergy Risk after Bee Pollen Supplementation, Molecules 27 (2022) 7733.

47-S. Gilles-Stein, I. Beck, A. Chaker, M. Bas, M. McIntyre, L. Cifuentes, A. Petersen, J. Gutermuth, C. Schmidt-Weber, H. Behrendt, C. Traidl-Hoffmann, Pollen derived low molecular compounds enhance the human allergen specific immune response in vivo, Clin. Exp. Allergy 46 (2016) 1355–1365. https://doi.org/10.1111/cea.12739.

48-M.A. Carrera, J.A.M. Martinez, M.D. Hernando, A.R. Fernandez-Alba, Simultaneous analysis of pesticides and mycotoxins in primary processed foods : The case of bee pollen, Heliyon 10 (2024) e33512. https://doi.org/10.1016/j.heliyon.2024.e33512.

49-A. Braciuliene, R. Stebuliauskaite, M. Liaudanskas, V. Zvikas, N. Sutkeviciene, S. Trumbeckaite, Changes in the Amino Acid Composition of Bee-Collected Pollen During 15 Months of Storage in Fresh-Frozen and Dried Forms, Foods 15 (2026) 207.

50-L.A. Fernández, M.A. Rodríguez, R.M. Sánchez, M. Pérez, L.M. Gallez, Long-term microbiological and chemical changes in bee pollen for human consumption: influence of time and storage conditions, J. Apic. Res. 60 (2021) 319–325. https://doi.org/10.1080/00218839.2020.1728867.

51-E.K.A. Taha, S.N. Al-Kahtani, E. Hegazy, N.M. Elwakeil, M.F. Osman, I.M. Taha, How can the protein and amino acid composition of bee pollen be preserved during long storage at ambient temperature?, J. Apic. Res. (2026) 1–10. https://doi.org/10.1080/00218839.2025.2587967.

52-O. Anjos, V. Paula, T. Delgado, L. Estevinho, Influence of the storage conditions on the quality of bee pollen, Zemdirbyste-Agriculture 106 (2019) 87–94. https://doi.org/10.13080/z-a.2019.106.012.

[53] J. Wang, Y. Chen, L. Zhao, X. Fang, Y. Zhang, Lipidomics reveals the molecular mechanisms underlying the changes in lipid profiles and lipid oxidation in rape bee pollen dried by different methods, Food Res. Int. 162 (2022) 112104. https://doi.org/10.1016/j.foodres.2022.112104.

[54] Y. Bi, J. Ni, X. Xue, Z. Zhou, W. Tian, V. Orsat, S. Yan, W. Peng, X. Fang, Effect of different drying methods on the amino acids, α-dicarbonyls and volatile compounds of rape bee pollen, Food Sci. Hum. Wellness 13 (2024) 517–527. https://doi.org/10.26599/FSHW.2022.9250045.

CHAPTER-8

NON-IONIZING RADIATION SOURCES IN OUR ENVIRONMENT

Mehmet ERDOĞAN[1]

1. INTRODUCTION

Electromagnetic radiation (EMR), which consists of combined electric and magnetic fields that behave like waves (Fig. 1), is a form of energy produced by the movement of electrically charged particles. It propagates through space or material media in the form of synchronized oscillating electric and magnetic fields. Unlike sound waves, which require a physical medium (like air or water) to travel, EMR can travel through the vacuum of space at the speed of light (speed of light in a vacuum, $c \cong 2.99\ 10^8 m/s$). It exhibits a dual nature, behaving simultaneously as a continuous wave and as a stream of discrete energy packets called photons. The energy quantum of electromagnetic radiation, carried by a photon, is given by the Equation (1).

$$E = hf = h\frac{c}{\lambda} \tag{1}$$

In Equation (1), h is Planck's constant with a value of h =6.6260693(11) $10^{-34}\ Js$, f is the frequency with unit Hz (s^{-1}), illustrating the quantized nature of light and radiation and c is speed of light.

If we oscillate a charge, we observe electromagnetic waves propagating in all directions. Let us refer to the charge generating these waves as the source charge. The simplest definition of an electromagnetic wave involves an electric field oscillating in one direction and a magnetic field oscillating perpendicular to it. Energy is transported in a direction perpendicular to both the electric and magnetic fields. This makes the electromagnetic wave a transverse wave, because the electric field (its amplitude) is perpendicular to the direction of wave propagation as shown in Fig. 1.

[1] Prof. Dr., Department of Physics, Faculty of Science, Selçuk University, Türkiye, merdogan@selcuk.edu.tr, meerdogan291@gmail.com, (ORCID: 0000-0003-1879-8500)

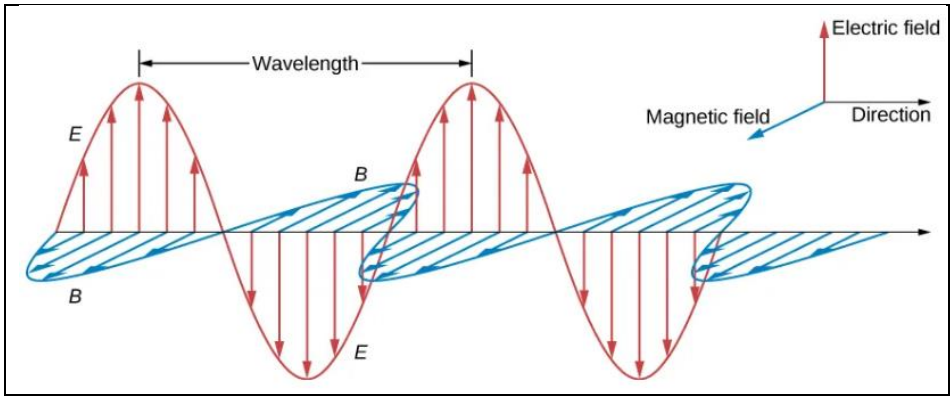

Figure 1. An image of an electromagnetic wave [1]

Since electromagnetic energy behaves like a wave, it exhibits all standard wave properties and characteristics:

Amplitude: This represents the peak strength or magnitude of the electric field (E).**Wavelength:** The spatial distance between consecutive points (λ) where the electric field reaches its maximum value.**Frequency:** The rate (f) at which the initiating source charge oscillates back and forth.**Wave Speed:** Determined by the fundamental relationship with $v_{wave} = \lambda f$.**Wave Interference:** Similar to acoustic waves, intersecting electromagnetic waves can either amplify or diminish one another.

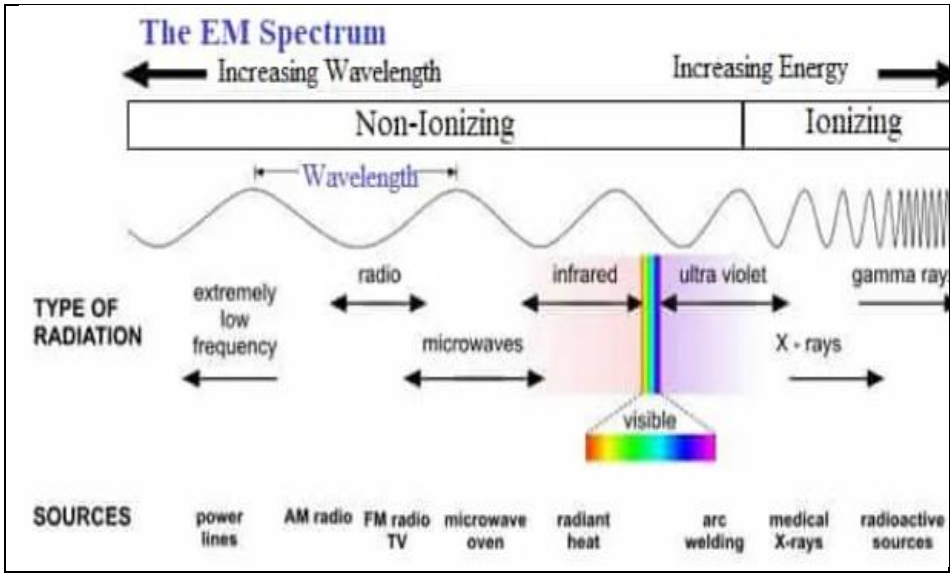

Figure 2. Electromagnetic spectrum [2]

Electromagnetic radiation, as shown in Fig. 2, can be classified into two types based on its interaction mechanisms with matter: ionizing and non-ionizing radiation. This category of electromagnetic radiation possesses the necessary energy threshold to detach tightly bound electrons from molecular or atomic structures, resulting in the creation of charged ions. This phenomenon is distinct to high-energy fields, which exhibit short wavelengths and elevated frequencies. Such radiation originates from radioactive nuclei or unstable atom and is discharged either as high-frequency electromagnetic waves including X-rays, cosmic rays, and gamma rays or in the form of particles like alpha, beta, and neutrons. The potent energy of ionizing radiation can inflict direct damage on cellular components, most notably the DNA sequence. Interacting with biological tissues at high doses, it significantly elevates risks associated with cellular aberrations, acute radiation syndrome, and various oncogenic pathologies [3].

Non-ionizing radiation is defined here as electromagnetic fields (EMFs) with a photon energy under 10 eV, featuring frequencies below 3.10^{15} Hz and wavelengths longer than 100 nm. It is divided into ultraviolet (100–400 nm), visible (400–780 nm), and infrared ranges (780 nm–1 mm), plus radiofrequency (100 kHz–300 GHz), low frequency (1 Hz-100 kHz), and static emissions (0 Hz) [4]. The categorization of electromagnetic radiation as a function of wavelength and frequency is depicted in Fig. 3.

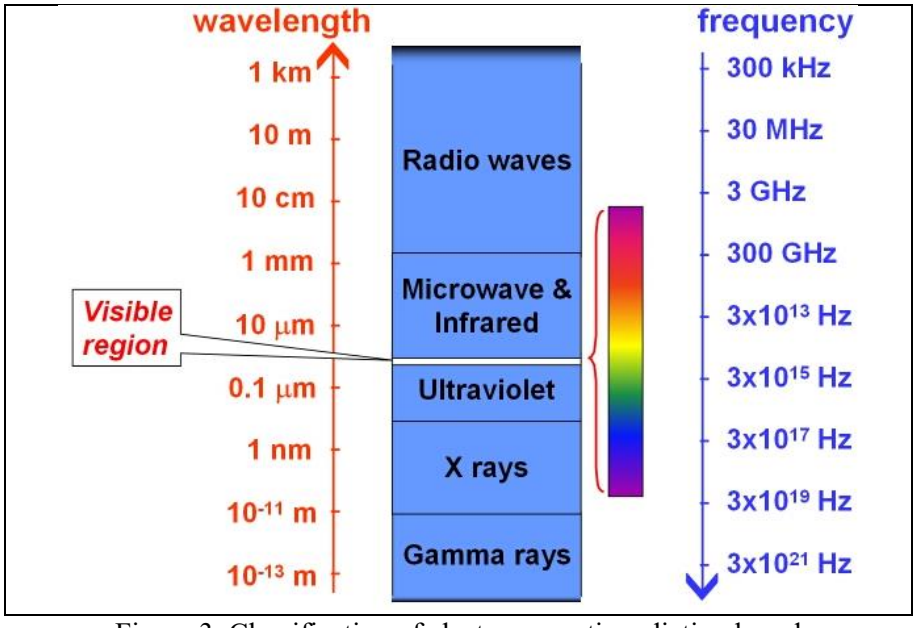

Figure 3. Classification of electromagnetic radiation based on wavelength and frequency [5]

2. SOURCES OF NON-IONIZING RADIATION

Non-ionizing radiation comes from both natural environments and human-made technologies. The radiation in our environment is categorized into two primary types: natural radiation, which occurs independent of anthropogenic activity and to which all living organisms have evolutionarily adapted, and artificial radiation, which stems from human access to electromagnetic energy. Natural radiation encompasses phenomena such as the thermal emissions of terrestrial bodies, solar radiation, cosmic radio waves that bypass atmospheric absorption, and spontaneous fluctuations in our planet's electric and magnetic fields, including atmospheric discharges. Conversely, anthropogenic radiation is primarily generated by high-voltage overhead power lines, broadcasting stations, telecommunication systems (such as mobile networks), radar and navigation infrastructure, electrical substations, domestic appliances, and household wiring. In essence, the non-ionizing radiation spectrum is bifurcated into two major categories, namely optical radiation and electromagnetic fields. [6].

Optical radiations are classified based on their position relative to visible light: higher-energy waves are ultraviolet (UV), while lower-energy waves are infrared (IR). Common UV sources include sunlight, welding techniques, sunlamps, germicidal sterilization lights, and discharge lamps. IR emissions primarily come from thermal industrial processes like steelmaking and glass fabrication. Additionally, the integration of coherent laser sources is rising significantly. Medical implementations of these technologies range from neonatal and UV phototherapy to surgical lasers and physiotherapy heat treatments [7].

Various bands of the electromagnetic fields serve distinct technological and medical purposes. For instance, microwaves are essential for modern telecommunications, satellite and radar links, mobile networks, TV transmitters, and household microwave ovens, while radiofrequency (RF) waves drive radio communications, television sets, and visual display units. Meanwhile, home electronics, everyday electrical machinery, building wiring, transformers, and high-voltage power lines are naturally surrounded by extremely low-frequency (ELF) electric and magnetic fields. Furthermore, this energy is heavily leveraged in the healthcare sector for advanced procedures, including magnetic resonance imaging (MRI), microwave hyperthermia, and both therapeutic and surgical diathermy [7].At the present time, electromagnetic radiation has become an integral component of the human living environment. Some of the electromagnetic radiation sources in our living spaces include mobile phones, tablets, computers, televisions, irons, microwave ovens, refrigerators, electric cookers, electric stoves, and all other electrical devices. The proliferation and continuous growth of diverse electrical devices, combined with the rapid

evolution of advanced telecommunications, have necessitated the monitoring of environmental electromagnetic field intensities. Consequently, regulating these exposure levels is crucial in both domestic and occupational settings to safeguard the public from the potential adversities of excessive field exposure [6].

3. BIOLOGICAL EFFECTS OF NON-IONIZING ELECTROMAGNETIC RADIATION

Although non-ionizing radiation is considered less detrimental to human health than ionizing radiation, continuous or repetitive use of related technologies remains a concern. Thermal induction represents the most prevalent consequence of non-ionizing radiation. While excessive heating precipitates tissue damage, low-level environmental exposure typically remains benign. To illustrate, the human body naturally dissipates harmless thermal energy, whereas a microwave oven concentrates sufficient non-ionizing radiation to heat food. Conversely, the long-wavelength segments of the spectrum—such as radiofrequency, Very Low-Frequency (VLF), and Extremely Low-Frequency (ELF)-seldom induce thermal changes, though they can facilitate surface electric charge accumulation on the body. Under extreme conditions, this low-frequency radiation interferes with neuromuscular responses. Additionally, despite lacking ionizing capabilities, infrared, visible, and ultraviolet wavebands possess adequate energy to trigger photochemical reactions. Intense exposure to these optical frequencies can induce cutaneous hyperpigmentation, photo-aging, and cataract formation. However, substantial ambiguity remains regarding the precise severity of outcomes resulting from both short-term and long-term exposure to different non-ionizing radiation modalities. Ultimately, natural ultraviolet (UV) radiation represents the most significant public health risk within this spectrum. Although individual photons of UV radiation lack the energy required to ionize atoms, they can nevertheless induce tissue damage by cleaving intra-molecular chemical bonds of the DNA helix, thereby introducing a long-term chronic risk of malignancy. This underlying mechanism must be carefully evaluated when establishing permissible exposure limits. Solar ultraviolet (UV) irradiation directly induces the generation of cyclobutane pyrimidine dimers (CPDs) and pyrimidine 6-4-pyrimidone photoproducts (6-4PPs), while UV-induced reactive oxygen species (ROS) further promote DNA damage. Investigating the detrimental impacts of very-long-wave UVA (>380 nm) and visible light (≥400 nm), Lawrence et al. documented significant alterations in gene expression and protein folding across both *in vitro* and *in vivo* models at 24 and 2 hours post-exposure, respectively, which included the formation of dark CPDs. Furthermore, oxidative stress triggered by endogenous cutaneous chromophores—such as melanin, β-carotene,

and protoporphyrin IX-inflicts multifaceted cellular damage. These collective findings underscore the critical necessity for developing efficient sunscreens targeting the near-380 nm UV spectrum [8].Conversely, IR and visible light radiation induce biological damage strictly through high-intensity, multi-photon processes. While the fundamental biological responses triggered by these two bands are virtually identical, coherent light sources such as lasers can generate substantially higher irradiances, thereby heating localized tissue volumes to temperatures sufficient to cause rapid physical alterations [7, 9].Microwave radiation (300 MHz – 30 GHz) possesses moderate wavelengths (1 mm to 1 m) and photon energy. It interacts with human tissues by creating standing waves through resonance, depending on tissue orientation. Environmental sources include broadcasting antennas, transmission equipment (cables, waveguides, heaters), and power supplies emitting radiation as a side effect. The associated health hazards depend heavily on frequency, power density, field exposure, and body orientation. Biologically, microwaves induce thermal effects (tissue heating) and electric currents. This heating is particularly hazardous to sensitive organs like the brain, eyes, stomach, genitals, liver, and kidneys, potentially causing cataracts, inductive burns, or contact burns from metallic implants and glasses [6]. The non-thermal radiofrequency radiation emitted by mobile phones is categorized as a Group 2B potential human carcinogen, with multiple studies linking it to an increased risk of cancer and tumor development [10]. A study investigating the effect of smartphone radiofrequency on platelet aggregation observed that ADP-induced aggregation was increased in both ischemic stroke patients and healthy individuals, while it was suppressed in blood samples from patients with polycythemia vera [11]. While non-thermal carcinogenic effects have been observed in animal studies, no definitive evidence confirms such effects in humans [6].Low-Frequency, Extremely Low-Frequency (ELF), and Static Fields (0 Hz – 10 MHz) include ELF fields (0 Hz – 300 Hz) induced by electrical currents in conductors, static fields (0 Hz) from natural sources like the Earth's magnetic field or friction, and low/very low-frequency radiation (up to 10 MHz) defined by low energy and long wavelengths (over 1 m). Although this radiation easily penetrates the human body, it rarely accumulates in tissues, and its biological energy transfer is weak. Extensive research has found no clear, permanent link between static or ELF fields and harmful effects on human health. Although static magnetic fields can induce small electrical potential differences within blood vessels, no confirmed adverse long-term health effects in humans have been established. In contrast, low-frequency alternating fields induce electric currents that may stimulate nerves and muscles, but there is currently no conclusive evidence of long-term adverse health effects.

Table 1. Biological Effects of Different Non-Ionizing Radiations [9]

	Radiation	Wavelength/ Frequency	Biological Effects
Optical Radiations	**UVC**	100 nm	Erythema, inc pigmentation (for skin) Inflammation of cornea (for eye)
	UVB	280 nm	Erythema, inc pigmentation (for skin) Skin cancer (long term exposure) Photochemical cataract (for eye) Photosensitive skin reactions
	UVA	315 nm	Erythema, inc pigmentation (for skin) Skin photo-ageing, Skin cancer (long term exposure) Photochemical & thermal retinal injury (for eye)
	Visible	400 nm 780 nm	Thermal retinal injury (for eye) Thermal retinal injury, thermal cataract (for eye)
	IRA	1.4 µm	Skin burn Corneal burn, cataract (for eye)
	IRB	3 µm	Skin burn Corneal burn, cataract (for eye)
	IRC	1 mm	Heating of body surface
Electromagnetic Fields	**Microwave**	300 GHz 1 GHz <100 KHz	Heating of body surface Heating with 'penetration depth of 10 mm Raised body temperature Cumulation of charge on body surface Disturbance of nerve & muscle responses
	Static	0 Hz	Magnetic field–vertigo/ nausea Electric field–charge on body surface

The primary public health risks are acute, such as electric shocks from physical contact or electromagnetic interference with life-supporting medical devices, including pacemakers and ferromagnetic implants [6].

The associated health hazards of non-ionizing radiation types are governed by their depth of penetration into the human body and the specific absorption profiles of diverse tissues as shown in Table 1.

4. NON-IONIZING RADIATION PROTECTION AND STANDARDS.

Numerous national and international regulations have been introduced to safeguard individuals from the potential harmful effects of non-ionizing

radiation. These recommendations are mainly developed and periodically revised by leading organizations, including the International Commission on Non-Ionizing Radiation Protection (ICNIRP) and the World Health Organization (WHO). For each scientifically established adverse effect, ICNIRP defines a corresponding health-effect threshold, representing the minimum exposure level at which that effect has been observed. These threshold values are determined conservatively to provide a high level of protection for the general population under normal exposure conditions.

Table 2. Basic restrictions for electromagnetic field exposure from 100 kHz to 300 GHz, for averaging intervals ≥ 6min.[a] [12]

Exposure scenario	Frequency range	Whole-body average SAR(Wkg^{-1})	Local Head/Torso SAR(Wkg^{-1})	Local Limb SAR(Wkg^{-1})	Local Sab(Wm^{-2})
Occupational	100 kHz to 6 GHz	0.4	10	20	NA
	>6 to 300 GHz	0.4	NA	NA	100
General public	100 kHz to 6 GHz	0.08	2	4	NA
	>6 to 300 GHz	0.08	NA	NA	20

[a]*Note:*
1."NA" signifies "not applicable" and does not need to be taken into account when determining compliance.
2.Whole-body average SAR is to be averaged over 30 min.
3.Local SAR and S_{ab} exposures are to be averaged over 6 min.
4.Local SAR is to be averaged over a 10-g cubic mass.
5.Local S_{ab} is to be averaged over a square 4-cm^2 surface area of the body. Above 30 GHz, an additional constraint is imposed, such that exposure averaged over a square 1-cm^2 surface area of the body is restricted to two times that of the 4-cm^2 restriction.

Since health risk is generally related to how much electromagnetic field (EMF) is absorbed by biological tissues, the threshold levels are expressed in terms of the strength of electromagnetic field absorption. For instance, at frequencies below approximately 6 GHz, where electromagnetic fields (EMFs) exhibit deep tissue penetration—necessitating the consideration of depth—exposure is appropriately quantified using the "Specific Absorption Rate" (SAR), defined as the absorbed power per unit of mass ($W.kg^{-1}$). In contrast, at frequencies exceeding 6 GHz, where electromagnetic fields (EMFs) are absorbed more superficially—rendering tissue depth less significant—exposure is more

accurately characterized by the density of absorbed power per unit area ($W.m^{-2}$), a metric designated as "absorbed power density (S_{ab}) (Table 2) [12].

Based on the different interaction mechanisms of low and high frequency fields with human tissue, ICNIRP divides exposure limits into specific operational zones. Accordingly, ICNIRP has established primary exposure criteria and defined threshold values to provide a clearer overview of how these limits vary according to the frequency spectrum. The basic limitations recommended by ICNIRP for EMF frequencies from 100 kHz to 300 GHz are given in Table 2.

REFERENCES

[1] University Physics, Volume 2, https://openstax.org/books/university-physics-volume-2/pages/16-2-plane-electromagnetic-waves, Access date:11.06.2026.

[2] https://www.rfwireless-world.com/terminology/ionizing-vs-non-ionizing-radiation, Access date:11.06.2026.

[3] Balasubramanian D, Agraharam G, Girigoswami A, Girigoswami K. "Multiple radiations and its effect on biological system – a review on in vitro and in vivo mechanisms", Annals of Medicine, Vol. 57, no. 1, 2486595, 2025.

[4] International Commission on Non-Ionizing Radiation Protection (ICNIRP), Guidelines for limiting exposure to electromagnetic fields, (100 kHz to 300 GHz). Health Physics, 118(5), 483-524, 2020.

[5] https://astronomy.swin.edu.au/cosmos/*/Electromagnetic+Spectrum, Access date:10.06.2026.

[6] Wojtczak M, Piotrowski Z. "Radiation standards review concerning non-ionizing radiation", Radioelectronic Systems Conference 2019, edited by Piotr Kaniewski, Jan Matuszewski, Proc. of SPIE, Vol. 11442, 114420J, 2020, doi: 10.1117/12.2565220.

[7] Kwan-Hoong Ng. "Non-Ionizing Radiations–Sources, Biological Effects, Emissions and Exposures", Proceedings of the International Conference on Non-Ionizing Radiation at UNITEN (ICNIR2003) Electromagnetic Fields and Our Health, 20-22 October 2003.

[8] Lawrence KP, Douki T, Sarkany RP, et al. "The UV/visible radiation boundary region (385–405 nm) damages skin cells and induces "dark" cyclobutane pyrimidine dimers in human skin in vivo", Sci Rep., 8(1), 12722, 2018.

[9] Martin C.J. & Sutton D.G. Ed. "Practical Radiation Protection in Health Care", Oxford University Press, Oxford p3-8, 2015.

[10] Belpomme D, Hardell L, Belyaev I, et al. "Thermal and non-thermal health effects of low intensity non-ionizing radiation: an international perspective", Environ Pollut., 242(Pt A):643–658, 2018.

[11] Olkhovskiy I, Stolyar M, Lagutinskaya D, et al. "The effect of mobile phone radiation on in vitro platelet aggregation in patients with Polycythemia vera and ischemic stroke", Biophysics, 64(1),62–66, 2019.

[12] International Commission on Non-Ionizing Radiation Protection (ICNIRP), "Principles For Non-Ionizing Radiation Protection", Health Phys. 118(5):477–482; 2020.

CHAPTER -9

CLEAN AND QUALITY DRINKING WATER PRODUCTION VIA BIOMIMETIC APPROACHES: THE NAMIB DESERT BEETLE AND OTHER NATURAL MODELS

Sabri ÜNAL[1], Oğuzhan ERKAN[2]

1.INTRODUCTION

Access to clean drinking water has become one of the most critical global problems of the 21st century. Climate change, increasing population, and polluted water resources threaten the sustainability of conventional water supply methods. In this context, the water collection strategies developed by living organisms over millions of years of evolution constitute a source of inspiration for human-made systems. This book chapter comprehensively addresses biomimetic approaches in clean drinking water production, focusing specifically on the hydrophobic-hydrophilic surface adaptation of the Namib Desert Beetle (*Stenocara gracilipes*). Additionally, water collection mechanisms of various natural models such as fog-harvesting plants, the desert kangaroo rat, web-weaving spiders, bromeliad plants, ferns, cacti, the thorny devil lizard, and mangrove trees are examined. The study analyzes the fundamental principles, water collection efficiencies, and potential for transfer to architectural/engineering applications of these biological systems. Furthermore, design criteria, material options, performance evaluation methods, and sustainability dimensions of biomimetic water harvesting systems are discussed. This comprehensive review aims to provide a theoretical framework for the development of nature-inspired innovative water production technologies.

1.1The Global Water Crisis and the Need for Sustainable Solutions

Although water is an indispensable resource for the continuity of life, the world is increasingly facing a problem of scarcity. According to United Nations data, approximately one quarter of the world's population lacks access to safe

[1] Prof. Dr., Department of Forest Entomology and Conservation/Faculty of Forestry, Kastamonu University, TÜRKİYE, ORCID: 0000-0002-2379-5331
[2] Undergraduate Student , Forestry Engineering Department,Faculty of Forestry, Kastamonu University, TÜRKİYE

drinking water, and this number is expected to increase with the effects of climate change (UNESCO, 2021). Rapid urbanization, increasing demand for agricultural irrigation, industrial pollution, and overuse of water resources lead to the degradation of freshwater ecosystems.Conventional water supply methods often rely on groundwater extraction, river regulation, or energy-intensive desalination plants. Each of these approaches has significant limitations in terms of energy consumption, environmental impact, or sustainability. The idea of passively harvesting water from the atmosphere, especially in arid and semi-arid regions, is increasingly attracting the attention of researchers.

1.2Biomimetics: Nature's Million-Year R&D

Biomimetics or biomimicry is an interdisciplinary approach that aims to produce solutions to human problems by imitating the structures, functions, behaviors, and processes of living organisms in nature (Benyus, 1997). Over millions of years of evolution, nature has developed highly optimized solutions in terms of energy efficiency, material optimization, and sustainability. Biomimetic applications in architecture and engineering appear across a wide range, from energy-efficient building envelopes to water management systems. Selçuk and Sorguç (2007) examined the effect of biomimesis on the architectural paradigm in detail and emphasized that the integration of natural systems into built environment design is critical for sustainability. Zari (2011) systematically evaluated the potential of biomimetic approaches to enhance sustainability in architectural design.This book chapter aims to comprehensively address biomimetic approaches in clean drinking water production. Specifically focusing on the unique water collection mechanism of the Namib Desert Beetle (*Stenocara gracilipes*), it also examines water collection strategies of various natural models such as fog-harvesting plants, the desert kangaroo rat, web-weaving spiders, bromeliads, ferns, cacti, the thorny devil lizard, and mangrove trees.

The main objectives of the chapter are:

1. To explain the fundamental principles and physical operation of water collection mechanisms in natural systems,
2. To evaluate the potential transfer of these biological systems to architectural and engineering applications,
3. To determine the design criteria and performance parameters of biomimetic water harvesting systems,
4. To analyze current applications and future research orientations,

5. To reveal the contribution of these technologies to sustainable development goals.

2. THE NAMIB DESERT BEETLE: NATURE'S WATER ARCHITECT

2.1. Taxonomy and Morphology

Stenocara gracilipes is a beetle species belonging to the order Coleoptera, family Tenebrionidae. This species is endemic to the Namib Desert in southwestern Africa, one of the driest regions in the world (Seely & Henschel, 2008). Annual rainfall in the Namib Desert is below 20 mm, and access to water is the greatest challenge for the continuation of life.Adult individuals are typically 15-20 mm in length, and their bodies are black. The beetle's most striking feature is the microscopic surface structures on its elytra (wing covers). These structures form the basis of the adaptation that allows the beetle to benefit from atmospheric water in foggy conditions.

2.2. Physics of the Water Collection Mechanism

The groundbreaking study by Parker and Lawrence (2001) elucidated the water collection mechanism of the Namib Desert Beetle in detail. The beetle's dorsal surface exhibits an arrangement of hydrophilic (water-attracting) bumps placed on a hydrophobic (water-repelling) background.

Table 1. Namib Desert Beetle Elytra Surface Properties

Feature	Hydrophobic Region	Hydrophilic Bump
Water contact angle	~120-130°	~60-70°
Surface roughness	High (microscopic)	Low
Bump diameter	-	~0.5-1.0 mm
Inter-bump distance	-	~0.5-1.5 mm
Function	Directing water droplets	Water nucleation ar

Microscopic water droplets (typically 1-40 microns in diameter) moving within the fog are carried onto the beetle's back by wind currents. The hydrophilic bumps enable the nucleation and accumulation of droplets. When the droplets

reach a certain critical size (approximately 1 mm), they move easily across the hydrophobic background towards the beetle's mouthparts (Hamilton et al., 2003).

The most striking feature of this mechanism is that it operates completely passively, requiring no energy input. The beetle initiates this efficient water collection process simply by adopting an appropriate body posture (usually a head-down position).

2.3. Ecological Context and Adaptive Value

The water collection adaptation of the Namib Desert Beetle has evolved in response to the unique ecological conditions of the desert. The dense fog layers that form in the morning hours in the Namib Desert are an important component of the region's water cycle. The beetles become active during these fog events and position their bodies perpendicular to the wind. Seely and Henschel (2008) estimate that this adaptation meets 50-80% of the beetle's daily water requirement. This situation not only enables the beetle to survive but also to reproduce under the harsh conditions of the desert.

2.4. Transfer to Architectural Applications: The Namibia University Hydrology Centre

The best example of the application of Namib Desert beetle water collection principles at an architectural scale is seen in the Namibia University Hydrology Centre building (Killen, 2011). In this structure, the beetle's elytra surface is mimicked by hydrophobic-hydrophilic coatings applied to large-scale metal panels.The building façade consists of panels with different tilt angles and is oriented to maximize water collection efficiency. The collected water is conveyed to storage tanks via a specially designed channel system. This application demonstrates that biomimetic principles can be successfully implemented at an architectural scale.

3. OTHER NATURAL WATER COLLECTION MODELS

3.1. Fog-Harvesting Plants

3.1.1. Tillandsia* Species (Air Plants)

Plants of the genus *Tillandsia*, belonging to the Bromeliaceae family, are epiphytic species (growing on host plants). These plants sustain their lives by obtaining water and nutrients from the atmosphere without direct contact with the soil. Special trichome structures on their leaf surfaces effectively capture fog droplets (Andrade, 2003).The leaf surface of *Tillandsia* species exhibits a complex morphology at the microscopic scale. The shape, density, and surface chemistry of the trichomes are the fundamental factors determining water

collection efficiency. Artificial surfaces inspired by these plants hold promise for water collection potential, especially in foggy regions.

3.1.2. Chilean Fog Bush (Flourensia thurifera)

Flourensia thurifera, growing in the arid coastal regions of Chile, is another plant species that has evolved to benefit from dense fog events. The leaf surface of this species, similar to *Tillandsia*, contains trichomes with high water capture capacity (Carter et al., 2007).The water collection mechanism of these plants is based on different physical principles in the processes of droplet nucleation and growth, unlike the Namib Beetle. Specifically, the micro-pressure differences between the trichomes facilitate the direction of fog droplets onto the surface.

3.2. Desert Kangaroo Rat (Dipodomys deserti)

The desert kangaroo rat is a rodent species living in the North American deserts that has developed extraordinary adaptations for metabolic water production. Although it feeds on dry seeds, this species can survive without needing drinking water (Schmidt-Nielsen, 1964).

The water balance strategy of the desert kangaroo rat is based on four fundamental mechanisms:

1. Metabolic water production: Water synthesis through the oxidation of fatty acids,
2. Kidney adaptations: The capacity to produce highly concentrated urine,
3. Minimization of respiratory water loss: Reduction of water loss through exhalation via complex structures in the nasal passages,
4. Behavioral adaptations: Reducing water loss by staying in underground burrows during the day.

These adaptations can serve as inspiration for closed-loop water life support systems and water-efficient building ventilation systems.

3.3. Web-Weaving Spiders (Family Uloboridae)

Spider webs have a remarkable capacity for capturing water droplets. The dew drops that form on spider webs, especially in the morning hours, demonstrate the water collection potential of this biological structure (Zheng et al., 2010).The water collection capacity of spider webs depends on three basic factors;

1. Microscopic knot structures: Periodic knots on the web threads create preferential sites for droplet nucleation.
2. Hydrophobic-hydrophilic pattern: The surface chemical heterogeneity of the web threads directs droplet movement.

3. Elasticity and tension: Deformation of the web under wind and droplet weight facilitates droplet coalescence and transport.

Table 2. Comparison of Water Collection Mechanisms of Natural Models

Organism	Basic Mechanism	Water Collection Efficiency	Energy Input	Scalability
Namib Desert Beetle	Hydrophobic-hydrophilic surface	0.5-1.0 L/m²/day	Passive	High
Tillandsia	Trichome structures	0.3-0.7 L/m²/day	Passive	Medium
Spider web	Knot/microfiber structure	0.2-0.5 L/m²/day	Passive	High
Cactus	Spine/groove system	0.1-0.3 L/m²/day	Passive	Medium
Bromeliad	Tank rosette	0.5-1.5 L/plant/day	Passive	Low

3.4. Bromeliad Plants

Many species of the bromeliad family collect water through a central tank formed by their rosette-shaped leaves (Benzing, 2000). These plants, known as "tank" bromeliads, host complex micro-ecosystems in the water reservoir formed at the base of the leaves.

The most remarkable feature of this system from an engineering perspective is the versatility of its water collection mechanism:

- Direct collection of rainwater,
- Direction of water flowing over the leaf surface,
- Capture of fog and dew droplets,
- Nutrient cycling through the accumulation of debris and organic matter.

This adaptation of bromeliads serves as an inspiring model for water harvesting and direction on sloped roof surfaces.

3.5. Ferns (Especially CheilanthesSpecies)

Ferns from arid regions draw attention with their adaptations to water scarcity. *Cheilanthes* species effectively collect fog and dew droplets thanks to the dense trichome and scale structures on their leaf surfaces (Nobel, 2006).Three basic elements stand out in the water collection strategy of these plants:

1. Leaf surface morphology: The folded and grooved leaf structure facilitates water direction.
2. Trichome density and morphology: High-density trichome structures provide a large surface area for water droplet nucleation.
3. Cuticle chemistry: Special wax layers enable controlled movement of water on the leaf surface.

3.6. Cacti (Especially Opuntia Species)

Cacti are plants specialized in water collection and storage. The spines of Opuntia* species, in particular, serve to capture water droplets and direct them towards the plant body (Ju et al., 2012).The water collection mechanism of cacti can be described as a three-stage process:

1. Capture: Conical structures on the spines nucleate fog droplets.
2. Coalescence: Small droplets merge on the spine surface to form larger drops.
3. Transport: The coalesced drops move towards the plant body via microscopic grooves on the spine.

Ju et al. (2012) demonstrated that this mechanism could be transferred to artificial surfaces using laser microfabrication techniques. The fabricated artificial spine structures exhibited water collection performance similar to their natural counterparts.

3.7. Thorny Devil Lizard (Moloch horridus)

The thorny devil lizard (*Moloch horridus*), living in the Australian deserts, can collect water through microscopic channels on its body surface (Bentley & Blumer, 1962). The skin surface of this species exhibits a complex combination of hydrophobic and hydrophilic regions.The remarkable feature of the lizard's water collection mechanism is not only the collection of water but also its direction to specific parts of the body (especially the mouth area). This direction occurs through capillary effects facilitated by the microscopic channel system on the skin.This adaptation is an inspiring model for engineering applications where water needs to be collected over large surface areas and directed to specific collection points.

3.8. Mangrove Trees

Mangrove trees are plants that live in saline water environments and have developed extraordinary adaptations for desalination (Tomlinson, 2016). These species take in seawater through their root systems, filter out salt, and direct freshwater to plant tissues.The desalination mechanism of mangroves consists of three main components:

1. Ultrafiltration roots: Special proteins in root cells retain salt ions while allowing water molecules to pass through.
2. Salt-secreting glands: Some mangrove species can expel accumulated salt through special glands in their leaves.
3. Water storage tissues: Freshwater is stored in various tissues of the plant for use during dry periods.

These mechanisms provide an important model for the development of low-energy water desalination technologies.

4. DESIGN OF BIOMIMETIC WATER HARVESTING SYSTEMS

4.1. Surface Engineering Principles

Surface engineering plays a fundamental role in the design of biomimetic water harvesting systems. Principles learned from the Namib Beetle and other natural models can be used to increase the water collection efficiency of artificial surfaces.

4.1.1. Wettability and Contact Angle

The interaction of a surface with water is characterized by the contact angle (θ):

- Hydrophilic surfaces: $\theta < 90°$ (water wets the surface)
- Hydrophobic surfaces: $\theta > 90°$ (water beads on the surface)
- Superhydrophobic surfaces: $\theta > 150°$ (water rolls off easily)
- Superhydrophilic surfaces: $\theta < 10°$ (water spreads rapidly)

The surface of the Namib Beetle exhibits a combination of these two extreme behaviors. Hydrophilic bumps ($\theta \approx 60\text{-}70°$) allow for the nucleation and accumulation of water droplets, while the surrounding hydrophobic background ($\theta \approx 120\text{-}130°$) enables the collected water to move easily.

4.1.2. Surface Roughness and Morphology

- The models by Wenzel (1936) and Cassie-Baxter (1944) explain the effect of surface roughness on wettability. On a rough surface, the contact angle is related to the roughness factor because the real surface area is larger than the geometric area.In natural systems, surface roughness is typically organized at two scales:

- Microscale: ~1-100 μm sized structures;Nanoscale: ~10-1000 nm sized structures

This hierarchical structuring plays a critical role in the processes of water droplet nucleation, growth, and transport.

4.2. Material Options and Production Technologies

The materials and technologies that can be used in the production of biomimetic water harvesting surfaces are summarized in Table 3

Table 3. Material and Production Options for Biomimetic Water Harvesting Surfaces

Material Type	Examples	Advantages	Disadvantages	Production Method
Polymers	PDMS, PMMA, PS	Low cost, easy processability	Low mechanical strength	Molding, casting, 3D printing
Metals	Aluminum, copper, titanium	High strength, good thermal conductivity	High cost, corrosion risk	Laser ablation, lithography
Ceramics	Silica, titania, alumina	Chemical resistance, UV stability	Brittle, high-temperature process	Sol-gel, CVD, PVD
Carbon-based	Graphene, carbon nanotubes	Excellent conductivity, high surface area	High cost, difficult production	CVD, electrophoretic deposition
Hybrid	Polymer-metal, polymer-ceramic	Combined properties	Complex production	Layer manufacturing, coating

4.3. Performance Evaluation Parameters

The performance of biomimetic water harvesting systems can be evaluated using the following basic parameters:1. Water collection efficiency (η): Ratio of collected water amount to the theoretical maximum (as a percentage)

1 $\eta = (m\_collected / m\_theoretical) \times 100$
2. Water collection rate (R):** Amount of water collected per unit area and time (L/m²/hour or L/m²/day)
3. Droplet nucleation density (N):** Number of droplets per unit area (cm^{-2})
4. Droplet growth rate (dr/dt):** Change in droplet radius over time (μm/s)
5. **Direction efficiency:** The rate at which collected water reaches the desired collection points (%)

Table 3. Comparative Performance of Artificial Surfaces Inspired by Different Natural Models

Model	Surface Type	Collection Rate (L/m²/day)	Droplet Diameter (mm)	Source
Namib Beetle	Hydrophobic + hydrophilic bumps	0.5-1.0	3-5	Parker & Lawrence (2001)
Spider web	Knotted microfiber	0.3-0.7	2-4	Zheng et al. (2010)
Cactus	Conical spines	0.2-0.5	3-6	Ju et al. (2012)
Tillandsia	Trichome-covered	0.4-0.8	2-3	Andrade (2003)
Hybrid (combined)	Multi-scale hierarchical	0.8-1.5	2-5	Chen et al. (2018)

5. BIOMIMETIC WATER HARVESTING APPLICATIONS

5.1. Architectural Façade Systems

The application of biomimetic water collection principles at an architectural scale has the potential to improve the environmental performance of buildings, especially in water-scarce regions.

5.1.1. Namib Beetle-Inspired Façade Panels

As in the example of the Namibia University Hydrology Centre, water-harvesting panels used on building façades contain hydrophobic-hydrophilic

patterns that mimic the beetle's elytra surface (Killen, 2011). Parameters to be considered in the design of these panels are:

- Panel tilt angle: Should be optimized according to local wind direction and precipitation regime.
- Surface pattern density:** The diameter, height, and spacing of hydrophilic bumps should be determined based on the expected fog droplet size distribution.
- Material selection:** Factors such as UV resistance, thermal expansion, mechanical strength, and cleanability should be considered.

Table 4. Optimal Panel Parameters According to Climate Conditions

Climate Type	Optimum Tilt	Bump Density	Recommended Material
Dense Fog	30-45°	High (>20/cm²)	PMMA + hydrophilic coating
Moderate Fog	45-60°	Medium (10-20/cm²)	Aluminum + anodization
Low Fog + Dew	15-30°	Low (<10/cm²)	Glass + TiO_2 coating
Coastal (Saline)	30-50°	Very high (>30/cm²)	Stainless steel + PTFE

5.1.2. Cactus-Inspired Directional Systems

The droplet transport mechanism observed on the conical spines of cacti inspires the design of water direction systems on building roofs. Using this principle, Ju et al. (2012) achieved 30% more water collection per unit area on artificial surfaces they developed.In these types of systems, the angle of the conical structures, surface roughness, and wettability gradient are critical factors determining the speed and direction of droplet movement. For maximum efficiency, the base diameter, aspect ratio, and surface energy gradient of the conical structures should be optimized.

5.2. Water Harvesting Meshes

The structural properties of spider webs can be successfully used in the design of large-scale water harvesting meshes. These meshes offer an effective method for benefiting from atmospheric water, especially in foggy regions.

5.2.1. Periodic Knot Structures

Zheng et al. (2010) elucidated the role of periodic knot structures in spider webs in droplet nucleation and coalescence and showed that these structures could be transferred to artificial meshes.Characteristic parameters of knot structures:

- Knot spacing: 200-500 μm
- Knot diameter: 2-3 times the thread diameter
- Knot morphology: Ellipsoidal or spherical

Polymer meshes developed based on these principles exhibited 40-60% higher water collection efficiency compared to conventional meshes under foggy conditions.

5.2.2. Multi-Layered Mesh Systems

Multi-layered systems formed by combining meshes with different pore sizes can provide effective water collection over a wide range of droplet sizes. In such systems:

- Top layer: Large pore size, for impaction and capture of fog droplets.
- Middle layer: Medium pore size, for droplet coalescence and growth.
- Bottom layer: Small pore size, for water direction and collection.

5.3. Capillary Action-Based Directional Systems

The microscopic channel system on the skin of the thorny devil lizard provides an effective model for directing water collected over large surfaces to specific points. This principle can be used especially in water harvesting applications on large roof surfaces.Design parameters of capillary channel systems:

- Channel width: 50-200 μm
- Channel depth:** 0.5-1 times the width
- Channel wall angle:** 30-60°
- Hydrophilic coating:** Contact angle <30°

By optimizing these parameters, more than 90% of the water collected on large surfaces can be directed to target collection points without any additional energy input besides gravity.

6. SUSTAINABILITY AND ECONOMIC EVALUATION

6.1. Energy Efficiency and Carbon Footprint

One of the most important advantages of biomimetic water harvesting systems is the minimal energy consumption due to their passive operating principle. At table -5 compares the energy consumption of different water supply methods.

Table 5. Energy Consumption Comparison of Different Water Supply Methods

Method	Energy Consumption (kWh/m³ water)	CO_2 Emissio
Conventional (groundwater pumping)	0.5-2.0	0.3-1.2
Reverse osmosis (seawater)	3.0-6.0	1.8-3.6
Reverse osmosis (brackish water)	1.5-2.5	0.9-1.5
Biomimetic fog harvesting	0.05-0.1	0.03-0.06
Biomimetic dew collection	0.02-0.05	0.01-0.03

The low carbon footprint of biomimetic systems offers a significant advantage, especially in the context of combating climate change. Furthermore, the operation and maintenance costs of these systems are significantly lower than those of conventional systems.

6.2. Economic Feasibility

The economic feasibility of biomimetic water harvesting systems depends on three main factors:

1. Investment cost: Surface production, assembly, and infrastructure costs.
2. Operating cost: Maintenance, cleaning, and possible repair expenses.
3. Value of water produced: Local water prices and the economic cost of water scarcity.

Economic analyses for Namib Desert Beetle-inspired systems show that the payback period varies between 2-5 years (Killen, 2011). This period is even shorter in regions where water scarcity is severe and conventional water costs are high.

6.3. Social and Environmental Benefits

The social benefits of biomimetic water harvesting systems are:

- Increasing water security for communities living in arid regions,
- Providing independent water supply in rural areas without access to conventional water infrastructure,
- Reducing the time and labor spent on water transport (especially for women and children),
- Strengthening adaptive capacity to climate change.

Environmental benefits are;

- Protecting aquifers by reducing groundwater extraction,
- Reducing energy consumption and associated carbon emissions,
- Preventing environmental impacts of conventional water facilities (brine discharge, habitat destruction, etc.),
- Technologies with a low ecological footprint, compatible with the natural water cycle.

7. FUTURE RESEARCH ORIENTATIONS

7.1. Bio-Inspired New Materials

Areas that future research should focus on;

1. Self-cleaning surfaces: Hybrid systems combined with lotus effect principles as a solution to the problem of dust and dirt accumulation reducing water collection efficiency.
2. Photocatalytically active surfaces: Integration of photocatalytic materials such as TiO_2 can provide water disinfection together with water collection.
3. Biodegradable materials: Water harvesting systems produced from compostable or recyclable materials to minimize environmental impact.

7.2. Multi-Functional Hybrid Systems

Combining different principles learned from natural models in a single system can create synergistic effects and enhance performance. For example:

- Hydrophobic-hydrophilic pattern of the Namib Beetle + Conical directional structures of the Cactus.
- Knotted structure of the spider web + Capillary channel system of the lizard.
- *Tillandsia* trichome structure + Tank collection mechanism of the bromeliad.

7.3. Smart and Adaptive Surfaces

The ability of natural systems to adapt to environmental conditions can be mimicked with smart material technologies;1. Temperature-sensitive surfaces: Polymers that change hydrophilic/hydrophobic properties within specific temperature ranges (e.g., PNIPAAm).2. pH-sensitive surfaces: Materials that change surface properties depending on the pH of rainwater.3. Wind-adaptive systems: Mechanical systems that change surface topography according to wind direction and speed.

7.4. Scaling-Up and Dissemination

Barriers to be overcome for transforming successful laboratory-scale prototypes into commercial-scale production and widespread use:

- Reducing production costs:** Developing high-throughput production techniques such as roll-to-roll production, nanoimprint lithography.
- Durability tests:Collecting performance and lifespan data under different climate conditions through long-term field studies.
- Standards and certification: Establishing test protocols and quality assurance systems in compliance with international standards.

8. POLICY AND IMPLEMENTATION RECOMMENDATIONS

8.1. Policy Framework for Local Governments

Policies that local governments can implement to disseminate biomimetic water harvesting technologies:

1. Incentive mechanisms: Tax reductions for buildings incorporating these systems, acceleration of construction permit processes, or direct subsidies.
2. Regulatory adjustments: Building regulations that mandate or encourage biomimetic water harvesting systems in new constructions.
3. Pilot applications in public buildings: Implementation of flagship projects in high-use buildings such as schools, hospitals, and public offices.
4. Integration of water harvesting infrastructure into the network: Necessary arrangements for harvested water to be fed into the city network.

8.2. Education and Capacity Building

Human resource development is critically important for the successful implementation of biomimetic Technologies; Integration into architecture and engineering curricula: Inclusion of biomimetic design principles in undergraduate courses, Vocational training programs: Certification programs for practitioners, Public awareness campaigns: Raising awareness about water conservation and alternative water sources. International Cooperation; The water

crisis in arid regions is a global problem and requires international cooperation for its solution, Knowledge sharing networks: Platforms where results of projects carried out in different countries are shared,Joint R&D projects: Testing and validation studies under different climate conditions, Technology transfer programs: Cost-effective transfer of technologies developed in developed countries to developing countries.

9.CONCLUSION

This study has comprehensively examined the potential of biomimetic approaches in clean drinking water production. The water collection mechanisms of various natural models, including the Namib Desert Beetle, fog-harvesting plants, the desert kangaroo rat, web-weaving spiders, bromeliads, ferns, cacti, the thorny devil lizard, and mangrove trees, have been detailed.Research findings show that natural systems offer significant advantages over man-made systems in terms of energy efficiency, material optimization, and passive operating principles in water collection processes. The transfer of these biological solutions to architectural and engineering applications offers an innovative path for sustainable water supply, especially in water-scarce regions.The most important advantages of biomimetic water harvesting systems are;1. Energy independence: Requires no external energy input due to its passive operating principle.2. Low environmental impact: Minimal carbon footprint compared to conventional water supply methods.3. Local adaptability: Potential to be customized for different climate conditions.4. Cost-effectiveness: Low operation and maintenance costs in the long term.5. Sustainability: Ecologically friendly technologies compatible with the natural water cycle.Future research should focus on new material technologies, multi-functional hybrid systems, smart and adaptive surfaces, as well as scaling-up and dissemination. Furthermore, the development of appropriate policy frameworks, educational programs, and international cooperation mechanisms is of great importance for the dissemination of these technologies.In conclusion, water collection strategies optimized over millions of years of evolution in nature offer a sustainable and innovative path to meet humanity's increasing water demand. The scientific understanding and successful technological transfer of these biological solutions have the potential to make a significant contribution to the solution of the global water crisis.

REFERENCES

Andrade, J.L. (2003). Dew deposition on epiphytic bromeliads. International Journal of Plant Sciences, 164(3), 479-487.

Bentley, P.J. & Blumer, W.F.C. (1962). Uptake of water by the lizard, Moloch horridus.Nature, 194, 699-700.

Benyus, J.M. (1997). Biomimicry: Innovation Inspired by Nature. New York: William Morrow.

Benzing, D.H. (2000). Bromeliaceae: Profile of an Adaptive Radiation. Cambridge: Cambridge University Press.

Carter, V., Schemenauer, R., Osses, P., & Streeter, H. (2007). The Atacama Desert fog collection project at Falda Verde, Chile. In *4th International conference on Fog, Fog Collection and Dew.

Cassie, A.B.D. & Baxter, S. (1944). Wettability of porous surfaces. Transactions of the Faraday Society, 40, 546-551.

Chen, Y., Wang, L., Xue, Y., Liu, M. & Jiang, L. (2018). Bioinspired hybrid surface for enhanced water collection. Advanced Materials Interfaces, 5(11), 1701618.

Hamilton III, W. J., Henschel, J. R., & Seely, M. K. (2003). Fog collection by Namib Desert beetles: correspondence. South African Journal of Science, 99(3), 181.

Ju, J., Bai, H., Zheng, Y., Zhao, T., Fang, R. & Jiang, L. (2012). A multi-structural and multi-functional integrated fog collection system inspired by cactus. Nature Communications, 3, 1247.

Killen, S. (2011). Biomimetic architecture: Namibian fog collection. Berlin: Springer.

Nobel, P.S. (2006). Physicochemical and Environmental Plant Physiology. Burlington: Academic Press.

Parker, A.R. & Lawrence, C.R. (2001). Water capture by a desert beetle. Nature, 414, 33-34.

Schmidt-Nielsen, K. (1964). Desert Animals: Physiological Problems of Heat and Water. Oxford: Oxford University Press.

Seely, M.K. & Henschel, J.R. (2008). Ecophysiology of atmospheric moisture in the Namib Desert. Atmospheric Research, 87(3-4), 260-268.

Selçuk, A.S. & Sorguç, G.A. (2007). Mimarlık paradigmasında biomimesis etkisi [The effect of biomimesis on the architectural paradigm]. Gazi Üniversitesi Mühendislik Mimarlık Fakültesi Dergisi, 22(2), 451-459.

Tomlinson, P.B. (2016). The Botany of Mangroves. Cambridge: Cambridge University Press.

UNESCO. (2021). The United Nations World Water Development Report 2021: Valuing Water. Paris: UNESCO.

Wenzel, R.N. (1936). Resistance of solid surfaces to wetting by water. Industrial & Engineering Chemistry, 28(8), 988-994.

Zari, M.P. (2011). Biomimetic approaches to architectural design for increased sustainability. In The SBSE Conference on Sustainability, Auckland.

Zheng, Y., Bai, H., Huang, Z., Tian, X., Nie, F.Q., Zhao, Y., Zhai, J. & Jiang, L. (2010). Directional water collection on wetted spider silk. Nature, 463, 640-643.

CHAPTER-10

GREEN ENERGY LITERACY THROUGH STEM EDUCATION: A PROPOSAL FOR AN INTERDISCIPLINARY AND REGIONAL STEM MODEL FOR TÜRKİYE

Ahmet YALKIN[1], Hasan UŞTU[2]

1. INTRODUCTION

The concept of STEM (Science, Technology, Engineering and Mathematics) was first introduced by the National Research Council (NRC) in the 1990s under the name SMET (Science, Maths, Engineering and Technology). In the early 2000s, under the leadership of the U.S. National Science Foundation (NSF), the concept evolved into a multidisciplinary approach. This approach was strategically integrated into educational policies with the aim of cultivating a qualified workforce capable of adapting to changing needs and technological competition. In recent years, efforts to integrate the STEM educational approach into education systems have gained significant momentum in many countries worldwide. Educators, policymakers and business and industry organisations emphasise the urgency of strengthening STEM skills in order to address current and future socio-economic challenges [23].

In this global context, STEM education is a pedagogical approach that transcends the mere formal juxtaposition of the four core disciplines. The literature defines STEM education as an integrated learning approach that enables students to analyse problems using discipline-specific knowledge, methods and forms of representation [4,20-23]. Sanders [20] describes the integrated STEM approach as the fundamental mechanisms that facilitate the transfer of science and mathematics from theoretical frameworks to real-world applications through technology and engineering. Bybee [4], on the other hand, emphasises the strategic importance of this approach in developing 21st-century skills, advancing scientific literacy and improving problem-solving practices.The STEM approach aims to transform students into active learners, defining integration as working in

[1] *Dr., Project Office, Tarsus University, Türkiye,
ahmetyalkin@tarsus.edu.tr, (ORCID: 0000-0002-1914-4608)
[2] Dr., Mersin Provincial Directorate of National Education, Mersin, Türkiye,
hasanuctu33@gmail.com, (ORCID: 0000-0002-1811-8280)

the context of complex phenomena or situations on tasks that require students to use knowledge and skills from multiple disciplines [8]. Vasquez, Sneider and Comer also emphasise the integration of disciplines in STEM education, highlighting that students' ability to apply knowledge of science, mathematics, technology and engineering together is crucial for understanding a problem [23]. According to this definition, the STEM educational approach can be described as a learning environment in which students seek answers to the questions “What do I know?” and “How can I use what I know to solve a problem?”. It can be said that the theoretical foundation of STEM education is linked to constructivist and application-based learning perspectives. The constructivist approach describes a process in which students make sense of knowledge by relating it to their own experiences, rather than through the direct transmission of information. STEM learning environments enrich this process through design, prototyping, and iterative refinement through testing. The engineering design process enables students to define the problem they face, identify constraints, develop solution proposals, create prototypes, and improve their designs based on the results obtained [11]. Jolly states that this process offers students opportunities for evidence-based decision-making and learning from mistakes rather than merely producing a final product [11].

Another important aspect of STEM in the learning process is that it enables students to think using multiple representations. Students do not merely describe a problem verbally; they also express it through graphs, tables, measurements, drawings, models, algorithms, or prototypes. Glancy and Moore’s evaluations of the STEM approach reveal that interdisciplinary learning can only deepen when students are able to establish connections between different forms of representation [10]. Therefore, quality STEM education aims to enable students to define a concept and apply it in design.

The importance of the STEM approach cannot be explained solely by global educational trends. Given Türkiye’s regional diversity, there is a perceived need for locally problem-based STEM models in areas such as energy, water, agriculture, transportation, industry, disaster safety, and environmental sustainability. The STEM Education Report published by the Ministry of National Education highlights the potential of the STEM approach to develop problem-solving skills, creativity, interdisciplinary thinking, and 21st-century skills in students [13]. The Türkiye Century Education Model, on the other hand, aims to foster the holistic development of students in terms of knowledge, skills, values, and actions; it centers on environmental awareness, responsibility, productivity, and a holistic approach to learning [14].In this section, STEM education is presented within the framework of an interdisciplinary and regional

model capable of developing green energy literacy. The section's fundamental premise is that addressing green energy literacy solely at the level of recognizing renewable energy sources may be insufficient today. This premise is based on the necessity of addressing the issue not only at the knowledge level but also in terms of comprehension, analysis, synthesis, and evaluation.It can be said that this section, by focusing on green energy literacy, aims to go far beyond the mere acquisition of knowledge-as mentioned above-by fostering an understanding of environmental terminology. In this context, students must be able to analyze the relationships between energy production, consumption, efficiency, carbon emissions, environmental impact, water use, local resources, and sustainable decision-making skills. To achieve this goal, STEM education, particularly when linked to regional problem areas, will provide a strong foundation for learning.

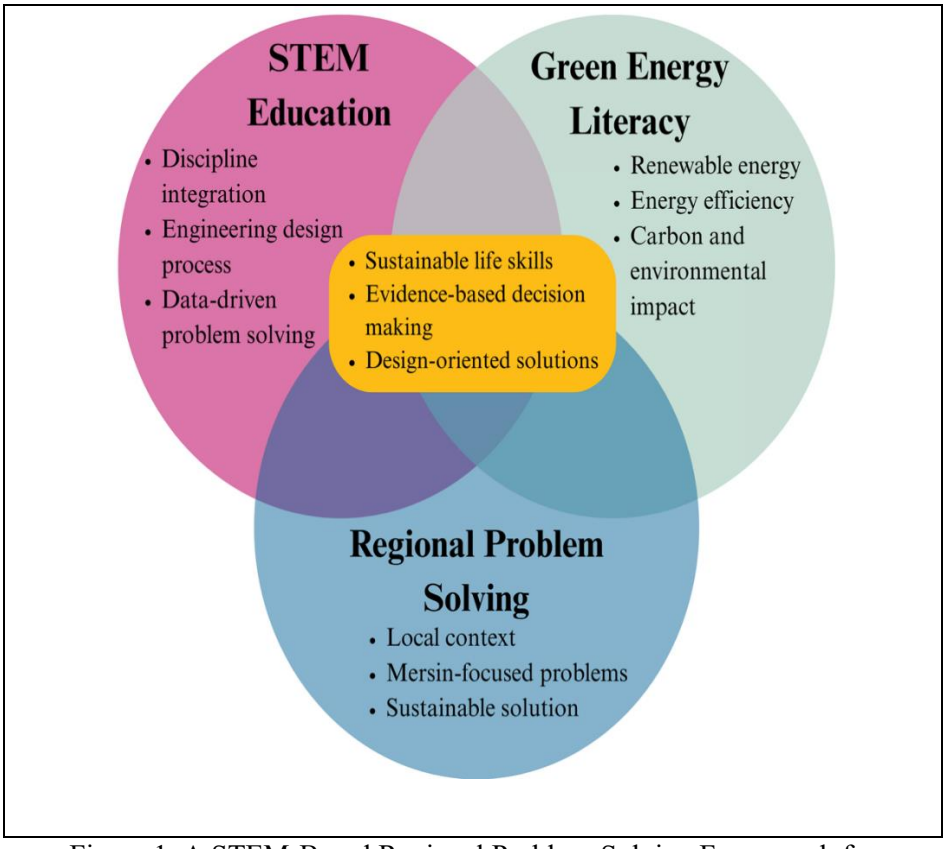

Figure 1. A STEM-Based Regional Problem-Solving Framework for Green Energy Literacy

Note: The model is structured using approaches such as integrated STEM, the engineering design process, multiple representations, and sustainable decision-making [4, 8- 14 ,20 -23].

2. GREEN ENERGY LITERACY: A CONCEPTUAL FRAMEWORK

Energy is a fundamental component of production, transportation, housing and communication practices in today's societies [1]. As Puspitasari et al. state, The energy transition from fossil fuels to renewable energy has become a pressing global priority to mitigate climate change impacts and ensure future energy security. It represents a multidimensional structure with environmental, economic and social implications. Fossil fuel-based industrialisation has increased production capacity while intensifying ecological pressure on nature [6]. This pattern implies that economic growth initially exacerbates environmental degradation but eventually contributes to improvements in environmental quality once a certain income threshold is surpassed. However, economic growth alone cannot resolve environmental issues, since energy consumption emerges as one of the most influential drivers of carbon dioxide emissions [6]. In this context, the incorporation of didactic mediation into developmentally suitable curriculum is regarded as a crucial approach to achieving significant and enduring educational results [22].The concept of green energy literacy has also brought to the forefront the need to restructure the concept of energy around the principles of environmental sustainability and social responsibility. In literature, this is defined as an interdisciplinary competency area in which individuals can track energy flows, analyse the consequences of consumption habits and integrate scientific data into social decision-making processes [22]. The 'green' emphasis is a concept that goes beyond simply adding renewable sources such as solar or wind to the curriculum. It refers to reducing carbon emissions across all processes, from production to consumption; internalising green innovation; and protecting ecosystems through a holistic approach [1], [6]. Students are expected to establish a direct connection between technical knowledge and environmental values, supporting cognitive knowledge with affective awareness and action-oriented behavioural steps [18].Since STEM education is inherently a multidisciplinary approach, it can be described as a pedagogical approach conducive to building this multidimensional literacy. Explaining the working principle of a solar panel through a theoretical text or visuals creates awareness in the student, but the level of awareness will differ when the same topic is addressed using a STEM-based approach. In the STEM approach, a student observes the duration of sunlight in a region. They can measure the energy produced by a small-scale panel. They can conduct a critical needs analysis. They discuss the cost-efficiency relationship of the system and evaluate how it offers a solution to an ecological problem. By overcoming social and psychological barriers related to the cost and complexity of technology, they

redefine renewable energy as a strategic asset [18]. Cognitive processes evolve into direct problem-solving and sustainable decision-making skills [22].

A similar integration can be examined in the water-energy nexus. Agricultural irrigation, energy consumption, drought, and food security are well-known issues. Having students design an irrigation system using a moisture sensor combines the goal of reducing water consumption with the concept of energy efficiency. Such constructivist and experiential practices, implemented from early childhood and primary education onwards, help ecological literacy become a mental habit [22]. As an interdisciplinary approach, STEM can move green energy literacy beyond the confines of a limited academic curriculum.

3. COMPARATIVE EDUCATION PERSPECTIVE: THE GERMAN MINT APPROACH AND IMPLICATIONS FOR TÜRKİYE

Taking a comparative approach to education can provide an important scientific foundation for developing an interdisciplinary and regional STEM model for Türkiye. Yalkın's doctoral study, which compares science curricula and STEM education policies in Germany, Ireland and Türkiye, shows that these countries have different structural priorities when it comes to STEM education [24]. The study examined dimensions such as curriculum objectives, learning domains, learning outcomes, teaching strategies, assessment and the feasibility of STEM policies. This indicates that any STEM model developed for Türkiye must be grounded not only in instructional activities, but also in policy, implementation, teacher capacity and regional context.The MINT concept, which was implemented in Germany, refers to the disciplines of mathematics, computer science, natural sciences and technology. The MINT approach in Germany offers a framework that supports individuals in these fields from an early age, linking them to career guidance and regional collaborations. Yalkın’s comparative education study shows that Germany takes a professional development, research-oriented approach to STEM education through regional networks [24]. In this context, MINT clusters operate using an ecosystem-based model to establish connections with universities, research centres, local governments and industrial organisations. The most valuable aspect of this model for Türkiye is arguably its demonstration of how STEM education can be linked to regional potential and local challenges.The German MINT system should not be regarded as a model that can be directly transferred to Türkiye. The evaluation of educational models must be conducted with a comprehensive consideration of the historical, economic, cultural, and institutional contexts in which they have emerged. Nevertheless, Germany's MINT cluster strategy has the potential to establish regional STEM ecosystems in Türkiye. Consequently, it would be more accurate

to consider it as a good example. Significant disparities are evident among the various regions of Türkiye with regard to energy resources, climatic conditions, economic activities, environmental risks and social needs. In summary, the pursuit of energy literacy and environmental management should commence in early childhood using evidence-based methods that position children as individuals who actively and competently contribute to sustainable transformation. In the Turkish education system, there has been a pervasive emphasis on integrating technology classrooms, robotics applications, project-based competitions, and teacher training programs to facilitate the integration of the STEM education approach. Whilst these endeavours are praiseworthy, it is broadly acknowledged that a multidimensional approach is imperative for a multidisciplinary field such as green energy literacy. It is imperative that students cultivate the capacity to discern energy-related issues as authentic concerns that are pervasive in their immediate surroundings.

4. THE MERSİN STEM STATION MODEL: A REGIONAL IMPLEMENTATION FRAMEWORK

The city of Mersin is characterised by a robust regional framework, offering a conducive environment for the integration of green energy literacy with STEM education. The city is characterised by numerous problem areas and real-life problems within its geographical location, including, but not limited to, the following: ports, logistics, agriculture, coastal ecosystems, tourism, rural life, mountain culture, water security, renewable energy potential, and disaster risks. The city of Mersin is notable for its diversity, which in turn has led to the establishment of a unique natural outdoor laboratory for interdisciplinary STEM learning. The "Mersin STEM Station Model" can be regarded as a regional framework designed to transform this potential into an educational structure. The fundamental principle of the model is predicated on the notion of treating mathematics not as a singular learning domain, but rather as a series of thematic STEM stations, meticulously structured according to diverse regional problem areas. The starting point of each station is the investigation of a local problem, with students subsequently exploring this problem by utilising their knowledge of science, technology, engineering, and mathematics. This approach serves to broaden the scope of STEM, extending its reach beyond the traditional confines of classroom-based activities. By promoting agency, critical thinking, and an inquiry-based culture, early childhood energy education, rooted in didactic mediation and CHAT frameworks, can establish a foundation for a scientifically literate and environmentally aware populace, advancing the goals of a sustainable future globally.The “Mersin STEM Station Model” is structured around five

stations. The first station is linked to the themes of the port city, urban life, and smart cities. The Port of Mersin provides a valuable learning environment with regard to heavy vehicle traffic, logistics density, fuel consumption, traffic congestion, and carbon emissions. Here, students can develop sensor-based smart intersection systems, algorithms to reduce traffic congestion, and energy-efficient logistics scenarios. Mathematical modelling, data analysis and engineering design are employed in this process. Green energy literacy is developed here through energy efficiency, carbon reduction and smart city planning.The second station could be established along the themes of history, agriculture and the rural-urban transition. The primary problem areas for this station are the Silifke Stone Bridge, the Göksu River, agricultural production and water pollution. Here, students can study the physical and chemical properties of water, design basic filtration systems, observe the effect of agricultural waste on water resources and devise ways to safeguard cultural heritage from environmental hazards. This station promotes green energy literacy by exploring the relationship between water management, agricultural production and environmental protection.The third station focuses on coastal ecosystems, agriculture, tourism and sustainability. The primary themes addressed in this study encompass the Göksu Delta, coastal pollution, microplastics, biodiversity, the impact of tourism and coastal agriculture. Ultimately, the primary target of this activity is to achieve a measurable shift in the community's paradigm from passive energy consumers to active, energy-literate citizens. In addition to this, they can create systems for the monitoring of biodiversity, as well as designs in the STEM subject which are intended to protect marine ecosystems. Persuasive and educational approaches are requisite to instill the understanding that renewable energy is a future investment that is economically and ecologically beneficial [4].The fourth station focuses on rural life, water and energy security. The Gülnar and Mut corridor provides a suitable context for exploring solar energy, wind potential, beekeeping, drought, irrigation and rural energy access. Students can develop solar-powered smart irrigation systems, beehive monitoring setups with temperature and humidity sensors, rainwater harvesting models or portable hybrid energy systems. The results suggest that environmental sustainability needs to be supported by a transition to renewable energy, energy efficiency measures, and green industrial policies, pointing to a transformation requirement aligned with Türkiye’s 2053 net-zero emission target.The fifth station is linked to the themes of natural disasters and resilient cities. In high-altitude regions such as Çamlıyayla, factors such as snow load, sloped terrain, drainage issues, landslide risk and climate conditions present significant STEM challenges for students. Here, students can develop models to examine the relationship between

roof slope, snow load, insulation, drainage and energy efficiency. Here, green energy literacy integrates with post-disaster energy security, resilient infrastructure, and sustainable building design.

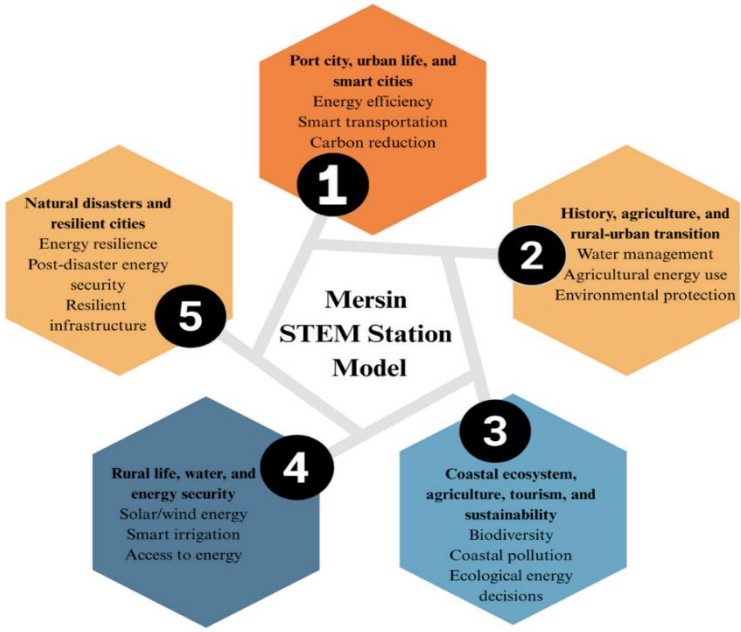

Figure 2. The Mersin STEM Station Model and Its Connections to Green Energy Literacy

Note. The model is based on German MINT clusters, interdisciplinary STEM components, the engineering design process, and a values-based approach to sustainability [11,14,15, 24].

5. PEDAGOGICAL DESIGN: 5E/7E, PROBLEM-BASED LEARNING, AND THE ENGINEERING DESIGN PROCESS

In order to ensure the effective implementation of the Mersin STEM Station Model, it is essential to establish a robust pedagogical framework. The 5E learning model is a pedagogical framework that organises the learning process for students through the stages of engagement, exploration, explanation, elaboration and evaluation [5]. In contrast, Eisenkraft's expanded 7E model places greater emphasis on identifying students' prior knowledge and transferring learned knowledge to new contexts through the emergence and dissemination stages [7]. The 7E model's expanded structure is particularly functional in a multidimensional field such as green energy literacy. Research underscores a persistent disparity between children's initial notions of energy and the intricate scientific understanding required for subsequent academic advancement [22].For instance, there may be a misconception that renewable energy sources have no

environmental impact, that energy efficiency merely involves electricity savings, or that solar energy has universal suitability. It can be demonstrated that the elicitation phase of the 7E model has the capacity to shed light on these misconceived ideas. Conversely, the application phase facilitates the transfer of the solution principle acquired in one area to another. It is conceivable that the sensor logic which has been developed for a rural energy station could be adapted for the monitoring of water quality in a coastal ecosystem or the control of drainage at a disaster monitoring station.The model is strengthened by problem-based learning, which establishes a connection to local issues. Felder and Brent's evaluations of STEM education demonstrate that exposure to real-world, open-ended problems is crucial for motivating students and developing their problem-solving skills [9]. In the context of Mersin, questions such as 'How can the fuel consumption of vehicles waiting around the port be reduced?', 'How are beekeeping activities in Gülnar affected by climate and energy conditions?', and 'How can a monitoring system be developed to preserve the balance of the Göksu Delta ecosystem?' directly link the learning process to local needs.Project-Based Learning is a pedagogical approach that ensures the transformation of problem scenarios into tangible products and design reports. As Jolly notes in his STEM design approach, when students work under real-world constraints, they acquire knowledge and develop skills in decision-making, testing, improvement and defending their solutions [11]. In this process, collaborative learning enables students to adopt different roles, while argument-based learning ensures they can justify their design decisions with evidence.This is a critical aspect of energy literacy. When a student claims that a system is more sustainable, for example, they must support this with evidence relating to energy consumption, cost, environmental impact, measurement data and ease of use.

6. THE TEACHER'S ROLE: FROM KNOWLEDGE TRANSMITTER TO DESIGNER OF A REGIONAL LEARNING ECOSYSTEM

The success of the regional STEM model is closely related to how the teacher positions their role. Instead of being someone who simply implements ready-made activities, the STEM teacher should act as a designer who transforms a real problem into an interdisciplinary learning experience. As Felder and Brent emphasize in their teaching approach, in effective STEM teaching, the teacher ceases to be merely a presenter of information; they become a guide who directs students' inquiry, application, discussion, and decision-making processes [9].This transformation is even more important in terms of green energy literacy. Cultural Historical Activity Theory provides an extensive framework for comprehending

learning as a dynamic, interactive, and historically contextualized process, particularly pertinent to early science and energy education [22] . However, when the teacher relates the topic of energy to the environment, ethics, economics, society, and local needs, students can develop a more holistic understanding. For example, when designing a solar-powered system, not only electricity production but also the region where the system will be used, the need it will meet, its cost, maintenance conditions, and environmental impact should be discussed. The teacher's task is to bring this multi-dimensional discussion into the learning process in a way that is appropriate to the student's level. The teacher's role as an ecosystem designer also requires establishing relationships with stakeholders outside the school. Universities, local governments, industrial organizations, agricultural units, energy experts, and environmental organizations are natural stakeholders of the regional STEM model. In the specific case of Mersin, areas such as the port, agriculture, coastal ecosystem, rural life, and disaster resilience can be considered as resources for out-of-school learning. Thus, the school ceases to be an institution detached from its environment and becomes a center that brings the city's energy and sustainability problems into a scientific learning context.

7. PROPOSAL FOR AN INTERDISCIPLINARY AND REGIONAL STEM MODEL FOR TÜRKİYE

The proposed interdisciplinary and regional STEM model for Türkiye should be based on three fundamental principles. The first principle is regional problem-based structuring. Each region should create STEM learning areas based on its own energy, environment, water, agriculture, industry, and disaster risks. While port, coast, agriculture, rural energy, and disaster resilience are highlighted in Mersin, different stations can be developed in another province. In this way, STEM education goes beyond centralized and uniform applications and becomes linked to local realities.The second principle is interdisciplinary learning architecture. The model is expected to facilitate the integration of the disciplines of science, technology, engineering and mathematics within a single activity. Additionally, it is anticipated that the model will serve to emphasise the distinct contributions of each discipline to the problem-solving process. Mathematics should be used for data analysis and modelling, while science should be used for conceptual explanation and experimental observation. It is imperative that technology is utilised for measurement and representation purposes, while engineering is employed for the development and optimisation of solutions. The research conducted by Nugraha, Kidman and Tan reveals that effective STEM learning is distinguished by the incorporation of interdisciplinary STEM

components, the inclusion of authentic problems, the utilisation of multiple representations, the promotion of engineering design, the facilitation of collaborative learning and an emphasis on student-centredness [15].The third principle pertains to the dimension of sustainability and ethical decision-making. The concept of green energy literacy is comprised of two core competencies. Firstly, it is imperative that students are able to recognise various energy technologies. Both analyses show that increases in GDP per capita affect CO2 emission positively, while increases in renewable energy consumption and patents related to green technology affect CO2 emission negatively [1]. The Turkish Century Education Model, predicated upon a value-based holistic education approach, posits that the focus of STEM applications should be broadened to encompass social benefit and environmental responsibility, in addition to technical achievement [14]. Consequently, the proposed model advocates for an assessment process that does not rely solely on the functionality of the product; rather the emphasis is on the student's capacity to define the problem, use data, collaborate, create a sustainability rationale and justify their chosen solution. In order to facilitate the implementation of the model, it is imperative that teacher training is planned concurrently, that a local stakeholder network is established, and that an assessment and evaluation system is developed. It is imperative that teachers develop a comprehensive understanding of STEM as an interdisciplinary learning architecture. It is imperative that students are able to relate the engineering design process, 5E/7E models, problem-based learning, and argumentation to local contexts. Local stakeholders have the capacity to furnish students with authentic data, field observations, and expert assistance. The measurement and evaluation process should monitor not only the products created by students, but also their scientific thinking and sustainable decision-making processes.

8. REGIONAL FRAMEWORK FOR IMPLEMENTATION, MONITORING AND SCALING OF STEM-BASED GREEN ENERGY LITERACY

The fundamental contribution of the Mersin STEM Station Model is its claim to place STEM education and green energy literacy within a regional context. However, in order to ensure that the educational value of this model does not remain at the conceptual level, it is necessary to define its implementation, monitoring, and scaling dimensions separately. As outlined in preceding chapters, the problem areas of concern to Mersin include the following: the port, agriculture, coastal ecosystems, rural energy, water security and disaster resilience. The incorporation of didactic mediation and Cultural Historical

Activity Theory into early childhood energy education is a significant pedagogical innovation and a crucial approach for achieving wider sustainability objectives in society [22]. One expectation of effective STEM education programs is that students are encouraged to make new and productive connections across two or more of the disciplines, which may be evidenced in improved student learning and transfer as well as interest and engagement [8], [15].The preliminary step in the process under consideration is the preparation of a "regional problem file" for each station. It is imperative that a number of elements are included in the designated file. The thematic designation of the station, in conjunction with the following information, is to be included: the local context of the problem; its interdisciplinary components; potential data sources; design constraints; safety aspects; sustainability rationale; and measurement tools. In order to illustrate this particular point, it would be beneficial to consider a file prepared in the context of ports and smart cities. A file of this nature may comprise a variety of data points, including, but not limited to, traffic density, waiting time, fuel consumption, carbon emissions, sensor data, and relationships between algorithmic decision-making. When giving due consideration to the context of ensuring the availability of energy and water in rural areas, a file might comprise a variety of indicators. Such indicators might include: the necessity for irrigation; the duration of daylight; humidity measurement; energy access; and indicators of water conservation. Consequently, these stations have evolved beyond their initial capacity to merely present headings, transforming into data-driven and design-oriented learning scenarios that educators can seamlessly integrate into their instructional practices. The present approach is in line with the findings of a number of assessments that have identified the central role of realistic and relevant problems in the context of learning STEM subjects [10,11,17].The subsequent stage of this process is to define the role of teachers. In the context of the implementation of STEM education at the regional level, the role of the teacher can be considered to be of crucial importance. The role of the teacher should extend beyond that of an intermediary in the implementation of a predetermined activity. Conversely, the teacher is optimally positioned to fulfil a function analogous to that of a designer, adapting the problem to the specific needs of the learning environment. Furthermore, the teacher must establish interconnections between various academic disciplines, meticulously structure the student's inquiry process, and scrupulously monitor learning evidence. Consequently, it is imperative that teachers address three fundamental questions prior to the implementation stage, in order to facilitate the smooth integration and subsequent utilisation of each station in the educational programme. The question of which scientific concept the student will use in this problem remains

unresolved. This prompts the question of which mathematical or technological representation will serve as an effective tool for visualising the subjects' cognitive processes. Which engineering decision will lead to a sustainable solution? The following questions are of a dual nature, encompassing two distinct yet interconnected aspects of pedagogical practice. The initial issue pertains to the role of the teacher in providing guidance, concerning how educators facilitate the development and progress of their students in the relevant disciplines. Secondly, and inseparable from the first, is the question of the teacher as the architect of the learning environment. This term is used to express the role of educators in shaping the physical and psychological spaces in which learning takes place. As Felder and Brent [9] have demonstrated, the role of the teacher in facilitating and supervising this process is of significant importance in the context of STEM education. In this manner, they furnish a substantial basis for the proposed framework. Sanders' integrative STEM approach has demonstrated the function of technological and engineering dimensions as pivotal interdisciplinary concepts, thus facilitating the real-life application of science and mathematics in a practical sense.The third stage of the process is not a rigid ordering of pedagogical models, but rather their flexible use in combination according to the needs of the station. It is important to note that the 5E and 7E models, problem-based learning, project-based learning, collaborative learning and argumentation-based learning should not be regarded as alternatives to each other. The community service program in Bungin Island successfully achieved its objective of enhancing energy literacy and acceptance by bridging the gap between technical advancements and coastal community realities through a Participatory Action Research approach [18].Whilst the 5E model provides a framework within which students can discover and explain the concept, the 7E model supports the identification of prior knowledge and misconceptions, and the transfer of learning to new contexts [5-7]. Problem-based learning involves the presentation of a local problem whose solution is not immediately apparent. Project-based learning is a pedagogical approach that transforms this challenge into a quantifiable, evaluable, and disseminable product. Whilst collaborative learning facilitates the distribution of roles within the group and the collective decision-making process, argumentation enables the student to defend the solution they have developed with evidence. It is evident that the pedagogical design employed by the Mersin STEM Station Model does not adhere to a singular methodology. Rather, it should be conceptualised as a flexible architecture that integrates diverse approaches within a unified learning flow, contingent on the inherent characteristics of the problem at hand [12,21,15].The fourth stage involves the monitoring of the students' learning process through both the product and process

evidence. The concept of green energy literacy cannot simply be reduced to the identification of energy sources, the explanation of carbon emissions, or the enumeration of renewable energy types. Additionally, the definition of the problem provided by the student, the data that is utilised, the identification of the design constraints, the criteria that is employed for testing solutions, and the evidence that has been presented in order to support the decisions made, must all be assessed. The assessment process is founded upon a quartet of categories of evidence: conceptual evidence, data evidence, design evidence, and argumentation evidence. The conceptual evidence demonstrates the extent to which the student has grasped the relationship between energy, the environment, efficiency, carbon emissions, and sustainability. The extant data demonstrate that the student has the capacity to interpret the problem situation quantitatively or qualitatively. The utilisation of tools such as measurements, tables, graphs, sensor outputs, or observation forms constitutes an integral component of this process. The utilisation of design evidence has been proven to facilitate the discernment of the solution development process in students. This is achieved through the use of prototypes, models, algorithms, drawings and technical reports, thus allowing for a more comprehensive assessment of the students' progress and development. The utilisation of argumentation evidence has been shown to facilitate student responses to the aforementioned inquiry with a robust scientific rationale. It is evident that the proposed framework finds congruence with a unified STEM approach, predicated upon a myriad of representation, engineering design and evidence-based decision-making processes [10,11],23].It has been posited that the fifth phase of the process pertains to the conceptualisation of assessment instruments in alignment with the station model. In this particular context, assessment based solely on classical tests is insufficient. At each designated station, the following tools may be used in conjunction: an assessment scale, a student portfolio, a design journal, a peer review form, a group presentation, and teacher observation notes. It is imperative that the assessment scales encompass evaluations of not only the efficacy of the product, but also of criteria such as problem definition, utilisation of data, consideration of engineering constraints, evaluation of environmental impact, collaboration and the defence of the solution in scientific language. The purpose of the student portfolio is to illustrate the alterations that have been made during the design process. It is evident that, within the same document, the following elements can be tracked: the initial concept, the results of preliminary trials, prototypes that have been unsuccessful in meeting the required standards, the decisions made regarding improvements, and the rationale behind the final design. Errors in the prototype are not excluded from the scope of assessment; rather, they provide evidence of the learning

process. At this juncture, the iterative nature of the engineering design process must be given due consideration as a pivotal component that fortifies students' academic resilience and problem-solving aptitude [3,11].The sixth stage of the programme is the establishment of a monitoring network based on the sharing of data and experience among teachers and local stakeholders. It is important to note that when educational institutions implement STEM models on a regional basis, they may encounter limitations in terms of the model's overall effectiveness if they do so independently. In the context of the station model, it is recommended that universities, local governments, industrial organisations, agricultural units, energy experts, environmental organisations, and science centres be recognised as natural stakeholders. These stakeholders have the capacity to furnish students with authentic data, field observation, expert opinions, laboratory support, or a project presentation environment. The development of such a structure is intended to prevent the solution developed by the student from remaining solely a classroom product; rather, it is intended to connect the solution to local needs and societal benefit. Yalkın's comparative education study, which emphasises the regional network and institutional collaboration logic through Germany's MINT approach, highlights the importance of non-school actors in models to be developed for Türkiye [24]. The OECD's approach to student agency and future skills also reveals that the student should be positioned as an active decision-maker and a subject producing societal contributions in the learning process [16].The seventh stage of the research process is concerned with the adaptability of the model to regions outside of Mersin. The Mersin STEM Station Model can be regarded not only as an application design specific to Mersin, but also as a model logic for establishing regional STEM ecosystems in Türkiye. The adaptable aspect of the model is not the names of the stations in Mersin, but rather the principle of starting from a local problem, designing an interdisciplinary learning task, developing an engineering solution, establishing a sustainability rationale, and monitoring evidence of learning. Consequently, the following issues can be addressed with a similar station logic: landslides, hydroelectric energy, and coastal security in the Black Sea; drought, solar energy, and agricultural irrigation in Central Anatolia; geothermal energy, agriculture, and coastal tourism in the Aegean; winter conditions, energy access, and disaster resilience in Eastern Anatolia; and industry, logistics, and air pollution in the Marmara region. This adaptation ensures that, instead of applying a centralized STEM model in the same way to every province, each region establishes a learning ecosystem nourished by its own ecological, economic, and social realities. In this respect, the model connects the integrity of knowledge, skills, values, and actions emphasised in the Turkish Century Education Model with a

regional application context [14].The final stage of this process is to establish a connection between green energy literacy and technical achievement, as well as ethical and social responsibility. It is of paramount importance for students to design a solar-powered irrigation system, a smart intersection algorithm, a biodiversity monitoring system, or a post-disaster energy security model. Nevertheless, it is imperative to consider the needs it aims to address, the resources it employs, the environmental costs it seeks to mitigate, and the social benefits it aspires to attain. In his seminal article on the subject of human agency, Bandura [2] asserts that human beings act not only as active participants in their own lives, but also as subjects who evaluate the consequences of their actions and take responsibility for them. Rap et al. [19] conducted research on student activism in relation to sustainability issues, which demonstrated that students should address environmental concerns not only through knowledge acquisition, but also by engaging in decision-making and action. Consequently, within the conceptual framework of the Mersin STEM Station Model, green energy literacy has been proposed to encompass not solely the capacity to identify energy technologies, but also to engage in scientific thinking, engineering design, environmental responsibility and the generation of social benefit.The structure proposed within this framework is intended to serve the implementation, monitoring and expansion of the STEM Station model, thereby transforming it from a conceptual proposition into a viable educational paradigm. The evaluation of the model's efficacy necessitates a comprehensive assessment that extends beyond the mere evaluation of students' factual knowledge. The evaluation process should encompass an assessment of students' aptitude for leveraging their knowledge to tackle local issues, the manner in which data has been integrated in decision-making processes, the engineering constraints considered, the sustainability rationale that has been developed, and the evidence that has been employed to substantiate their proposed solutions. It is evident that the relationship between STEM education and green energy literacy cannot be regarded solely as an abstract discourse. Rather, it should be regarded as a pragmatic paradigm, integrating regional development, environmental responsibility, and a culture of scientific thinking within a unified learning environment.

9. CONCLUSION

The present study puts forward the argument that green energy literacy should be regarded as a key component of contemporary STEM education. It is imperative that students are provided with opportunities to engage with the nexus between energy production, consumption, efficiency, carbon emissions, water

usage, environmental impact, and social benefits, as opposed to solely relying on lecture-based instruction to comprehend these complex concepts.It is asserted that the enhancement of such relationships may be realised through interdisciplinary learning processes, wherein students are tasked with working on authentic problems, engaging in critical thinking about data, developing prototypes, testing their solutions, and justifying their decisions.The MINT cluster approach in Germany demonstrates that STEM education can be strengthened through regional networks, out-of-school partners, and hands-on learning processes [24]. For Türkiye, adapting this approach to local conditions is more meaningful than directly replicating it. The Mersin STEM Station Model will serve as a strong example of this adaptation. The city's problem areas – such as the port, agriculture, coastal ecosystems, rural life, water-energy security, and disaster resilience – provide opportunities to address green energy literacy in a local and hands-on manner.The model proposed in this section aims to transform STEM education from a mere collection of activities into a regional learning ecosystem. The notion of green energy literacy as an educational achievement that endures is predicated on the capacity of students to analyse the energy and environmental challenges of their surroundings by means of scientific data, on the ability of teachers to transform these challenges into interdisciplinary learning experiences, and on the transformation of schools into learning centres that collaborate with local stakeholders. The paradigm emphasizes that significant science education involves cultivating new modes of being and doing in the world, in addition to the acquisition of knowledge or skills.

REFERENCES

[1] Atik, H., Kışlacık, N., İnce, K., Çelik, M., Ekmekçi, F., & Demir, H. M. (2026). 2005 Dünya sosyal gelişme zirvesi sonrası yeşil inovasyonun CO_2 emisyonuna etkisi: Sistem GMM yöntemi. *Uluslararası Yönetim İktisat ve İşletme Dergisi, 22*(1), 156–177. https://doi.org/10.17130/ijmeb.1626328

[2] Bandura, A. (2006). Toward a psychology of human agency. *Perspectives on Psychological Science, 1*(2), 164–180. https://doi.org/10.1111/j.1745-6916.2006.00011.x

[3] Bevan, B., Gutwill, J. P., Petrich, M., & Wilkinson, K. (2015). Learning through STEM-rich tinkering: Findings from a jointly negotiated research project taken up in practice. *Science Education, 99*(1), 98–120. https://doi.org/10.1002/sce.21151

[4] Bybee, R. W. (2010). Advancing STEM education: A 2020 vision. *Technology and Engineering Teacher, 70*(1), 30–35.

[5] Bybee, R. W., Taylor, J. A., Gardner, A., Van Scotter, P., Powell, J. C., Westbrook, A., & Landes, N. (2006). *The BSCS 5E instructional model: Origins, effectiveness, and applications*. BSCS.

[6] Dereli, S. (2026). Yeşil dönüşüm bağlamında Türkiye'de ekonomik büyüme, enerji ve karbon emisyonları ilişkisi: Çevresel Kuznets Eğrisi yaklaşımı. *Üçüncü Sektör Sosyal Ekonomi Dergisi, 61*(1), 261–282. https://doi.org/10.63556/tisej.2026.1754

[7] Eisenkraft, A. (2003). Expanding the 5E model. *The Science Teacher, 70*(6), 56–59.

[8] English, L. D. (2016). STEM education K–12: Perspectives on integration. *International Journal of STEM Education, 3*, Article 3. https://doi.org/10.1186/s40594-016-0036-1

[9] Felder, R. M., & Brent, R. (2016). *Teaching and learning STEM: A practical guide*. Jossey-Bass.

[10] Glancy, A. W., & Moore, T. J. (2013). *Theoretical foundations for effective STEM learning environments* (Working paper). Purdue University. http://docs.lib.purdue.edu/enewp/1

[11] Jolly, A. (2017). *STEM by design: Strategies and activities for grades 4–8*. Routledge.

[12] Mansilla, V. B. (2005). Assessing student work at disciplinary crossroads. *Change: The Magazine of Higher Learning, 37*(1), 14–21. https://doi.org/10.3200/CHNG.37.1.14-21

[13] Millî Eğitim Bakanlığı. (2016). *STEM eğitimi raporu*. Yenilik ve Eğitim Teknolojileri Genel Müdürlüğü.

[14] Millî Eğitim Bakanlığı. (2024). *Türkiye Yüzyılı Maarif Modeli öğretim programları ortak metni*. Talim ve Terbiye Kurulu Başkanlığı. https://tymm.meb.gov.tr/ortak-metin

[15] Nugraha, M. G., Kidman, G., & Tan, H. (2024). Interdisciplinary STEM education foundational concepts: Implementation for knowledge creation. *EURASIA Journal of Mathematics, Science and Technology Education, 20*(10), Article em2523. https://doi.org/10.29333/ejmste/15471

[16] OECD. (2019). *The future of education and skills 2030: OECD learning compass 2030*. OECD Publishing.

[17] Pleasants, J. (2020). Inquiring into the nature of STEM problems. *Science & Education, 29*(4), 831–855. https://doi.org/10.1007/s11191-020-00135-5

[18] Puspitasari, P., Hanaldi, W., Alinra, R. R., Hasanah, M., Nugrahanto, C. A., & Sriyatun. (2026). Strengthening energy literacy through renewable energy socialization for coastal communities. *Ta'awun: Jurnal Pengabdian Kepada Masyarakat, 6*(1), 62–73. https://doi.org/10.37850/taawun.v6i01.1165

[19] Rap, S., Blonder, R., Sindiani-Bsoul, A., & Rosenfeld, S. (2022). Curriculum development for student agency on sustainability issues: An exploratory study. *Frontiers in Education, 7*, Article 871102. https://doi.org/10.3389/feduc.2022.871102

[20] Sanders, M. (2009). STEM, STEM education, STEMmania. *The Technology Teacher, 68*(4), 20–26.

[21] Spelt, E. J. H., Biemans, H. J. A., Tobi, H., Luning, P. A., & Mulder, M. (2009). Teaching and learning in interdisciplinary higher education: A systematic review. *Educational Psychology Review, 21*(4), 365–378. https://doi.org/10.1007/s10648-009-9113-z

[22] Topaloglou, N. G., & Kotsis, K. T. (2026). Cultivating energy literacy in early childhood: Didactic mediation within a cultural-historical framework. *European Journal of Contemporary Education and E-Learning, 4*(2), 103–113. https://doi.org/10.59324/ejceel.2026.4(2).09

[23] Vasquez, J. A., Sneider, C. I., & Comer, M. W. (2013). *STEM lesson essentials, grades 3–8: Integrating science, technology, engineering, and mathematics*. Heinemann.

[24] Yalkın, A. (2024). *Almanya, İrlanda ve Türkiye'deki fen bilimleri dersi öğretim programları ve STEM eğitimi politikalarının karşılaştırılması* (Tez No. 909118) [Doktora tezi, Mersin Üniversitesi]. Ulusal Tez Merkezi.

CHAPTER-11

MULTIVARIATE OPTIMISATION IN ORGANIC SYNTHESIS, SMART FLOW CHEMISTRY AND AUTONOMOUS LABORATORY APPROACHES

Ahmet YALKIN[1]

1. INTRODUCTION

The success of an organic reaction depends both on the chemical methodology of the reaction and on its being carried out in a selective and feasible manner under suitable conditions. The hypothetical effects of variables such as temperature, catalyst, solvent, concentration, reaction time, purification process and flow rate can define the framework of the classical OFAT (one factor at a time) approach. For this reason, reaction optimisation processes are now increasingly associated with data-driven methods and algorithmic decision-making support. Among these data-driven and algorithmic decision-making support tools, current technologies such as machine learning, computer-aided synthesis planning (CASP), smart flow chemistry and self-driving laboratories (SDL) can be cited.In this section, which examines all these contemporary approaches, multivariate optimisation problems in organic synthesis are addressed using the synthesis of heterocyclic compounds, such as pyrimidine carboxamide derivatives, as an example. In addition, a multi-dimensional assessment is presented, evaluating recent developments related to reaction prediction, process analytics technologies (PAT), retrosynthesis, Bayesian optimisation, data standards, laboratory safety and STEM education.Drawing on current literature, an "Artificial Intelligence Integrated Organic Synthesis Framework" comprising digital information, prediction, experimental application, feedback and decision-making layers has been proposed. Within this framework, artificial intelligence and automation tools are treated not as systems intended to replace the chemist, but rather as components of a research infrastructure that integrates experimental expertise, data, analytical measurements and decision-support mechanisms.In today's world, research in the natural sciences is increasingly centred on more complex data structures and multivariate problems. It can be said that organic chemistry is also part of this transformation. For many years, organic chemistry has continued to develop through synthesis processes based on laboratory

[1] Dr., Project Office, Tarsus University, Turkey, ahmetyalkin@tarsus.edu.tr, (ORCID: 0000-0002-1914-4608)

practice, combined with the scientist's experience, chemical knowledge and intuition. However, it is stated that organic synthesis has now evolved into a field of research linked to data management and decision optimisation [1].Among the key drivers of this transformation are the sheer volume of data generated in laboratories and the rapid increase in the number of experimental variables. Following the integration of chemical knowledge with technology, it is often not possible to experimentally test all possible conditions. Historically, the optimization of chemical reactions has been performed by manual experimentation guided by human intuition and through the design of experiments where reaction variables are modified one at a time, which is a labor-intensive, time-consuming task that requires exploring a high-dimensional parametric space [16,17].

In today's rapidly evolving technological landscape, machine learning models, computer-aided synthesis planning systems (CASP), process analytics technologies and autonomous experimental platforms have begun to be utilised as tools to help mitigate these limitations. To this end, the concept of a self-driving laboratory (SDL) describes a system in which automated experiments are integrated with data-driven decision-making, with the goal of accelerating the application of the scientific method [16]. The convergence of continuous flow chemistry, automation, and artificial intelligence (AI) defines the emerging field of intelligent flow chemistry. By transitioning from passive tools to agentic systems capable of autonomous decision-making, this paradigm promises to drastically accelerate discovery timelines and ensure high data reproducibility [3].

As a result of these developments, the integration of artificial intelligence and automation into synthesis reactions could be interpreted as leading to a reduction in the researcher's role. However, critical decisions such as reaction safety, the immediate assessment of unexpected by-products, risks arising during scale-up, and the interpretation of analytical data still require chemical expertise. Current developments aim to support chemists' experimental decision-making processes with more robust data sources [11,16].

2. THE PARAMETER SPACE IN ORGANIC SYNTHESIS: A STUDY OF HETEROCYCLIC COMPOUNDS

Reaction optimisation is not a process that can be explained by evaluating different independent variables individually. It can be described as a complex and intricate process that can be optimised by evaluating multiple variables simultaneously. The parameters listed above—such as solvent polarity, temperature, catalyst, ligand and concentration - simultaneously influence product yield and selectivity. These relationships are often non-linear. For example, whilst increasing the temperature typically increases the reaction rate, it can also accelerate thermal

decomposition and the formation of by-products. The choice of solvent, meanwhile, is not solely related to solubility but also plays a decisive role in the stability of the transition state. Chen et al. [3] emphasize that multivariable reaction spaces often exceed what can be efficiently explored through manual screening; under these conditions, OFAT optimization may miss interactions among solvent, temperature, catalyst and concentration.In chemistry, numerous reaction steps can be cited as examples of this situation. The synthesis steps for heterocyclic compounds are presented as examples in this section. The preparation of pyrimidine carboxamate derivatives consists of interlinked stages such as the synthesis of intermediates, acid chloride activation, condensation with amines, and chromatographic purification. Low purity at any stage can directly affect the yield and selectivity in subsequent reaction steps. Similarly, the stability of reagents such as acid chlorides is highly sensitive to the humidity and temperature of the environment. Yalkın [19] has demonstrated the purification, traceability and reproducibility issues encountered in organic synthesis studies through a five-step synthesis of amide derivatives containing a pyrimidine ring, characterised by FT-IR, ^{1}H-NMR and ^{13}C-NMR, using a practical example.One of the key challenges in experimental optimisation is reproducibility. Minor variations in details such as the rate of reagent addition, stirring conditions, temperature profile and atmosphere control can have a significant impact on product yield and purity. Traditional laboratory records often report only the reagents used and the yield obtained. Details regarding the manner in which the experiment was conducted may be missing. Consequently, the utilization of automated systems enables more precise documentation of experimental protocols, enhancing repeatability and reproducibility, while digitization facilitates data recording and sharing [15,16].

Table 1. Comparison of conventional and autonomous optimization approaches in organic synthesis *on [3,11,15,16]*

Feature	Conventional approach	Autonomous approach
Experimental design	Researcher intuition	Algorithm-assisted
Number of parameters	Limited	Multivariable
Data collection	Manual	Automated
Analytical monitoring	Offline	Real-time
Optimization	Trial and error	Bayesian/active learning
Use of negative data	Generally limited	Systematic
Reproducibility	Operator-dependent	High
Resource use	Higher	More efficient
Decision-maker	Chemist	Chemist + algorithm

3. ALGORITHMIC SYNTHESIS PLANNING: REACTİON PREDICTION, RETROSYNTHESIS AND CASP

One of the fundamental challenges in synthesis planning is selecting which of the numerous processes that appear theoretically feasible are actually feasible in the laboratory. It is evident that classical retrosynthetic analysis is shaped by practical constraints such as cost, intermediate stability, functional group tolerance and purification difficulties. Thakkar et al. [15] treat computer-aided synthesis planning as a decision-support approach that can assist route exploration, while still requiring chemists to judge feasibility, functional group compatibility and practical laboratory constraints. However, the feasibility of the reaction steps proposed by the algorithms must ultimately be assessed in conjunction with chemical knowledge and experience [15,16].In these synthesis planning systems, parameters such as reaction prediction, molecular sequences and molecular graphs are processed within digital systems. Graphs can model molecular topology by treating atoms as nodes and bonds as edges. However, the success of these systems also depends on the algorithms used, the quality of the training data, and the accuracy of experimental records [15,18].

Current CASP platforms provide synthesizability predictions by jointly evaluating criteria such as process duration, step yield, and selectivity. Particularly in the development of heterocyclic compounds and drugs, which form the basis of our example, it is not sufficient for a molecule to be computationally predictable Xiao et al. [18] place synthesis at a critical stage of drug and materials research; therefore, a computationally promising structure still needs to be prepared, purified and evaluated under real experimental conditions. In structures containing dense functional groups, such as pyrimidine carboxamide derivatives, steric effects, electronic properties and the isolability of intermediates demonstrate that theoretical predictions do not always align with experimental results [19].One of the most challenging aspects of algorithmic planning is the prediction of reaction conditions. Even if the product structure can be predicted, determining the appropriate combination of solvent, base, catalyst or temperature is often more difficult. One of the main reasons for this is a lack of data. Whilst successful reactions are generally reported in the literature, low-yield or failed experiments are often not documented. The absence of negative data creates a bias whereby machine learning models perceive the chemical space as more ordered than it actually is [11,16]. Consequently, the development of reliable models requires that unsuccessful conditions be reported alongside appropriate data [11,15,16]. As both successful and unsuccessful reaction processes are reported on CASP platforms, algorithmic predictions can yield more successful results.A short and seemingly efficient sequence of steps suggested by algorithms may, in laboratory practice, involve toxic reagents, highly exothermic steps, or by-products that are difficult to separate [17].

Large language models (LLMs), which have been integrated into synthesis planning processes in recent years, provide useful interfaces for procedure generation and information retrieval. To mitigate these risks, by adopting in-context learning and the ReAct (Reasoning and Acting) paradigm, agentic systems decompose complex synthesis objectives into logical subtasks and dynamically deploy external computational tools. This framework ensures that generative outputs are grounded in verifiable chemical data [3,16]. Algorithmic synthesis planning does not so much eliminate the organic chemist's role as enable them to make more informed decisions within the vast literature and reaction data. The evaluation of critical factors such as selectivity, scalability, purification strategies and safety remains the fundamental responsibility of experimental expertise [11,15,16].

4. SMART FLOW CHEMISTRY AND AUTONOMOUS LABORATORY WORKFLOWS

Flow chemistry has long been utilised as a powerful experimental framework that enables the precise control of reaction parameters. This sub-section examines smart flow chemistry and workflows in autonomous laboratories. In syntheses conducted via flow chemistry, unlike in traditional batch systems, reagents move continuously through microchannels or pipelines. By providing superior heat dissipation and millisecond-level residence time control, flow architectures enable automated platforms to safely manage ultrafast kinetics and extreme exotherms while accelerating optimization through cost-aware algorithmic search [3,17].However, not every organic reaction can be transferred to flow systems. However, flow chemistry faces limitations in handling poorly soluble reagents, lacks dedicated databases for automated synthesis planning, and typically lacks translatability between flow and batch chemistries. Hence, batch-type synthesis remains practical for chemists due to its status as a standard protocol in mass production and development [4,17]. Therefore, the preferred approach is not to prioritise a specific technology, but to select the reaction platform best suited to the chemical problem.Chen et al. [3] describe process analytical technologies as the sensory layer of intelligent flow chemistry, since real-time analytical information can be used to monitor conversion, purity and selectivity during optimization. Data obtained from analytical instruments such as HPLC, LC-MS, FT-IR and NMR can be fed directly into optimisation algorithms; parameters such as conversion rate, product purity and selectivity can be evaluated whilst the experiment is in progress [3,11].

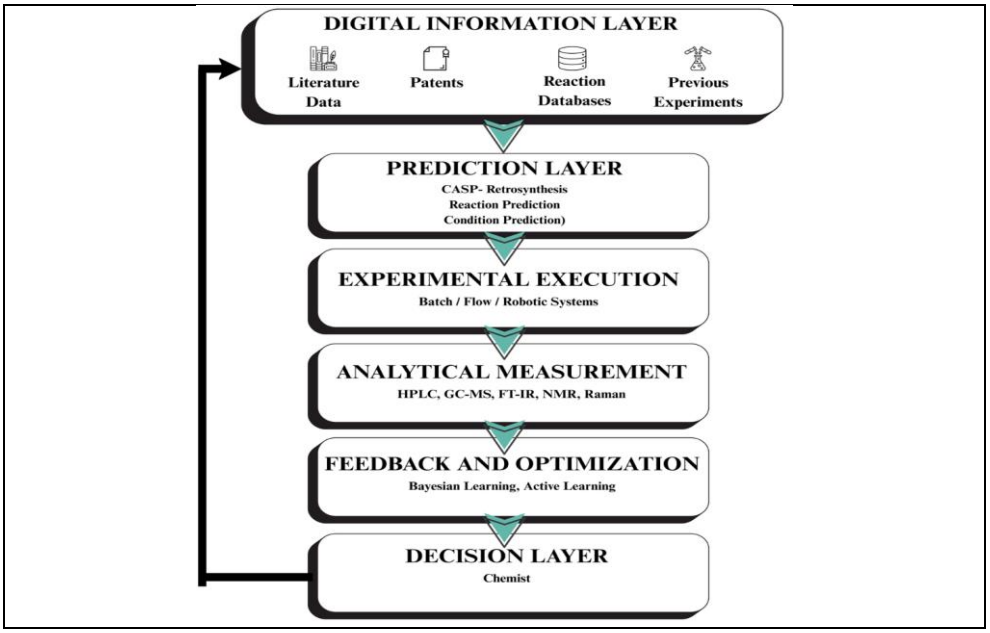

Figure 1. The closed-loop experimental optimisation process in self-driving laboratory systems [3,4,11,16].

Self-driving laboratories unify artificial intelligence (AI) with automated robotic platforms to realize autonomous experimentation, where the closed-loop workflow is generally sub-divided into four steps: design, make, test, and analyze (DMTA) [11,16]. These systems are not limited to liquid transfer alone. To operate such systems, the software component of an SDL is composed of three distinct parts: (1) the control and communication system of the automated hardware of the laboratory, (2) the data extraction, management, and analysis of experimental output, and (3) the decision-making experimental planner [11,16].Autonomous platforms currently under development serve a variety of research objectives. Ha et al. [4] present Synbot as a layered robotic chemistry platform in which AI software, robot-control software and physical robotic execution are linked to support autonomous organic synthesis. The Chemputer platform, on the other hand, enables the standardisation of experimental procedures via a chemical programming language and their reproducibility in modular reactors [12]. The mobile robotic chemist approach developed by Burger and colleagues proposes the integration of autonomous support into experimental processes without altering existing laboratory infrastructure [2]. Fluidic autonomous laboratories developed for inorganic crystallisation and material synthesis provide significant examples of the integration of characterisation data into algorithmic decision-making mechanisms [10,13]. This diversity of laboratory equipment necessitates that the stages of synthesis planning, experimental

implementation and analytical measurement be operated within a single integrated research ecosystem, rather than being managed by separate, disconnected devices [3,16].To this end, the proposed "Artificial Intelligence Integrated Organic Synthesis Framework" (Figure 2) addresses the process across five layers: digital information, prediction, experimental implementation, feedback and decision-making. Thus, the generation, interpretation and conversion of data into new experimental decisions can be evaluated within the same workflow.

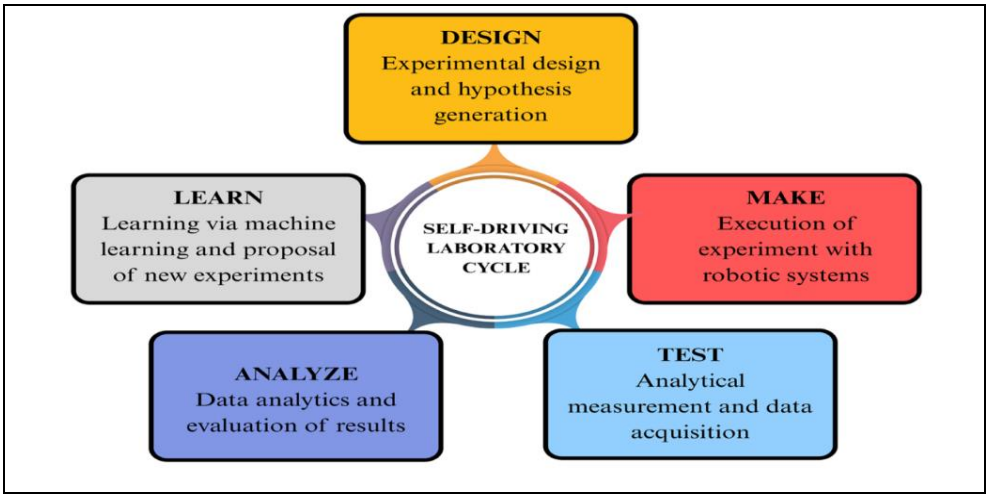

Figure 2. Artificial Intelligence-Integrated Organic Synthesis Framework

The solution that the framework presented in Figure 2 brings to the laboratory is the integration of technologies that do not communicate with one another into a common decision-making cycle. CASP systems can predict synthesis workflows, flow systems can optimise specific conditions, and robotic platforms can execute experiments. However, these tools do not, on their own, represent the entire synthesis process. The proposed framework integrates algorithmic prediction, robotic execution and analytical feedback within the same data stream. Such an approach does not eliminate the chemist's role; on the contrary, it further highlights the importance of interpreting and overseeing experimental decisions. The assessment of intermediate products carrying an explosion risk, safety issues that may arise during scale-up, or the interpretation of unexpected analytical results remain decision-making areas that still require expert chemical knowledge. For this reason, autonomous systems should be regarded as tools that assist the researcher's expertise rather than replacing them [11,16].

5. AREAS OF APPLICATION: HETEROCYCLIC COMPOUNDS, MATERIALS AND SUSTAINABILITY

Autonomous laboratory systems provide a data-driven common ground for collaboration between organic synthesis and pharmaceutical research. Establishing structure-activity relationships in drug development often requires the synthesis, purification and comparative evaluation of a large number of analogue compounds. Candidate molecules bearing a pyrimidine skeleton and enzyme inhibitors are typical examples in this regard. Closed-loop flow systems enable more controlled screening of parameters such as solvent, temperature, concentration and flow rate in these systems [18]. However, heterocyclic derivatisation still requires significant laboratory effort due to intermediate purity, chromatographic separation and characterisation [19].The data-driven optimisation approach is not limited to organic synthesis alone. Sadeghi et al. [10] show that self-driving fluidic laboratories can be used for the autonomous development of lead-free metal halide perovskite nanocrystals by connecting synthesis, characterization and experiment selection within the same workflow. In these systems, real-time data obtained from spectroscopic sensors enables the modelling of relationships between precursor concentration, flow rate and material performance. The direct translation of characterisation results into new experimental conditions enhances the capacity for high-throughput experimentation. Similarly, the optimisation of reaction conditions by algorithms at the microvolume scale contributes to sustainable chemistry objectives by reducing reagent consumption, solvent usage and the volume of chemical waste. However, whilst performance in material synthesis can often be defined by a few measurable parameters, additional variables in organic synthesis—such as selectivity, by-product formation and purification requirements—make the optimisation problem more complex.

6. SECURITY, DATA STANDARDS AND ETHICS

The integration of robotic systems into laboratory work will also bring with it new responsibilities regarding safety and data management. For example, in laboratories using mobile robotic arms, high-pressure pumps and automatic valve systems, physical safety cannot be left solely to the researcher's vigilance. Computerised prediction systems are increasingly being used to detect chemical leaks, pressure surges or equipment-related accidents at an early stage. Systems based on visual language models that can monitor the use of personal protective equipment and detect abnormal conditions in the experimental environment are emerging as key components of laboratory safety. Munguia-Galeano et al. [9] extend the self-driving laboratory discussion to safety monitoring by showing that visual language model-based systems can support laboratory supervision and robot

decision-making in chemically active environments.With the increasing prevalence of autonomous systems, cybersecurity and ethical considerations have also gained importance. The malicious manipulation of chemical workflows or their use in the synthesis of regulated substances are among the risk areas increasingly discussed in the literature [7]. Similarly, large language models (LLMs), whilst offering useful tools for preparing experimental procedures, can generate critical errors from a safety perspective. Issues such as the failure to identify explosive intermediates, inappropriate solvent recommendations, or the use of fabricated sources demonstrate that these systems should be regarded not as independent decision-makers, but as support tools used under expert supervision.Another factor limiting the effectiveness of autonomous systems is data quality. In chemical synthesis processes, the process steps from experimental setups that fail to achieve the desired outcome are generally not published. The failure to publish data from these experiments means that artificial intelligence technologies are fed only with successful results. This is important because the current endemic publication bias is detrimental to ML approaches as “negative” results are as important as “positive” ones for training models [11]. To develop reliable predictive models, negative data must also be systematically recorded and shared. Furthermore, it is of great importance that experimental processes are documented alongside information regarding quantity, duration, temperature, purification steps and the equipment used. Machine-readable data structures and standardised protocol formats are regarded as key tools for enhancing the comparability and reproducibility of studies conducted across different laboratories [15,16].

7. CHEMİSTRY EDUCATION IN THE AGE OF ARTIFICIAL INTELLIGENCE AND IMPLICATIONS FOR STEM

The increasing role of machine learning, artificial intelligence technologies and autonomous laboratory systems in organic synthesis research has brought new areas of competence to the fore in chemistry and STEM (Science, Technology, Engineering, and Mathematics) education. In a research environment where a multidisciplinary approach is increasingly being adopted across many fields, leading to the widespread adoption of autonomous systems, it may no longer be sufficient for students to learn merely experimental techniques. It is of great importance that chemists capable of adapting to new technologies develop skills such as data literacy, algorithmic thinking and statistical experimental design alongside laboratory practices [6,8].It could be argued that the effective use of generative AI tools in educational settings is also linked to positioning these systems as aids that support scientific thinking. Tassoti [14] argues that prompt design becomes educationally meaningful in chemistry when students are guided to question, refine and evaluate

generative AI outputs rather than simply accepting them. However, rather than directly accepting synthesis processes or experimental conditions suggested by artificial intelligence, these must be critically evaluated in terms of thermodynamics, reaction kinetics and laboratory safety [20].An approach that integrates technology, pedagogy and subject knowledge provides an important framework for reflecting this transformation in educational programmes [5]. One of the most beneficial practices in undergraduate chemistry education may be the gradual incorporation of modular flow systems, open-source data analysis tools and basic automation applications into laboratory training, rather than relying on high-cost systems. In this way, students can be trained not merely as individuals who produce experimental results, but as researchers capable of interpreting data-driven decision-making processes.

8.CONCLUSION

It can be said that artificial intelligence technology, which has rapidly become part of our lives in recent years, is a topic of ongoing debate amongst chemists. The use of artificial intelligence in organic synthesis is most often seen in terms of algorithmic success, robotic hardware or autonomous platforms. From a laboratory perspective, the issue is more concrete: how should the experiment be planned, why should certain conditions be selected, how should the resulting product be monitored, and how should failed attempts be recorded? The approach proposed in this section evaluates AI-assisted synthesis through these questions. This is because the success of synthesis depends not so much on the design of the target molecule, but rather on how traceable, reproducible and chemically justifiable the experimental process is.

Multi-step heterocyclic syntheses, such as those involving pyrimidine carboxamides, clearly demonstrate how theoretical planning is affected by experimental limitations. Intermediate purity, moisture control, temperature profiles and chromatographic separation processes are not isolated steps. Even the slightest tolerated impurity at any stage can lead to yield losses that are difficult to compensate for in subsequent stages, the formation of secondary by-products or complex mixtures that are difficult to separate chromatographically [17,19]. In this context, the true potential of CASP tools, reaction prediction algorithms, and autonomous laboratory equipment should be evaluated based not only on the outputs they generate in a digital environment, but also on their applicability under physical laboratory conditions. A reaction route that appears flawless and short in a computational environment does not necessarily guarantee a successful outcome in a physical laboratory setting.That said, the ‘Artificial Intelligence-Integrated Organic Synthesis Framework’ should not be viewed as a form of automation that renders chemists redundant. Rather, it should be understood as an analytical thinking

model that makes complex experimental workflows measurable. When digital prediction, robotic action and real-time analytical data converge within the same system, researchers will have access to more information, including that relating to the outcome, as well as the data at each process step. Nevertheless, all of these operational challenges in chemical synthesis still rely directly on the researcher's chemical knowledge, as well as their intuition, experience, and attention to detail [11,16].Rather than building high-cost autonomous platforms, Turkey's first step might be to establish a robust culture of digital experimentation. Widespread adoption of electronic laboratory notebooks, development of open chemical data sources and creation of standardised recording formats through university–industry partnerships could strengthen the data infrastructure necessary for reliable autonomous synthesis studies [11,15,16].This infrastructure would support reproducibility in organic synthesis studies, enabling chemists to engage with data-driven experimental design from the outset [6,8,20]. The enduring scientific value of autonomous synthesis will not rest on massive computational power, but on well-documented experiments, careful laboratory validation and the expertise to chemically interpret the data [11,16].

REFERENCES

[1] Abolhasani, M., & Kumacheva, E. (2023). The rise of self-driving labs in chemical and materials sciences. *Nature Synthesis, 2*(6), 483–492. https://doi.org/10.1038/s44160-022-00231-0

[2] Burger, B., Maffettone, P. M., Gusev, V. V., Aitchison, C. M., Bai, Y., Wang, X., Li, X., Alston, B. M., Li, B., Clowes, R., Rankin, N., Harris, B., Sprick, R. S., & Cooper, A. I. (2020). A mobile robotic chemist. *Nature, 583*(7815), 237–241. https://doi.org/10.1038/s41586-020-2442-2

[3] Chen, Y., Tan, X., Wu, T., Tang, B., & Wen, Z. (2026). Intelligent flow chemistry: A new paradigm for artificial intelligence-driven synthesis and discovery. *CCS Chemistry, 8*, 2667–2686. https://doi.org/10.31635/ccschem.026.202607484

[4] Ha, T., Lee, D., Kwon, Y., Park, M. S., Lee, S., Jang, J., Choi, B., Jeon, H., Kim, J., Choi, H., Seo, H.-T., Choi, W., Hong, W., Park, Y. J., Jang, J., Cho, J., Kim, B., Kwon, H., Kim, G., ... Choi, Y.-S. (2023). AI-driven robotic chemist for autonomous synthesis of organic molecules. *Science Advances, 9*(44), Article eadj0461. https://doi.org/10.1126/sciadv.adj0461

[5] Iyamuremye, A., Niyonzima, F. N., Mukiza, J., Twagilimana, I., Nyirahabimana, P., Nsengimana, T., Habiyaremye, J. D., Habimana, O., & Nsabayezu, E. (2024). Utilization of artificial intelligence and machine learning in chemistry education: A critical review. *Discover Education, 3*, Article 95. https://doi.org/10.1007/s44217-024-00197-5

[6] Khoo, J. Z. Y., Hollinger, F., Han, J. Y., Lin, C., Tsai, C.-C., Schwartz Poehlmann, J. K., Anzola, D., Choo, Y. S. L., & Fung, F. M. (2026). Tipping point in the future readiness of artificial intelligence and chemistry education. *Journal of Science Education and Technology*. Advance online publication. https://doi.org/10.1007/s10956-026-10330-8

[7] Lee, J., Persaud, B., Del Castello, B., Berke, A., & Zilgalvis, G. (2025). *Documenting cloud labs and examining how remotely operated automated laboratories could enable bad actors* (PE-A3851-1). RAND Corporation. https://doi.org/10.7249/PEA3851-1

[8] Maisincho-Asqui, M.-P., Bastidas-Chalán, R., Armijos-Hurtado, S., Alcocer-Vallejo, M., & Gavilanes-López, S. (2026). Artificial intelligence in undergraduate chemistry education: A review. In M. V. García, C. Gordón-Gallegos, P. C. López-López, & M. Botto-Tobar (Eds.), *Proceedings of the International Conference on Computer Science, Electronics and Industrial Engineering (CSEI 2024)* (Lecture Notes in Networks and Systems, Vol. 1532, pp. 197–212). Springer. https://doi.org/10.1007/978-3-031-98890-5_13

[9] Munguia-Galeano, F., Zhou, Z., Veeramani, S., Fakhruldeen, H., Longley, L., Clowes, R., & Cooper, A. I. (2026). Chemist Eye: A visual language model-powered system for safety monitoring and robot decision-making in self-driving laboratories. *Digital Discovery, 5*, 2209–2220. https://doi.org/10.1039/d6dd00062b

[10] Sadeghi, S., Bateni, F., Kim, T., Son, D. Y., Bennett, J. A., Orouji, N., Punati, V. S., Stark, C., Cerra, T. D., Awad, R., Delgado-Licona, F., Xu, J., Mukhin, N., Dickerson, H., Reyes, K. G., & Abolhasani, M. (2024). Autonomous nanomanufacturing of lead-free metal halide perovskite nanocrystals using a self-driving fluidic lab. *Nanoscale, 16*(2), 580–591. https://doi.org/10.1039/d3nr05034c

[11] Seifrid, M., Pollice, R., Aguilar-Granda, A., Chan, Z. M., Hotta, K., Ser, C. T., Vestfrid, J., Wu, T. C., & Aspuru-Guzik, A. (2022). Autonomous chemical experiments: Challenges and perspectives on establishing a self-driving lab. *Accounts of Chemical Research, 55*(16), 2454–2466. https://doi.org/10.1021/acs.accounts.2c00220

[12] Steiner, S., Wolf, J., Glatzel, S., Andreou, A., Granda, J. M., Keenan, G., Hinkley, T., Aragon-Camarasa, G., Kitson, P. J., Angelone, D., & Cronin, L. (2019). Organic synthesis in a modular robotic system driven by a chemical programming language. *Science, 363*(6423), Article eaav2211. https://doi.org/10.1126/science.aav2211

[13] Szymanski, N. J., Zeng, Y., Huo, H., Bartel, C. J., Kim, H., & Ceder, G. (2021). Toward autonomous design and synthesis of novel inorganic materials. *Materials Horizons, 8*(8), 2169–2198. https://doi.org/10.1039/d1mh00495f

[14] Tassoti, S. (2024). Assessment of students use of generative artificial intelligence: Prompting strategies and prompt engineering in chemistry education. *Journal of Chemical Education, 101*(6), 2475–2482. https://doi.org/10.1021/acs.jchemed.4c00212

[15] Thakkar, A., Johansson, S., Jorner, K., Buttar, D., Reymond, J.-L., & Engkvist, O. (2021). Artificial intelligence and automation in computer aided synthesis planning. *Reaction Chemistry & Engineering, 6*(1), 27–51. https://doi.org/10.1039/d0re00340a

[16] Tom, G., Schmid, S. P., Baird, S. G., Cao, Y., Darvish, K., Hao, H., Lo, S., Pablo-García, S., Rajaonson, E. M., Skreta, M., Yoshikawa, N., Corapi, S., Akkoc, G. D., Strieth-Kalthoff, F., Seifrid, M., & Aspuru-Guzik, A. (2024). Self-driving laboratories for chemistry and materials science. *Chemical Reviews, 124*(16), 9633–9732. https://doi.org/10.1021/acs.chemrev.4c00055

[17] Velasco, P. Q., Hippalgaonkar, K., & Ramalingam, B. (2025). Emerging trends in the optimization of organic synthesis through high-throughput tools and

machine learning. *Beilstein Journal of Organic Chemistry, 21*, 10–38. https://doi.org/10.3762/bjoc.21.3

[18] Xiao, W., Su, H., Ma, Y., Ma, Y., Lu, W., Wang, L., Ge, L., Yuan, M., Jiang, L., Liang, L., & Liu, X. (2025). Integration of machine learning and automated synthesis for accelerated drug and material research. *ChemistrySelect, 10*(2), Article e04970. https://doi.org/10.1002/slct.202504970

[19] Yalkın, A. (2017). *Multifonksiyonel yeni heterosiklik bileşiklerin sentezi* (Tez No. 483450) [Yüksek lisans tezi, Bozok Üniversitesi]. Ulusal Tez Merkezi.

[20] Yim, K.-H., & Lui, M. Y. (2026). Supporting undergraduate students' learning in practical chemistry courses through AI-supported experimental design. *Journal of Chemical Education*. Advance online publication. https://doi.org/10.1021/acs.jchemed.5c01311